UNIVERSITAT DE BARCELONA

Using Phosphorodiamidate Morpholino Oligomers (PMOs) to characterize the role of neurofibromin in cell physiology

Josep Biayna Rodríguez

USING PHOSPHORODIAMIDATE MORPHOLINO OLIGOMERS (PMOs) TO CHARACTERIZE THE ROLE OF NEUROFIBROMIN IN CELL PHYSIOLOGY

Facultat de Farmàcia

Programa de Doctorat en Biomedicina

Universitat de Barcelona

Memòria presentada per:

Josep Biayna Rodríguez

Per a optar al títol de:

Doctor per la Universitat de Barcelona

Directors/tutors:

Eduard Serra i Arenas **Conxi Lázaro García**

Tesi realitzada a l'Institut de Medicina Predictiva i Personalitzada del Càncer (IMPPC) i l'Institut d'Investigació Biomèdica de Bellvitge (IDIBELL)


IDIBELL
Institut d'Investigació Biomèdica de Bellvitge


UNIVERSITAT DE
BARCELONA


IMPPC
Institut de Medicina Predictiva
i Personalitzada del Càncer

- GENER 2016 -

Poco somos conscientes de todo lo que pasa aunque estemos rodeados de silencio. Y es que ahí, cualquier pequeño detalle tiene mucho más valor. Se aprende a conocer los gestos, las miradas, las medias sonrisas...Las sonrisas enteras pueden incluso sonar a carcajada. Te vuelves cómplice ineludible del más leve sonido. Se tejen historias, enfados y vidas nuevas alrededor de un mundo silencioso que avanza implacable.

—— I.R ——

Als meus pares Avis en Francesc i la Gabrijela

Sempre he cregut que totes aquelles decisions que prenem modelen el que serem i el que hem sigut. Des de la més petita a la més gran de les accions sempre en traiem alguna cosa. Però realment darrere de tot el que fem, les persones que ens envolten són les que tenen més influència en nosaltres. En aquesta tesi, m'agradaria agrair a totes aquelles persones que m'han acompanyat en aquest viatge.

Les meves primeres paraules són per a l'**Edu**, ell va donar-me l'oportunitat d'iniciar la meva aventura científica al IMPPC, fet pel qual sempre li estaré agraït. Gràcies a la seva paciència, ajuda, guia però sobretot per transmetre'm la seva passió i entusiasme envers la ciència tanco aquesta etapa amb una gran satisfacció i riquesa personal. Gràcies per tot. Aprofitar també per agrair a tota la gent del nostre lab; l'**Ernest** amb qui vaig iniciar el meu aprenentatge i amb el qual he acabat vivint moltes experiències (sobretot viatges), el **Bernat** el nostre "bioinfo todo terreno" que en general sap de tot (literalment), una font d'opinió i consells a la que sempre m'ha agradat escoltar, la **Meri** que amb el seu somriure tan característic, sempre he tingut un suport davant tots els dubtes que podien aparèixer, especialment pel que fa a cultius i la **Eli** defensora fèrria del JP i una crack en el *running* com del NGS.

Si hi ha algú, amb la qual he passat grans moments i sincerament s'ha convertit en una de les millors persones que he conegut és l'**Imma** (Lada). Amb ella he compartit vivències, ha estat al meu costat tant en els bons com els mals moments i sempre amb un somriure. En aquesta tesi també hi ha una part teva, ja que sense la teva ajuda, consells i amistat aquesta no hagués sigut possible.

També agrair a tota la gent que ha passat pel nostre laboratori i amb els quals hem compartit molt bons moments. Em refereixo a la **Núria**, l'**Helena**, la **Rocío**, la **Noelia** i ara últimament un tal **José Marcos**. Així com a tota la gent de l'IDIBELL, a la **Conxi** per haver confiat sempre en mi, pel seu gran suport i ajuda prestada i com l'Edu un gran exemple a seguir, la **Juani** sempre disposada a donar un cop de mà, l'**Eva** i el **Joan**.

No ho recordo molt bé, però una vegada algú em va comentar que l'IMPPC era com una gran família nombrosa i que en certa manera treballar allà era com estar a casa teva. Amb molta seguretat, ara puc dir que cadascú de vosaltres m'ha

aportat alguna cosa.

Per començar, agrair als MAPs, la família nombrosa dins la "IMPPC family" (ara ja no en són tants). El **Miquel Àngel Peinado**, la **Mònica**, la **Mireia**, el **Quim**, la tècnic amant dels animals i d'energia inesgotable la **Mar**, la **Raquel**, la **Berta**, l'**Elvira** amb les seves paraules d'ànim en tot moment i la senyoreta **Yaiza** una gran persona, a la qual m'hi uneix una gran confiança i respecte. També la **Izaskun**, ja que gràcies a les seves sortides per la muntanya he pogut respirar una mica quan les situacions eren difícils i al **Llorenç** amb el qual ens han unit converses de gran transcendència (Mòbils i Bola de Drac).

Agrair també a tota la gent del Marcus Buschbeck lab, començant precisament pel **Marcus** promotor de "l'IMPPC *running team"*, així com l'**Anna**, la **Vane**, el **Julien**, el **David**, la **Sarah** amb la qui he compartit dinars de cap de setmana parlant de les meravelles de França i el **Roberto** una gran persona i el millor cuiner del campus (ho sento Bernat!!). També agraïr a tota la gent del grup de la Mayka, la **Jessica**, l'**Àlex**, l'**Anna**, la **Sara** així com el **Francisco** i el **Jorge**, gràcies als dos per totes les emocionants sortides nocturnes per Barna.

El meu agraïment a la gent del Fumi lab, a l'**Emili** una persona que sempre ha estat molt comprensiva i a la que li agrada escoltar, al **Fumii** per tots els seus consells sobre com afrontar la ciència i la **Miyako** a tots els seus petits regals i detalls de Japó.

A tots els integrants del Perucho Lab, l'entusiasta per la ciència **Sònia Forcales**, la **Gabrijela** (ja en parlaré després), el duo Pin i Pon **Jordi** i **Cristian** amb els quals sempre hem tingut temps de riure plegats (Bueno, Bueno...), el **Taka** que s'ha convertit en el meu *sensei* de la pesca, la **Lucie,** la **Irene,** l'**Andreu**, el **Sergio** i la **Bea.** També a la gent del Yokota lab, el **Francesco**, la **Fuyumi,** la italiana amb més marxa i bon rollo la **Sabrina** i a la segona membre del "*running team*" **Sònia Solé.**

I a la resta de gent de l'IMPPC el **Lauro**, la **Raquel**, el **Gabriel**, el **Rafa**, l'**Anna Carreras**, el *IT-duo* **José** i **Adri**, la **Tanya**, l'**Edu Casas**, el **David izquierdo**, la **Sílvia,** l'**Oscar,** la **Harvey,** el **Juan,** l'**Inaki** i l'**Oliver**. Com a tota aquella gent, que ha passat pel nostre centre i amb els quals he compartit molts bons moments

com el **Charlio**, l'**Edu Porta**, l'**Aida Arcas**, el **Víctor**, la **Neus**, la **Melanija**, el **Sergi**, l'**Anna Díez**, la **Marta** i la **Susana**.

A tots els companys de l'Institut Carreras, la **Lourdes**, la **Vera** per tots els moments d'ànim en la recta final d'aquesta tesi, l'alegre **Jordi**, la **Paula** la *runner* professional que m'ha ajudat en algun que altre article, la **Nuri**, la **Laura**, la **Mar**, la **Érica**, la **Joao,** la **Rocío**, la **Eulàlia,** el **Josep** i el **Francesc Solé**.

Al llarg d'aquesta tesi, he tingut l'oportunitat de conèixer a gent que s'han convertit en uns grans amics, em refereixo als membres del "G8" o "e-biometges"; la meva parella de taula en cada esdeveniment el Sr. **Dani Rodrigo**, la veïna de l'IGTP amant de Nova York i del millor cava del món (no faré publicitat però comença per F) l'**Aida**, la Gironina experta en snowboard i *Arrays* l'**Anna Puiggros**, la **Marina** amb la qual ens uneix un vincle molt fort amb les bones sèries i l'anime, i la culé i exploradora **Tanit**. Sense oblidar-me de la "e", el **Jeudiel** amb el qual sempre quedo atrapat en multitud de converses, "*l'Apple boy"* **David**, l'**Ignasi** i de l'artista de Manlleu **Marc**. Finalment dos membres inicials del G8, el **Miguel**, el Mexicà conegut tant en grans ciutats com en els pobles més petits de Catalunya, i el **Pablo** un Murcià amant de les camises i de la bona història.

Aprofitar també per agrair als meus amics de la UdG, per tots els anys que hem passat i les experiències viscudes. A l'**Anna Bahí** i el **Dani Lucena**, amb els quals hem compartit un munt de somnis, reptes, vivències i alguns dels millors moments assaborint i recordant els secrets de la comarca de Selva (som i sempre serem els tres magnífics). I finalment al **Pedro Calvete**, el **Joaquim Olivés** i el **Sergi Compte,** per estar presents sempre quan els necessites.

El meu sincer agraïment, a tres persones que han sigut molt importants en la meva educació i que segurament sense ells ara potser no hauria arribat on sóc, es tracta d'en **Ricard Martín**, l'**Ani Dunjó** i la **Marina Roldán**. Moltes gràcies per tot. Agrair també a tota la gent de **Principia**, ja que entre tots i amb molt d'esforç hem pogut crear una finestra per divulgar la ciència en totes les seves vessants.

També a la meva família, els quals els hi haig d'agrair una gran part de tot. Sense ells res d'això seria possible. Als meus pares, que sempre han posat la meva educació com una prioritat a la seva vida intentant que fos el més feliç possible fent el que m'agrada. El meu **pare**, al qual sempre li estaré agraït per ser la primera persona que em va portar cap al camí de la ciència, ja que un petit microscopi de plàstic pot canviar moltes coses. A la meva **mare,** per tot el suport que sempre m'ha donat tant en els moments fàcils com difícils. Al meu germà **Francesc**, que tot i que no se'n adoni som molt més semblants del que es pensa. Als tres gràcies per haver estat al meu costat i haver-me recolzat sempre. Als meus **avis**, per tot el suport, ajuda i paciència que sempre m'han brindat, especialment el meu avi **Antonio** que allà on sigui mai no va defallir en ajudar-me. També als meus **tiets,** per tot el seu suport i al **Molina**, que tot i que malauradament no podrà veure aquesta tesi, sempre va estar orgullós de mi.

I finalment, a la **Gabrijela** a la persona amb la qual he passat i passaré els millors anys de la meva vida. Pel teu suport incondicional en tot aquest procés, per aguantar els nervis i la pressió en aquesta recta final, gràcies per dibuixar-me un somriure cada matí, per ajudar-me en cada moment. Sense tu, res hauria sigut possible. Però sobretot gràcies per entendrem i estimar-me cada dia.

ACRONYMS

AA	Amino acid
AC	Adenylyl cyclase
ALT	Alternatively spliced exon
AON	Antisense oligonucleotide
ATCC	American type culture collection
ATP	Adenosine triphosphate
APP	Amyloid precursor protein
bFGF	Basic fibroblast growth factor
BSA	Bovine serum albumin
CALM	Café-au-late macules
cAMP	Cyclic adenosine monophosphate
CELF	CUG-BP and ETR-3 Like Factors
CS	Cancer syndrome
CNS	Central nervous system
CSR	Conserved splicing region
CSRD	Cysteine/serine-rich domain
CUG-BP	Cytosine-Uridine-Guanine-binding protein
CTD	C-terminal domain
Dusp6	Dual specificity phosphatase 6
dNTP	Deoxyribonucleotide triphosphate
DMEM	Dulbecco's modified eagle medium
dNF	Dermal neurofibroma
DTT	Ditiotretiol
E23a	Exon 23a
EGF	Epidermal growth factor
EPEI	Ethoxylated polyenthylenimine
ERK	Extracellular signal-regulated kinase1
ES	Embryonic stem
ESE	Exonic splicing enhancer
ESS	Exonic splicing silencer

ETR-3	ELAV-type RNA-binding Protein
EV12	Ecotropic viral integration site
FBS	Fetal bovine serum
G418	Geneticin
GAP	GTPase activating protein
Gap43	Growth associated protein 43
GDP	Guanosine diphosphate
GEF	Guanine Nucleotide Exchange Factor
GIST	Gastrointestinal stromal tumor
GRD	Gap-related domain
GTP	Guanosine-5'-triphosphate
hn-RNPS	Heterogeneous nuclear ribonucleoproteins
Inc	Inclusion
LOH	Loss of heterozigosity
LRD	Leucine-rich domain
MBNL1	Muscleblind-like protein 1
MBNL2	Muscleblind-like protein 2
MAPK	Mitogen-activated protein kinases
Mmp3	Matrix metallopeptidase 3
MPNST	Malignant peripheral nerve sheath tumor
mRNA	Messenger RNA
NBM	Neurobasal medium
NF1	Neurofibromatosis Type I
NF2	Neurofibromatosis Type II
NGF	Nerve growth factor
NIH	National Institute of Health
NMD	Non-sense mediated decay
OMGP	Olygodendrocyte-myelin gycoprotein
PBS	Phosphate buffered saline
PH	Pleckstrin homology
PI3K	Phosphatidylinositide 3-kinases
PKA	CAMP-dependent Protein Kinase

PMO	Phosphorothioate morpholino oligomer
PNS	Peripheral nervous system
RNA	Ribonucleic acid
RRM	RNA recognition motif
RT-PCR	Reverse transcription PCR
SCs	Schwann cells
SEM	Standard error of the mean
Skp	Skipping
snRNA	Small nuclear RNA
SRE	Splicing regulatory elements
SS	Splice site
TIA-1	T-cell intracellular antigen 1
TIAR	T-cell intracellular antigen 1 related protein
TSG	Tumour suppressor gene
UBO	Unidentified bright objects
ΔE	Exon skipping

TABLE OF CONTENTS

INTRODUCTION

The Neurofibromatoses

The Neurofibromatoses (NF) is a group of autosomal dominant neurocutaneous disorders that share as a main clinical manifestation, the development of multiple tumors involving Schwann cells or their precursors. Three major forms of NF are recognized as distinct entities: the neurofibromatosis type 1 (NF1), neurofibromatosis type 2 (NF2), and schwannomatosis. All these three forms have a distinct genetic origin and pathogenesis.

The neurofibromatosis type I is caused by mutations in the *NF1* gene and is characterized mainly by the presence of dermal neurofibromas and café-au-lait spots among other clinical manifestations. NF2 is caused by mutations in the *NF2* gene. Most distinctive trait of NF2 is the occurrence of bilateral vestibular schwannoma. As a consequence, about 90% of these patients suffer from hear loss and deafness. In schwannomatosis patients develop cranial and also spinal and the peripheral nerves schwannomas among other lesions (MacCollin M et al., 1996).

Neurofibromatosis type I can be classified in a group of genetic disorders that share alterations in genes involved in the Ras/MAPK pathway (Denayer E et al., 2008). This group, called RASopathies, comprises NF1, LEOPARD syndrome, Noonan syndrome, Costello syndrome and the Legius syndrome among others.

Neurofibromatosis Type I

Neurofibromatosis type 1 (NF1) is an autosomal dominant inherited disease that affects about one in 3,000-4000 individuals worldwide (Huson SM et al., 1989) with a complete penetrance at the age of 8 (DeBella K et al., 2000). Patients with NF1 have clinical manifestations involving many different organs and systems with a highly variable clinical expression even among members of the same family.

Introduction

Clinical aspects of NF1 disease

Neurofibromatosis Type I patients exhibit a variable clinical expressivity. The most frequent clinical manifestations of this disease are the presence of cafe au lait spots on the skin, Lisch nodules (iris hamartomas), and the development of multiple neurofibromas (benign tumors of the peripheral nervous system). During paediatric ages can also develop optic pathway gliomas (benign tumors of the optic nerve) and bone abnormalities. Predisposition to develop peripheral and central nervous system tumors and cognitive problems are the two most burdening clinical manifestations. The diagnostic criteria for NF1 were established by the National Institute of Health (NIH) in 1987 and are still valid today since they were only slightly modified. A patient is diagnosed with NF1 if he/she present two or more of the clinical criteria (summarized in **Table 1**). After approximately 8 years 95-97 % of patients have two or more of the NF1 diagnostic criteria and after 20 years nearly 100 % fulfil clinical criteria (DeBella K et al., 2000).

Diagnostic criteria for NF1 (NIH Consensus Conference, 1987).
Six or more café-au-lait spots of over 5 mm in prepubertal individuals and over 15 mm in postpubertal individuals.
Two or more neurofibromas of any type or one plexiform.
Freckling in the axillary or inguinal regions.
Optic glioma.
Two or more Lisch nodules
A distinctive osseous lesion such as sphenoid dysplasia or thinning of long bone cortex with or without pseudoarthrosis.
A first-degree relative with NF1.

Table 1: NF1 diagnostic criteria according the NIH Consensus conference in 1987**. Adapted from:** NIH, 1988.

The frequency of the different clinical manifestations present in NF1 is summarized in **Figure 1**. **Café-au-late macules** (CALMs) are hiperpigmented lesions caused by the presence of big melanosomes inside the melanocytes. Almost all patients with NF1 have 6 or more CALMs in the first year of life (DeBella K et al., 2000). **Lisch Nodules** are asymptomatic hamartomas of the iris that appear in over 90% of adult NF1 patients. **Optic pathway gliom**as (OPG) or grade I pilocytic astrocitomas occur in about 15% of NF1 patients, which are detected by magnetic resonance imaging (MRI) before 6 years of age (Listernick R et al., 2007). At least 20% of NF1 patients with optic glioma will develop a tumor of the central nervous system (CNS). Sometimes, these tumors experience a very fast growth, causing considerable vision dysfunctions, neurological deficits and endocrine problems (Listernick R et al., 2007).

Bone abnormalities affect the vertebral column, the long bones and the sphenoid. Scoliosis is present in about 10-25% of the patients (Friedman JM & Birch PH, 1997). Other bone alterations are the sphenoid dysplasia and the dysplasia of the long bones, which frequencies are reduced. Pseudoarthrosis is more common in tibia and becomes evident during the first years of life, consequence of bone fractures in the tibia (DeBella K et al., 2000; Friedman JM & Birch PH, 1997) (**Figure 1A**).

One of the major clinical complications of Neurofibromatosis type 1 (NF1) patients is the development of different tumor types that arise in nervous and non-nervous tissues. The peripheral nervous system is particularly affected, with the development of multiple bening dermal neurofibromas (dNFs), bening plexiform neurofibromas (pNFs) and malignant peripheral nerve sheath tumors (MPNSTs). The number of dNFs is highly variable, ranging from tens to thousands of tumors in a single patient. Plexiform neurofibromas affect about 30-50% of NF1 patients,

are thought to be congenital and can affect large regions of tissue since they develop from multiple fascicles or large nerves. dNFs do not progress towards malignancy but certain pNFs transform into MPNSTs. Approximately 8–13% of NF1 patients develop MPNSTs hyperploid soft tissue sarcomas (Evans DG et al., 2002; Huson SM et al., 1989). Bi-allelic inactivation of the *NF1* gene is a key event in tumor initiation for both benign and malignant lesions (Colman et al., 1995; Legius E et al., 1993; Sawada S et al., 1996; Serra E et al., 1997). dNFs and pNFs are composed of different cell types, but only Schwann cells bear a double inactivation of the *NF1* gene (Kluwe L et al., 1999; Maertens O et al., 2006; Serra E et al., 2000) (**Figure 1B**). Due to its invasive growth, propensity to metastasize, and limited sensitivity to chemotherapy and radiation, MPNST has a poor prognosis.

A)

Clinical Manifestation	Frequency (%)
Café-au-laite spots	85
Skin-fold freckling	85
Lisch nodules	90-95
Cutaneous neurofibromas	>99
Plexiform neurofibromas	30-50
MPNST	2-5
Pheochromocytoma	2
OPG	15
Cerebral gliomas	2-3
Pseudoarthrosis of tibia	5
Scoliosis	10-25
Severe Cognitive Impairment (IQ<70)	4-8
Learning problems	30-60
Epilepsy	6-7

B)

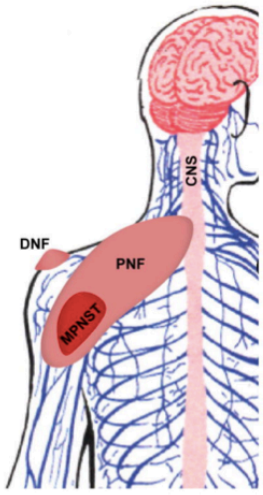

Figure 1: A) Principal clinical manifestations in NF1 patients. In dark grey tumoral manifestations and in light grey non-tumoral manifestations associated with the CNS. **Adapted from:** Ferner R et al., 2006. **B)** Different tumor types associated with the Peripheral Nervous system. DNF: Dermal neurofibroma, PNF: Plexiform neurofibroma, MPNST: Malignant Peripheral Nerve Sheet Tumor. **Adapted from:** Reilly KM, 2009.

Clinical manifestations associated with the CNS

The cognitive and learning impairments are one of the most common complications in children with NF1 and do not improve in adulthood. Between 4% to 8% of NF1 individuals fall into the intellectually impaired range (IQ<70%) compared to the 3% in the general population (North et al., 1997).

Children with NF1 have specific learning difficulties that include visual spatial problems, impaired visual motor integration with abnormal ocular saccades, language deficits, and disorder of executive function. Problems that are typically associated with the NF1 phenotype include attention deficit hyperactivity disorder, which responds to methylphenidate medication and poor socialization. Autistic spectrum disorder has occasionally been associated with NF1, but prospective studies are necessary to assess the frequency of this complication. Academic difficulties and school failure are the most common reported complication of NF1 in childhood and are present in 40% to 60% of the cases (reviewed in Acosta et al., 2006; Ferner et al., 2007; North et al., 1997; Ozonoff S, 1999; Levine et al., 2006).

In NF1 patient's structural brain abnormalities can be found. One of the most common finding is the brain size associated with macrocephaly. Although the studies correlating the brain volume and the cognitive function in NF1 patients are not conclusive, some studies found a positive correlation between the larger corpus callosum volume (the main white matter structure) with the academic underachievement, lower intelligence and the visual spatial impairment (Kayl AE et al., 2000; Pride N et al., 2010). Another frequent brain abnormality is the appearance of unidentified bright objects (UBOs) that had been observed as areas of increased T2-weighted signal intensity on MRI in 50% to 93% of children with Neurofibromatosis 1. It has been suggest that the presence of UBOs can be

connected with the cognitive impairment in NF1 patients (DeBella K et al., 2000b).

Genetic aspects of *NF1*

Structure of the *NF1* gene

The *NF1* gene is located in the pericentromeric region of chromosome 17q11.2 and spans more than 300 Kb of genomic DNA (Li Y et al., 1995; Marchuk DA et al., 1995). It's composed of 61 exons, four of which are alternatively spliced exons: 9a, 10a-2, 23a and 48a, and are mainly expressed in a specific tissues and during the development (Viskochil DM, 1998). Intron 27a contains three genes, Olygodendrocyte-Myelin Gycoprotein (OMGP), Ecotropic Viral integration site (EVI2A and EVI2B) that are transcribed in the opposite direction (Cawthon RM et al., 1991; Viskochil D et al., 1991). Some OMGP gene mutations had been associated with cognitive disturbances, but there is no correlation between this gene and the phenotype observed in NF1 patients (Martin IC et al., 2009).

A high number of pseudogens of *NF1* gene are distributed in different chromosomes, specially around the pericentromeric regions of chromosomes 2,14,15 and 22 (Régnier V et al., 1997).

The *NF1* gene mutational spectrum

Neurofibormatosis type I is a hereditary cancer syndrome (CS). The CS are genetic diseases with Mendelian inheritance that confer a high predisposition to develop cancer. Often hereditary cancer syndromes are caused by germline mutations in tumor suppressor genes (TSGs). The proteins encoded by most tumor

suppressor genes inhibit cell proliferation or survival. At the somatic level, the total inactivation of tumor suppressor genes leads to tumor development by eliminating negative regulatory proteins.

Tumor suppressor genes normally follow the model of double hit proposed by Knudson in 1971, which involves the bi-allelic inactivation of the gene to contribute to tumor formation. Individuals with germline mutations need a second mutation in the somatic cell to induce the tumor to develop (Knudson AG, 1971). The double *NF1* gene inactivation had been reported in various tumours associated with NF1, such as neurofibromas, pNFs, MPNST, juvenile myeloid leukemia (JMML), astrocytomas, among others (revised in De Raedt TM et al., 2008). The double inactivation was also reported in other associated NF1 features like the café-au-laite spots (De Schepper et al., 2008; Maertens O et al., 2007) and pseudarthrosis of the thibia (Stevenson DA et al., 2006).

At the constitutional level, studies regarding *NF1* mutations describe more than 1000 different mutations affecting *NF1* gene (Messiaen L & Wimmer K, 2008). There are no mutational hot spots although some of these mutations have recurrence (Ars E et al., 2003). In *NF1* we can find point mutations, big deletions affecting the whole gene (microdeletions) and exon copy number variations. Deletions that involve the *NF1* gene and surrounding genes represent 5% all mutations (Clementi et al., 1996); exon copy number variation represents 2-5% (Messiaen L & Wimmer K, 2008; Wimmer C et al., 2006) and the rest of mutations (90%) are point mutations (18% missense, 26% frameshit and 21% nonsense). It's important to mention that splicing mutations occur with frequency of 27% in NF1 patients (Messiaen L & Wimmer K, 2008). Most of these splicing mutations affect the canonical splicing sites (GT/AG) but also nonsense, missense or frameshit mutations can have an effect in the splicing process (Ars E et al.,

2000b; Ars E et al., 2003; Messiaen L et al., 2000). Splicing *NF1* mutations can be classified in 5 different groups (Wimmer et al., 2007).

Classification of splicing mutations in *NF1*
Exon skipping resulting from mutations at authentic splice sites (type I)
Cryptic exon inclusion caused by deep intronic mutations (type II)
Creation of de novo splice sites causing loss of exonic sequences (type III)
Activation of cryptic splice sites upon authentic splice-site disruption (type IV)
Exonic sequence alterations causing exon skipping (type V)

Table 2: Classification of the different types of splicing mutations in the *NF1* gene. **Adapted from:** Wimmer K et al., 2007.

Gene expression

The full-length *NF1* mRNA transcript is ubiquitously expressed across a range of tissues, with highest levels in cells and tissues from the central and peripheral nervous system, such as the brain, spinal cord and the peripheral nervous system. The mRNA transcript is about 11-13 Kb in length (Marchuk DA et al., 1991; Xu GF et al., 1990a).

The *NF1* gene can generate five different isoforms. Two of the main *NF1*-isoforms are termed type I and II, and are formed by an alternative splicing of an exon located within the NF1-GRD region (**Figure 2A**). Type II contains an exon of 63-bp (exon 23a) that encodes for 21 amino acids in the center of NF1-GRD region, with a reduced GAP-Ras activity compared to the exon 23a less type I isoform (Andersen LB et al., 1993; Uchida T et al., 1992) (See below: The NF1

protein: neurofibromin). Type I isoform is predominantly expressed in neurons of the adult CNS (**Figure 2B**) (Suzuki Y et al., 1991; Takahashi K et al., 1994).

Several other isoforms have been identified in humans and rodents: the **3' ALT** that includes the alternative spliced exon 48a, the **5' ALT2** that includes the alternative exon 9a, the **5' ALT1** that misses the exons 21 to 27a and the isoform with the alternative exon **10a-2** that is believed haeve a housekeeping function at the intracellular membrane. (Kaufmann D et al., 2002b). The isoform 5' ALT2 is mainly expressed in the central nervous system. It has been found enriched in neurons of the forebrain, specifically septum, striatum, cortex, hippocampus and olfactory bulb. The pattern of *NF1* exon 9a expression correlates with the postnatal maturation of these neurons and suggests a role of *NF1* in neuronal differentiation (Danglot et al., 1995; Geist & Gutmann, 1996).

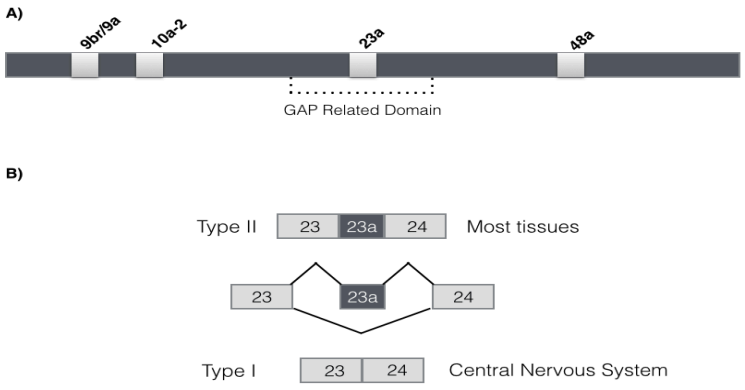

Figure 2: Alternatively spliced exons of the *NF1* gene. **A)** Alternatively-splice exons 9a, 10a-2, 23a and 48a. Exon 23a is located in the GAP related domain. **B)** Type II and Type I isoforms. Exon 23a is included in most tissues and skipped in the central nervous system. **Adapted and modified from:** Barron VA & Lou H, 2012.

RNA studies identified some *NF1* transcripts with an unknown biological function. These transcripts miss some constitutive exons ΔE4b, ΔE7, ΔE8,

ΔE10b, ΔE29, ΔE29/30, ΔE30, ΔE33, ΔE34, ΔE37, ΔE43, ΔE45 (Kaufmann D et al., 2002a; Park VM et al., 1998; Thomson SA & Wallace MR, 2002; Vandenbroucke I et al., 2002a; Vandenbroucke I et al., 2002b) or the insertion of a cryptic exon like the one between the exons 4a and 4b (ins4a-2) (Ars E et al., 2000a). Although some of them are tissue specific, their expression levels are reduced. As an example, the transcript *NF1*- ΔE29 is specific for the brain and cerebellum and the *NF1*- ΔE4b is mainly expressed in blood, heart tissue and cerebellum (Vandenbroucke I et al., 2002b). Different explanations could be that all this plethora of exon-less isoforms represents errors in the process of splicing or that they have a specific biological function at low expression levels.

Phenotype-genotype correlation

Among NF1 patients there is an important variability regarding the different clinical manifestations, even in patients with the same constitutional mutation. This variability in the phenotype cannot be explained only by mutations in the *NF1* gene. Epidemiologic studies suggest the presence of genes that alter the somatic mutation rate or even genes that regulate the splicing mechanism. For example in some cases in patients with the same splicing mutations the variability in their clinical phenotype is explained by a differential expression of aberrant transcripts.

The NF1 protein: Neurofibromin

Neurofibromin is a protein of 2818 amino acids (AA) and 220-280kDa (DeClue JE et al., 1991; Gutmann DH et al., 1991) and the product of the *NF1* gene. It is ubiquitously expressed across a range of tissues, but it's mostly expressed in cells of neurological origin like neurons, Schwann cells and olygodendrocytes (Daston

MM et al., 1992). Neurofibromin is highly conserved among vertebrates with sequence identity commonly > 90% (Bernards A et al., 1993). The yeast *Saccharomyces cerevisiae* has two orthologs of the *NF1* gene, IRA1 and IRA2, whose products have a high sequence identity and homology with neurofibromin and that have been demonstrated to participate in Ras and cAMP dependent pathways (Buchberg AM et al., 1990; Xu GF et al., 1990b).

The NF1 GAP-Related domain and RAS

In its central region (aa 1205-1536) neurofibromin contains a small domain (GAP-related domain, GRD) with a high sequence similarity to the GTPase activating protein (RasGAP) family (Martin GA, et al. 1990). The structure of the GRD consists in a central catalytic domain GAP and an extra domain called GAPex. The structure is similar to the catalytic domain of the p120GAP (Martin GA, et al. 1990).

Ras proteins are a group of small GTPases that regulate cell growth, proliferation and differentiation. Ras is activated by guanine nucleotide exchange factors (GEFs) that release GDP and allow GTP binding. GTPase activating proteins (GAPs) terminate Ras signalling by stimulating intrinsic GTPase activity. Neurofibromin acts a negative regulator of Ras signalling. This protein downregulates the biological activity of the small guanine nucleotide binding protein (GNBP) Ras increasing the hydrolysis of Ras-bound GTP, the active form of Ras. Active GTP-bound Ras interacts with several downstream effector proteins: Raf kinases, Ral-GDS, phosphatidylinositol 3-kinase (PI3K)/Rac/Rho and PI3K/Akt/mTOR (Castellano E & Downward J, 2011) (**Figure 3**).

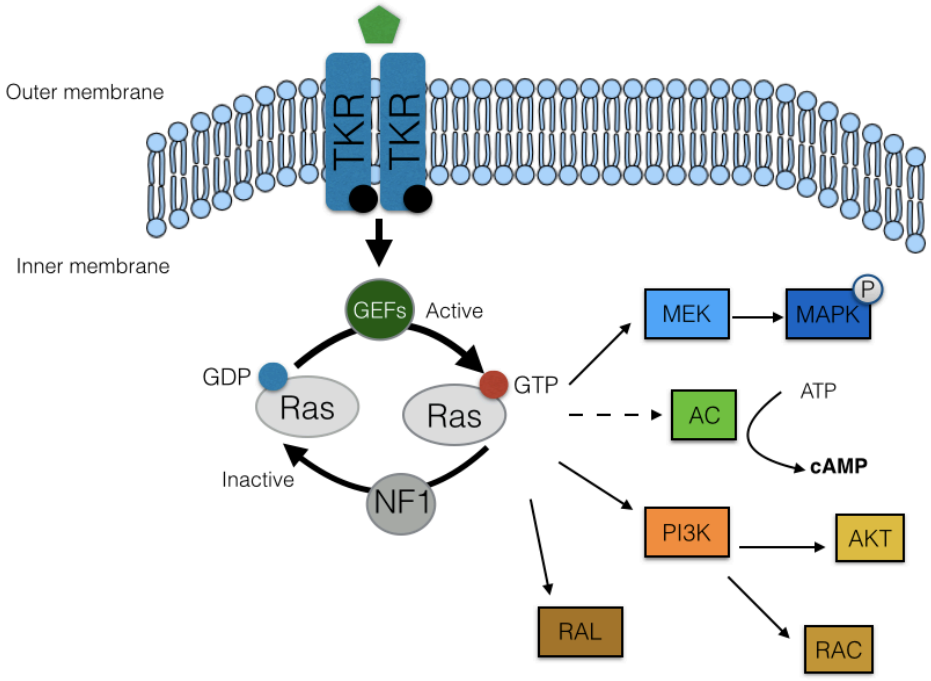

Figure 3: Schematic representation of Ras regulation by neurofibromin and its downstream signalling pathways. **Adapted and modified from:** Diggs-Andrews KA & Gutmann DH, 2013.

Alternative splicing is important to regulate cellular activity of some proteins. In the case of NF1 the biochemical analysis of both isoforms (with or without E23a) indicated a tenfold lower GAP activity for the type II transcript. It is still unclear how this biochemical difference translates at the physiological level (**Figure 4**).

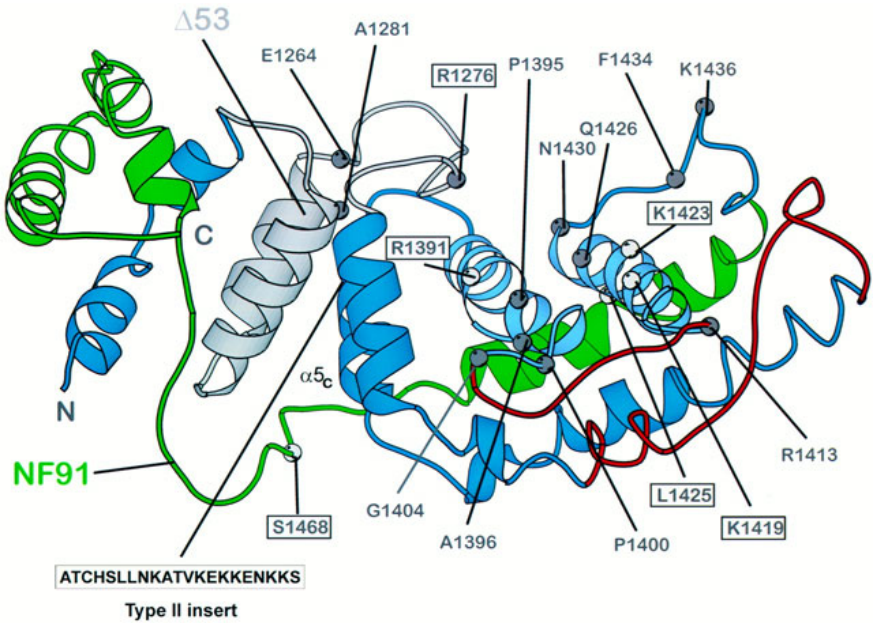

Figure 4: Ribbon representation of the GAP Related domain (GRD). The representation shows the different missense mutations identified in NF1 patients in the GRD, and the position of exon 23a insertion. **Adapted from:** Scheffzek K et al., 1998.

The SEC14-PH and other neurofibromin domains

Recently, structural analyses have identified a Sec14 homologous segment (N-terminal) and an adjacent pleckstrin homology (PH)-like domain (C-terminal), a bipartite module (aa 1560-1816) that allow neurofibromin to bind to membrane phospholipids (D'Angelo et al., 2006).

Sec14-like domains have been found in a number of lipid binding proteins such as α-tocopherol transferprotein (αTTP) and supernatant protein factor (SPF) (Stocker A, 2004) and also in several signal regulatory proteins including Rho specific guanine-nucleotide exchange factors (RhoGEFs), RhoGAPs, RasGAPs and phosphotyrosine phosphatases (PTPases) and neurofibrin (Phillips SE et al., 2006). They commonly bind lipid ligands. The Pleckstrin Homology (PH) portion of this bipartite module is involved in membrane recruitment process and they can

promote the binding to specific proteins. Apart of these domains, it has been postulated the existence of other domains identified by sequence analysis of neurofibromin: the **CSRD** domain (aa 543-909), rich in serine and cysteine residues, which contains multiple phosphorylation sites for protein kinase cAMP dependent (PKA) (Izawa I et al., 1996); the **LRD** domain (aa 1530-1950) rich in leucine repeats and the **CTD** domain (aa 2260-2818) containing three sites of phosphorylation for PKA and two for MAPK. (Izawa I et al., 1996; Tokuo H et al., 2001).

Neurofibromin regulation and function

Although the best characterized biochemical function of neurofibromin to date is the GAP-RAS activity, there is also experimental evidence, mainly obtained using *Drosophila melanogaster* as a model, that indicate a role of neurofibromin in regulating cyclic AMP-dependent signalling pathways, although the responsible mechanisms have remained elusive. Adenylate cyclase synthesizes cAMP from ATP which in turn activates PKA, that then phosphorylates several proteins, involved in different biological processes. Activation of AC through neurofibromin could be possible in different ways: one dependent on RAS-GAP and the GRD domain, and the other one by regulating the subunit of $G\alpha_s$ of G heterodimeric proteins (Hannan F et al., 2006). Neurofibromin has been associated with three cytoskeletal elements: microtubules (tubulin) (Bollag G et al., 1993), microfilaments (actin) (Li C et al., 2001), and filamentous keratin. Moreover, interaction between the amyloid precursor protein (APP) and the GRD was identified (De Schepper S et al., 2006). APP has been proposed as a vesicle cargo receptor for kinesin-1 in neurons and melanocytes. Interaction with caveolin-1 has been reported and it's implication in modulating Ras, AKT and focal adhesion kinase (FAK) (Boyanapalli M et al., 2006) (**Figure 5**).

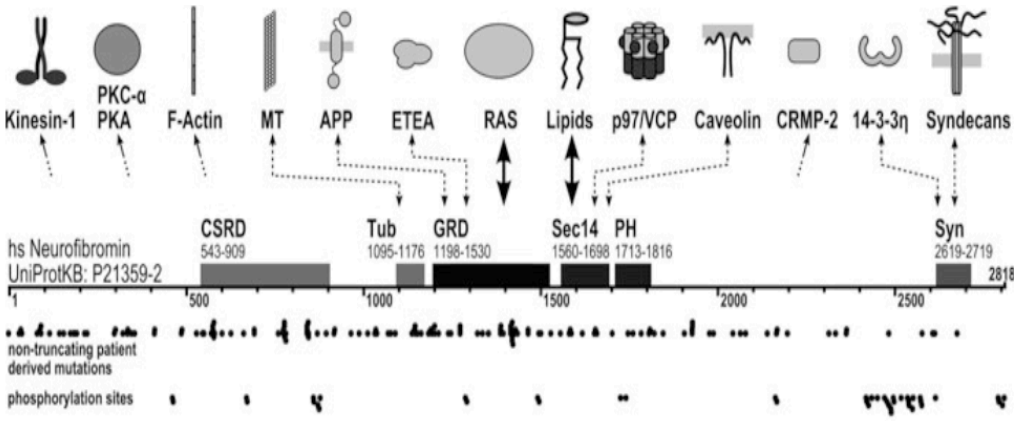

Figure 5: Scheme of neurofibromin domains and all reported interaction partners. The putative phosphorylation sites and the position of non-truncating mutations identified in patients are indicated with black dots. **Adapted from:** Scheffzek K & Welti, 2012.

Neurofibromin interacts also with collapsin response mediator protein-2 (CRMP-2) and collapsin response mediator protein-4 (CRMP-4) in rat brain. These interactions with CRMPs suggest a possible contribution of neurofibromin in tumorigenesis and neuronal morphogenesis (Lin Y & Hsueh Y, 2008) (**Figure 5**).

Molecular and cellular pathogenesis of cognitive and learning impairments in NF1

NF1 animal models to study human cognitive symptoms

Animal models have played a role in understanding the molecular and cellular mechanisms associated with NF1. In order to study NF1, mice with heterozygous null mutations in the *NF1* gene (*NF1* $^{+/-}$) were generated. These mutants show cognitive deficits similar to the ones observed in humans. Since neurofibromin is

a negative regulator of Ras signaling, increases in Ras activity and MEK/ERK have been detected in the hippocampus and cortex of *NF1* $^{+/-}$ mice (Li W et al., 2005). In addition, the spatial learning defects observed in *NF1*$^{+/-}$ mice were rescued with an inhibitor of the Ras signalling, a Farnesyl transferase inhibitor (FTI) (Costa RM et al., 2002). Similar results were obtained with Lovastatin that reduce RAS signalling, with the isoprenylation of Ras. Lovastatin rescued the water maze *NF1*$^{+/-}$ mice and their deficits in attention. The studies using *NF1*$^{+/-}$ mice showed a possible correrelation between the long-term synaptic plasticity specifically in hypoccampus and spatial learning and memory (Li W et al., 2005). Evidences show that increased Ras signaling results in an increased GABA-mediated inhibition in *NF1*$^{+/-}$ mice (Cui Y et al., 2008).

The role of Neurofibromin as a positive regulator of adenylate cyclase (AC) was also studied with *NF1* null Drosophila mutants. These mutants showed a reduced AC activity and deficits in olfactory learning. This phenotype was rescued by the expression of rutabaga a constitutively active AC (Guo HF et al., 2000). The relationship between the AC-PKA signaling with the cognitive deficits is unclear, but in *NF1*$^{+/-}$ mice hippocampal and retinal ganglion neurons decreased the growth cone area and neurite length and increased apoptosis. The phenotype was reversed elevating the cAMP levels (Brown J et al., 2010; Brown J et al., 2012).

In order to determine the role of the isoform type I (*NF1* exon 23a), Costa and collaborators (Costa RM et al., 2001) generated a mutant mouse harboring a homozygous deletion in exon 23a. The results showed behavioral impairments without any other alteration, such as tumor formation. This study suggests the possible relation between the *NF1* signaling via RAS/MAPK pathway and the learning defects observed in patients.

The alternative splicing

The splicing process is a post-transcriptional event in which introns are removed from the pre-mRNA and exons joined in the mRNA. This process takes place in the nucleus. Once the mRNAs are produced, they are transported to the cytoplasm and translated by the ribosomes.

In order to leave the nucleus, the mRNA must pass through the double lipid bilayer of the nuclear envelope. The mRNA protects and identifies itself by adding two nucleotides sequences in both ends of the strand. During the RNA processing, a specialized methyl-guanine nucleotide (CAP) is added to the 5'end. This CAP sequence protects the mRNA from degradation and facilitates binding with the ribosome. To the 3' end is added a long chain of adenine nucleotides called Poly(A) tail, that protects from the degradation.

Recognition splice sites and other splicing sequences

Consensus splice sites

Generally, introns start from a GU dinucleotide sequence and end with an AG sequence. They are called as donor and acceptor site, respectively. Another important sequence within the intron is the branch site located 20 - 50 bases upstream of the acceptor site. The consensus sequence of the branch site is CU(A/G)**A**(C/U), where the adenosine (A) is conserved in all genes. These sequences are important for correct identification of the exons and the selection of the splicing sites. There is also a polypyridmidine rich region located between the 3' splice site (ss) and the branch site (**Figure 6**).

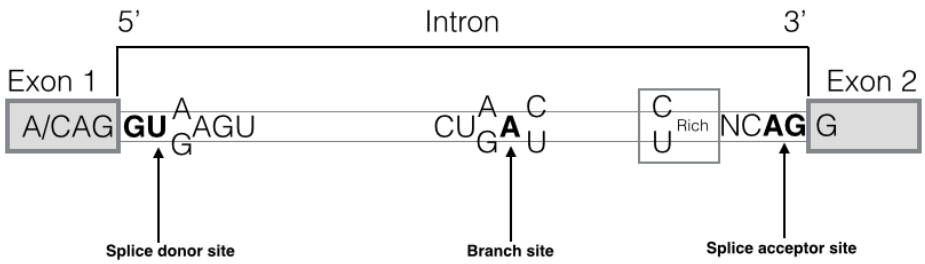

Figure 6: The consensus sequence for splicing. In bold are shown the consensus splice sites, the 5' donor site and the 3' acceptor site and the surrounding conserved regions respectively. The branch site with the conserved adenosine (A) is located Between 20-50 bp upstream of the 3' acceptor site.

Splicing regulatory elements and associated factors

There are other *cis* regulatory elements that help the splicing machinery to regulate the splicing process. These elements are classified in two groups; the exonic splicing enhancers (ESEs) or silencers (ESSs), that promote or inhibit the inclusion of the exon they reside in, and the intronic splicing enhancers (ISEs) or silencers (ISSs), that enhance or inhibit usage of adjacent splice sites or exons from an intronic location. These splicing regulatory elements (SREs) function by recruiting *trans*-acting splicing factors that activate or suppress splice site recognition or spliceosome assembly (Ast G, 2004; Chen M & Manley JL, 2009; Matlin AJ et al., 2005).

The enhancer elements ESEs and ISEs are cis-acting RNA sequences that contain binding sites for SR family proteins. These proteins are required for both constitutive and regulated splicing, with a modular structure that contains at least

two N-terminal RNA recognition motif (RRM) and a C-terminal arginine/serine rich domain. The SR act as a positive regulators of the splicing (binding to the ESE through the RRM domain), and also they can distinguish between authentic exons and pseudo-exons and inhibit the action of close silencer elements (Chen M & Manley JL, 2009; Matlin AJ et al., 2005).

The splicing silencers (ESSs and ISSs) are cis-acting RNA elements on which complex bind members of heterogeneous nuclear ribonucleoproteins (hnRNPs), a group of more than 20 proteins. These proteins contain a RRM and a KH-type-RNA-binding domain and an alternative auxiliary domain for protein-protein interaction. hnRNPs proteins act as negative regulators of splicing by inhibiting the splicing process by interfering with the spliceosome and the SR proteins (Chen M & Manley JL, 2009; Matlin AJ et al., 2005).

The splicing process

The RNA splicing process is performed by small nuclear RNAs (snRNAs) that recognize the intron-exon boundaries. These molecules snRNAs are five (U1, U2, U3, U4, U5 and U6) and they are involved in the splicing of the majority of pre-mRNA. Each of them is complexed with at least seven protein subunits to form a small nuclear ribonucleoprotein (snRNP). This assembly of RNA and protein molecules form the spliceosome complex.

The splicing process occurs in two consecutive transesterification reactions. In the first one, the adenosine residue of the branch site induces a nucleophilic attack on the 5' ss generating two intermediates; a free exon and a lariat-exon. In the second step, OH group left by the nucleophilic attack of the exon located at the 5' SS attacks the phosphoryl group at the 3' ss to generate the ligated spliced exons and the lariat intron (Baralle M & Baralle D, 2012) (**Figure 7**).

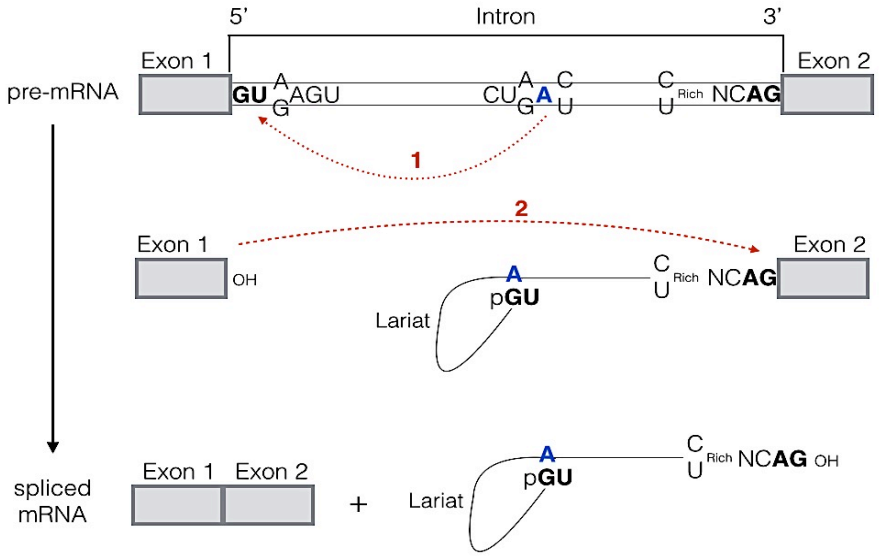

Figure 7: Schematic representation of the splicing reaction with the two consecutive transesterification reactions. In the step 1) the adenosine residue of the branch site carries out a nucleophilic attack on the 5' splice site, generating a free 5' exon 1 and the lariat-exon 2 complex. 2) Exon 1 (free OH left at 5'ss) attack the 3'ss splice site of the next exon to generate the ligation of both exons at the lariat intron.

Regulation of exon 23a alternative splicing of the *NF1* gene

Usually alternative exons are under specific regulation with different protein factors. Exon 23a is regulated by different regulatory elements and factors in a cell-type dependent way. Two families of proteins act as negative regulators by promoting exon 23a skipping. These two families are the Hu and the CELF proteins. There are four members in the Hu protein family, HuR , HuB, HuC and HuD while for the CELF proteins, there exist six members: CUG-BP1, ETR-3, CELF3, CELF4, CELF5 and CELF6 (Zhu H et al., 2008 ; Barron VA et al., 2010). It's important to mention that these families are brain-specific (Ladd AN, 2012), where as we mention previously exon 23a is skipped (Type I).

Exon 23a inclusion is enhanced by two families of proteins, the TIA-1/ TIAR and MBNL family (Fleming VA et al., 2012). These two families are widely expressed. It had been demonstrated that TIA-1/ TIAR proteins bind to AU-rich sequences (functioning as ISE) flanking both sides of the exon, and promoting exon 23a inclusion by binding U1 and U6snRNPs to the 3'ss. The Hu proteins bind to the AU-rich sequences competing for the binding sites with TIA-1/TIAR proteins (Zhu H et al., 2008). This competition is resolved depending on the final balance of the different factors present in a particular tissue (Baralle M & Baralle D, 2012; Barron VA & Lou H, 2012) (**Figure 8**).

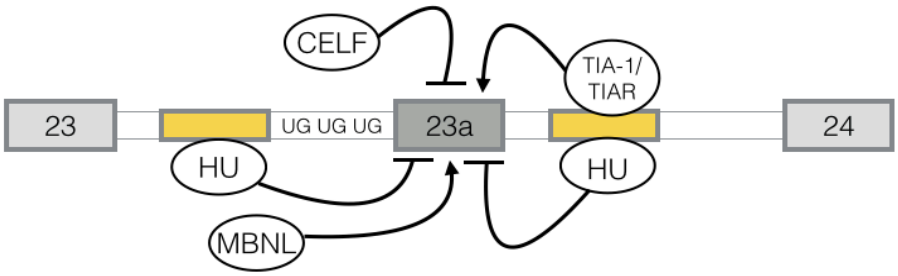

Figure 8: Schematic representation of the exon 23a splicing regulation. Constitutive exons 23 and 24 are shown in light grey boxes and alternatively-splice exon 23a is shown as a dark grey box. Splicing factors are shown in circles. HU proteins and CELF proteins promote the skipping of exon 23a by binding the intronic splicing silencers elements (yellow boxes) and the UG-rich upstream elements respectively. TIA-1, TIAR proteins and MBNL family promote exon 23a inclusion. **Adapted from:** Barron V & Lou H, 2012.

Antisense Oligonucleotides

The term antisense oligonucleotides (AONS) defines a group of oligonucleotide analogues (13–25 nucleotides) and other sequence-specific binding polymers that

are designed to block the translation of selected mRNAs and control normal splicing events. Antisense oligonucleotides constitute one of the most promising advances in the treatment of intractable disease.

First generation of AONS were used to silence gene expression based on RNase H cleavage of their targeted RNA. After that, next class comprised agents that function by a steric blockage mechanism, independent of the RNase H activity. With this steric blockage AONs are capable to block promotor elements, inhibiting gene expression or interfere with splicing process by blocking splicing regulatory elements and associated factors (Morcos PA, 2007; Summerton JE, 2007).

Regarding steric block AONs; one of the main concerns regarding the design of the sterick bloackage AONs is the degradation by the intracellular endonucleases and exonucleases. In order to avoid this degradation, different chemical strategies have been used for AON design and synthesis, including the 2'-O-methyl phosphorothioate (2'OMe), locked nucleic acids (LNA), petide nucleic acids (PNA) and the phosphorodiamidate morpholino oligomers (PMOs).

Phosphorodiamidate Morpholino Oligomers (PMOs) and delivery vehicle

PMOs are non-ionic DNA analogs available from Gene Tools LLC, where a morpholino ring replaces the deoxyribose backbone and an uncharged phosphorodiamidate linkage replaces the charged phosphodiester intersubunit linkage (**Figure 9**). Each morpholino ring is properly positioned with each of the DNA bases (A, C, G, T), so that a 25-base PMO specifically binds to its complementary strand of RNA via Watson-Crick pairing. Morpholino ring makes also PMOs more resistant to the nucleases. Moreover, the negative charge of the

backbone confers less interaction with cellular proteins or enzymes (Summerton J & Weller D, 1997).

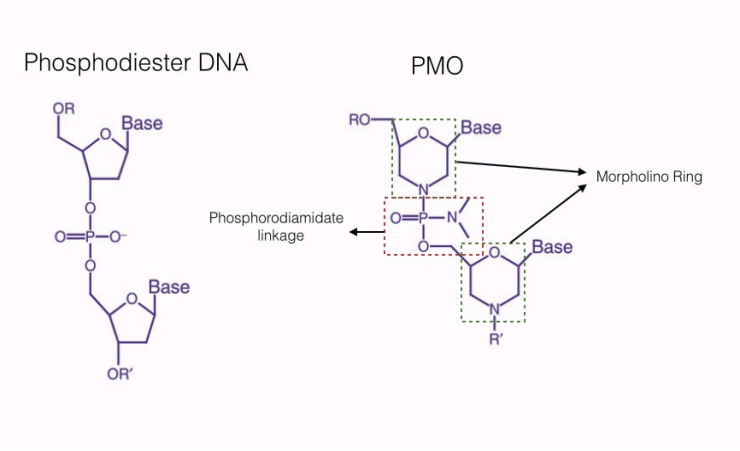

Figure 9: Structures of DNA and PMO. In green the Morpholino ring replacing the deoxyribose backbone and in red the phosphorodiamidate linkage. **Adapted from:** Corey DR & Abrams JM, 2001.

The PMOs are designed to specifically bind to its selected target site and block the access of cell components. This property can be used to block translation, splicing, miRNAs and the ribozyme activity at the cellular level. In this project we were interested in the use of PMOs as a splice-blocking tool, by blocking sites involved in splicing pre-mRNA with the final goal to modify and control the cellular splicing events.

An important feature of PMO efficiency is the method used to deliver them inside the cell. PMOs can be delivered into cultured cells by different transfecting methods. However, Endo-Porter (EPEI) reagent gives excellent efficiencies in cultured cells. EPEI is a weak-base amphiphilic peptide, designed to deliver PMOs into the cytosol and nuclear compartment by endocytosis-mediated process, preventing the damage to the cell membrane. This mechanism prevents

cell toxicity associated with the classical delivery systems (Morcos PA, 2001; Summerton JE, 2005).

Functional applications of PMOs: Splicing modulation

The uses of AON-mediated therapies to restore gene function by modulating aberrant splicing have been increasing in the last few decades. The first studies to use AONs as therapeutic tools for genetic diseases were obtained in B-thalassemia. In this case an abnormal splicing event caused by activation of cryptic sites was corrected with the use of AON technology (Dominski Z & Kole R, 1993). Since then a progressive number of reports applied the AON technology to modulate splicing events in different diseases like the cystic fibrosis, Duschenne Muscular dystrophy (DMD), NF1, NF2, the Hutchinson-Gilford syndrome among others.

As mentioned above, PMOs are good therapeutic agents to modify and control cellular splicing events by blocking sites involved in splicing pre-mRNA. In that sense, the most promising advances have been done in the treatment of DMD. DMD is caused by mutations that disrupt the reading frame of the human DMD gene, generating a lack of functional distrophyn protein in skeletal muscles. Selective removal of exons flanking these mutations can result into a restoration of the reading frame and thus of dystrophin expression, in both *in vitro* DMD patient cells and also *in vivo* animal models. In dystrophin-deficient mouse (mdx) model of DMD, PMOs were use to target the skipping of exon 23 after intramuscular injection. Results showed excellent safety profiles and consistent and sustained exon skipping levels. On the other hand, in DMD patients, due to the existence of mutational hot spots for example exon 51 skipping would have

the potential capacity to treat 13% of DMD cases, and already there are some clinical trials based on this principle (Popplewell L, 2012; Wang Q et al., 2010).

Regarding NF2 disease, about 25% of the point mutations affect the correct splicing of the *NF2* gene (Selvanathan et al., 2010; Kluwe et al., 1997, Evans DGR, 2009). One particular type of these mutations are the deep intronic mutations. A mutation-specific PMO was designed and used *in vitro* to restore normal NF2 splicing in patient's fibroblasts. In addition, merlin (*NF2* protein) levels were recovered after PMO treatment (Castellanos E et al., 2012).

As mentioned before, splicing mutations occur with a frequency of 27% in NF1 patients (Messiaen L & Wimmer K, 2008), that provides a unique opportunity towards the utilization of splicing therapeutic approaches based on PMO technology. Although many of them will be difficult to restore using PMOs, those affecting splicing and located inside introns are the best mutation types to be faced by PMO treatment. In this context, three different *NF1* deep intronic mutations (c.288+2025T>G, c.5749+332A>G, and c.7908-321C>G) were identified in our lab. All these mutations created novel donor splice sites, causing pathogenic inclusion of cryptic exons in the mRNA. In order to inhibit and prevent their inclusion, PMOs were targeted against these new donor splice sites and the normal splicing of the *NF1* gene was restored *in vitro* using different patient-derived primary cells (Pros E et al., 2009). A fourth mutation generating a cryptic acceptor site (c.3198 - 314G>A) was also detected in another patient and corrected using specific PMOs (Fernández-Rodríguez J et al., 2011) (**Figure 10A**). In conclusion, both studies showed that PMO treatments were durable and specific, had an impact on the function of neurofibromin, and opened a new door to the possibility of therapeutic strategies for this type of mutations, or to modify at will the alternative splicing of the *NF1* gene (**Figure 10B).**

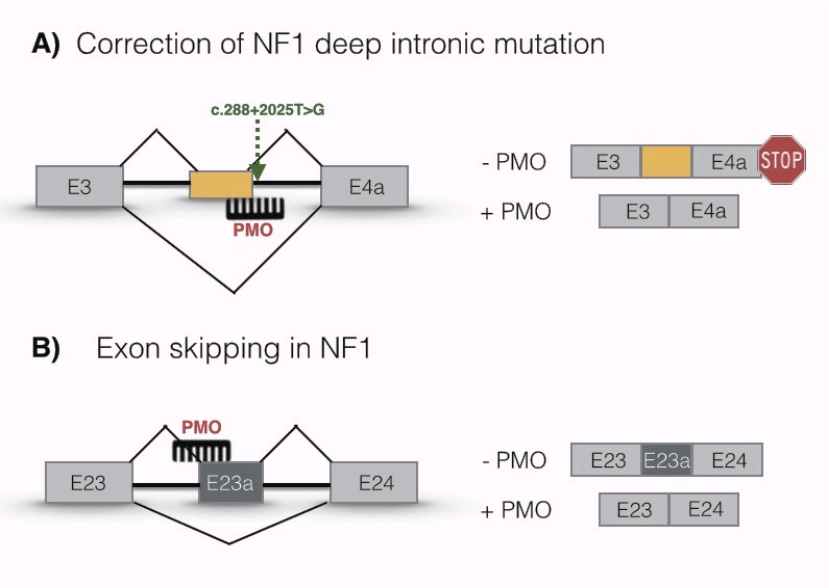

Figure 10: A) Schematic representation of a deep intronic mutation (c.288+2025T>G) and the PMO designed to avoid the inclusion of the resulting cryptic exon (yellow). **Adapted from:** Fernández-Rodríguez J et al., 2011. **B)** Schematic representation of exon 23a skipping modulation by the use of PMOs targeting the acceptor site.

Cellular models to study central nervous system

Homogeneous cultures of neuronal cells are challenging since mature neurons do not undergo cell division. In order to overcome these limitations a group of immortalized cell lines have been established derived from neuronal tumors. These cell lines have the advantage of being able to expand easily *in vitro* and provide with a rather homogeneous cell culture. A good example is the PC12 cell line, generated from a rat adrenal medullary pheochromocytoma. The use of this cell line allowed for instance a better understanding of neurodegenerative diseases and neurotoxicology.

PC12 cell line as a neuronal model system

PC12 is a cell line derived from rat adrenal medullary pheochromocytoma (a tumor from the adrenal gland) that can be stimulated to differentiate into sympatethic-like neurons in the presence of neurotrophic factors like nerve growth factor (NGF) (Greene LA & Tischler AS, 1976). In the presence of serum, PC12 cells acquire a round morphology and proliferate to high density. In contrast, in the presence of NGF, PC12 cells undergo a neuronal differentiation process by stopping cell division, promoting the extension of neurites, becoming electrically excitable (Das et al., 2004) and increasing the synthesis of several neurotransmitters like acetylcholine or γ-amiinobutyric acid. In addition to NGF, the differentiation of PC12 can be induced by other factors such as cytokines and basic fibroblast growth factor (bFGF), cell adhesion proteins like NCAM or N-Cadherin 1 and drugs like cholera toxin or potassium (Doherty P et al., 1992; Gunning PW et al., 1981).

A different number of metabolic changes have been observed during differentiation process; the enzymatic activity of lactate dehydrogenase (LDH) is down-regulated and NADH-dehydrogenase activity is increased during differentiation (Ohuchi T et al., 2002). The expression of neuronal markers is increased during this biological process, such as B-Tubulin III (*Tubb3*), Neurofilament (*Nefl*), *Gap43*, Synapsin I (*Syn1*), *Mmp3*, *Dusp6* (Das KP et al., 2004; Ohuchi T et al., 2002).

PC12 neuronal model is particularly useful to study neurite outgrowth, the process in which neurons promote extensions during development, in order to establish neuronal connections. In PC12 growing-neurites, characteristic morphological features can be observed. For instance, the presence of large

varicosities containing catecholamines that are involved in the process of neurite outgrowth or the presence of growth cones containing filopodia and lamellipodia in the distal end of neurites. These growth cones are used by PC12 cells for sensing the environment and guiding neurite extension (Mingorance-Le Meur A et al., 2009).

RAS/MAPK pathway in PC12 differentiation

The Ras/MAPK pathway is highly conserved through evolution and plays an important role in different cellular processes, like cell proliferation, differentiation or survival. In PC12 cells, the use of epidermal growth factor (EGF) induces a transient ERK activation and cell proliferation. In contrast, NGF induces differentiation through TrkA receptor, by a sustained activation of ERK/MAPK pathway via Ras family proteins (Kaplan DR, 1998). Neuronal differentiation by NGF is characterized by the expression of early transcription factors that promote a secondary activation of NGF-responsive genes. But still the molecular mechanisms behind that process are not completely understood (Brightman FA & Fell DA, 2000; Marshall CJ, 1995; Vaudry D et al., 2002).

The learning and memory defects observed in NF1 knockout mice studies indicated that functional modulation of Ras pathway was essential and that neurofibromin plays an important role as a GAP in neuronal cells. In PC12 cells was observed that regulation of Ras and NF1-GAP was essential for normal neuronal differentiation and that regulation of alternative splicing through exon 23a may be important in modulating Ras-related neuronal functions (Hinman M et al., 2014; Metheny LJ & Skuse GR, 1996; Yunoue S et al., 2003).

Other neuronal model systems

Although PC12 cells are one of the best-characterized neuronal differentiation systems to date, one of the major problems is that the genes leading to immortalization and transformation have not been identified. This provides the necessity to find other possible neuronal differentiation models, in order to study more in detail the central nervous system neurons.

The H19-7 cell line

The H19-7 cell line was derived from early embryonic day (E17) rat hippocampal cells and conditionally immortalized by retroviral transduction of temperature sensitive tsA58 SV40 (SV from simian virus) large T antigen. In general, H19-7 cells provide a good model for neuronal differentiation of central nervous system neurons. Similarly to PC12 cells, H19-7 cells respond differentially to EGF and FGF. At the permissive temperature (33ºC), EGF treatment induces proliferation, whereas at the nonpermissive temperature (39ºC) addition of bFGF induces differentiation.

H19-7 cells exhibit specific expression of neuronal markers (NFP, MAP-2 and GAP43) in the differentiation conditions (Eves EM, 1992). Moreover, the importance of hippocalcin in the signalling pathway of bFGF-induced neurite outgrowth was demosntreated. Suppression of hippocalcin results in an inhibition of neurite outgrowth and provides evidences that this protein could be the target of the signalling pathway of bFGF (Oh D et al., 2008). On the other hand, the ERK1/2 are early expressed and phosphorylated in differentiating H19–7 cells. However, in comparison with PC12, in H19-7 cells this process is not sufficient for neuronal differentiation and the activation of the upstream signalling component, Raf is necessary (Kuo WL et al., 1996).

Introduction

One of the major problems with H19-7 cell cultures are the high levels of apoptosis when cells are induced to differentiate at 39ºC in the presence of bFGF. In presence of this factor H19-7 cells undergo apoptosis by a Fas-independent mechanism by activation of a TNFα death pathway (Eves EM et al., 2001). Moreover, recent reports suggest that lysophosphatidic acid (LPA) is involved in the suppression of apoptosis in differentiating H19-7 cells by activation of β-catenin/TCF signalling pathway (Sun Y et al., 2013).

OBJECTIVES

Objectives

The role of neurofibromin, the product of the Neurofibromatosis Type 1 (NF1) gene, in cell physiology is still not well understood. Considering the different traits associated to NF1 it is clear that neurofibromin participates in processes of proliferation and differentiation of different cell types. The Ras-GAP activity of neurofibromin is its best characterized biochemical function, a function that is regulated by the alternative splicing of exon 23a. In this thesis we intended to better understand the role of alternative splicing of exon 23a during neuronal differentiation, with the aim that in the future it could provide information on the learning and cognitive issues related to this disease.

Due to the large size of neurofibromin, the difficulty of manipulating it *in vitro* and the necessity to mimic, as much as possible, the physiological conditions of the cell, we proposed to use Phosphorodiamidate Morpholino oligomers (PMO) as an oligonucleotide antisense technology to modify the exonic composition of *NF1* mRNA while preserving the endogenous neurofibromin expression levels.

The objectives of this thesis are:

1. To develop a system, based on the use of antisense oligonucleotides (PMOs) to modify at will the alternative splicing of exon 23a of the *NF1* gene, without altering its endogenous physiological expression.

2. To set up a group of functional assays for assessing proliferation, differentiation and signaling in two cell-based differentiation model systems.

3. To study the role of the alternative splicing of exon 23a in two different models of neuronal differentiation using PMOS.

Objectives

4. To compare the effect of modifying the alternative splicing of exon 23a on neuronal differentiation with the effect caused by a knockdown of neurofibromin using PMOs.

5. To better understand the function of neurofibromin in the RAS/MAPK and cAMP/PKA pathways during the process of neuronal differentiation.

MATERIALS AND METHODS

Cell culture

Cell lines

The cell lines used in the project are described in the **Table 3**. We had 2 cell lines as neuronal models and one control human cell. Most of these cell lines are commercially available in the American Type Culture Collection (ATCC).

Name	Origin	Species	Culture Medium
PC12	Adrenal Gland	Rat	RPMI 1640
H19-7	Brain/Hippocampus	Rat	DMEM
293T	Kidney	Human	DMEM

Table 3: List of cell lines used in the thesis project, their cellular origin, species and culture medium without supplements.

Cell culture medium and solutions

Cell culture medium:

Dulbecco's Modified Eagle Medium (DMEM): DMEM High Glucose with sodium pyruvate (Biowest). Supplemented with L-glutamine (Gibco) and Penicillin Streptomycin (Gibco).

Roswell Park Memorial Institut Medium (RPMI 1640): RPMI 1640 (Biowest). Supplemented with L-glutamine (Gibco) and Penicillin Streptomycin (Gibco).

Schwann Cell medium (SCM): DMEM (Gibco), with 10% FBS (Gibco), 500U/ml penicillin/streptomycin (Gibco), 0.5mM 3-iso-butyl-1-methilxantine

(IBMX, Sigma), 2.5 μg/ml insulin (Sigma), and 10 nM b1-heregulin (Peprotech).

SCM+Fo: SCM with 0.5μM forskolin (Sigma).

Cell culture solutions:

Freezing medium: 10% DMSO (Sigma-Aldrich), 40% FBS (Biowest) and 50% Cell culture media (DMEM, RPMI).

Parafromaldehyde 4%: Paraformaldehyde dissolved in hot water (60ºC) and diluted with PBS.

Antibody S100: Polyclonal rabbit anti-cow S100, Dako. Dilution 1:1000 in PBS-FBS 10%.

1x Trypsin working solution: 5ml of 0.5% Trypsin-EDTA (10X) in Phosphate-buffered saline (PBS) (Biowest).

Cell culture experimental procedures

PC12 Coating: Filtered Collagen IV (25 ug/ml) (Corning) was added to tissue culture dishes and incubated at RT. After 1h, plates were washed two times with sterile PBS. Cultures were maintained at 37 ºC in a 95% with 5% CO_2.

PC12 cell medium: For proliferative conditions PC12 cells were cultured in RPMI medium supplemented with 10% fetal bovine serum (FBS). For the induction of differentiation, the medium was replaced with 1% FBS-RPMI medium, supplemented with 50 ng/ml NGF (Promega). Cultures were maintained at 37 ºC with 5% CO_2.

H19-7 Coating: Filtered Poly-L-Lysine (0.1 mg/ml) (Sigma-Aldrich) was added to tissue culture dishes and incubated at RT. After 10 min, plates were washed two times with sterile PBS.

H19-7 cell medium: Cells were maintained in DMEM supplemented with 10% fetal bovine serum, 200 mg/ml of G418 (Calbiochem) (selection for the T antigen plasmid) and 1 mg/ml of puromycin (selection for the IGF-IR) (Sigma-Aldrich) at 33 ºC with 5% CO_2. For differentiation experiments, H19-7 cell lines were washed extensively and shifted to the no-permissive temperature of 39ºC with 5% of CO_2 in 1X N2 (Calbiochem) DMEM medium and 10 ng/ml bFGF (Invitrogen).

Schwann cell culture (SC +/-): Primary Schwann cells previously isolated in our lab from an NF1 patient nerve biopsy, were thawed and cultured on plates coated with Poly-L-Lysine (0.1mg/ml) and laminin (4μg/ml) in SCM+Fo medium, and were incubated at 37°C and 10%CO_2. The next day, medium was replaced by SCM for 2-3 days. For proliferative conditions, cells were cultured in SCM+Fo medium for 1 day, and replaced with SCM for 2-3 days, repeting this process in cycles (1day SCM+Fo, 2-3 days SCM, 1day SCM+Fo, …). For differentiation conditions, cells were cultured with SCM+Fo constantly for 5 days. At this point, cells were harvested for protein extraction.

Purity evaluation of neurfibroma-derived Schwann cells by S100 staining: The S100 proteins are a family of low-molecular-weight proteins normally present in cells of peripheral nervous system, especially in SCs. Immunofluorescence for S100 was performed as follows: cells grown on a glass coverslip were washed with PBS and fixed with 4% paraformaldehyde for 15 minutes at RT. After two consecutive washes with PBS, cells were permeabilized with PBS/Triton-X 0.1% for 10 minutes at RT. Cells were washed and blocked with one PBS/FBS 1 % and one PBS/FBS 10% wash. Cells were incubated with 100 uL of primary antibody under a coverslip for 1h at RT. Cells were washed three times with PBS/FBS 1%. Secondary antibody (anti-rabbit) was incubated for 45 minutes at RT. After three washes with PBS/FBS 1%, coverslips were dried on a filter paper and mounted

with Vectashield containing DAPI. Cells were visualized on an inverted microscope (Leica DMI 6000B).

Trypsinization: The culture media was removed and the layer of cells was washed with sterile PBS. Pre-warmed trypsin (37ºC) was added to cover the cell layer, and the plate was incubated at 37ºC for 5 minutes. Cell suspension was centrifuged at 1200g for 5 minutes and resuspended in cell culture media.

Cell freezing: Cells were centrifuged and 1 ml of freezing medium was added. The cell vial was placed in the freezing container at -80ºC for 24h, until placing them in liquid nitrogen.

RNA analysis

RNA extraction and quantification

TRIPURE isolation: The standard method for RNA extraction of the samples was TRIPURE isolation (Roche). In the first step, cells were lysed with TriPure and chloroform (Sigma-Aldrich) to separate the sample into three phases. RNA was recovered from the colourless aqueous phase via isopropanol (Sigma-Aldrich) precipitation. The RNA pellet was rinsed two times with 75% ethanol (VWR), and finally the dry RNA pellet was resuspended in 15 to 20 µl of DEPC-treated ddH_2O and kept on -20ºC.

RNA quantification: The RNA quality and quantity was assessed using the nanodrop spectrophotometer and a gel electrophoresis analysis. For an accurate quantification, size and integrity of the RNA was determined with Bioanalyzer (RNA Nano Assay: 25-500 ng/μl), according to manufacturer instructions.

RT-PCR

Reverse transcription was performed with SuperScript® II First-Strand Synthesis System (ThermoFisher scientific) with random hexamers (Life Technologies, SA) on 1-3 ug of RNA following manufacturer's instructions.

Detection of exon skipping levels

PCR amplifications were carried out with 1μl of the cDNA samples and different set of primers (summarized in **Table 4**) for each exon. PCR was performed with *Taq* DNA Polymerase (Roche) according to the manufacturer's recommendations. The PCR products were evaluated by 2% agarose gel electrophoresis to verify the expected product size. Each pair of primers (desalted and purified, Invitrogen) was tested with an *in silico* PCR to evaluate the specificity.

qPCR analysis

In order to evaluate the differentiation levels across the different experimental conditions, a quantitative PCR (qPCR) was performed with PC12 and H19-7 neuronal cell lines samples. Relative expression was determined using SYBR Green I master mix (ThermoFisher scientific) according to manufacture's instructions. Reactions were run on Light Cycler® 480 II Real Time PCR system (Roche) with 480 Multiwell plate 384 (Roche). Conditions of amplification were as follows: 95ºC for 10 min; 40 cycles of 95ºC for 10s, 59ºC for 30s and 72ºC for 20s, finally a melting curve of 95ºC for 5s and 65ºC for 1 min. The expression levels were normalized using *Rpl29* and *Rpl19* reference genes. . Each pair of primers (desalted and purified, Invitrogen) for qPCR analysis was tested with an *in silico* PCR to evaluate the specificity. Primers used in **Table 4**

Primer Name	Sequence 5' – 3'	Specie
Control E3 Forward	CAGAACACACATACCAAAGTCA	Rat
Control E3 Reverse	GACCAGCATTGTTTCATCTA	Rat
Forward E23a	CAGAGTTCCCCTCGCAGCTTCG	Rat
Reverse E23a	CTCCGTGCCAAGTCGGAGTTGC	Rat
Forward E23a	TTAGAACCATCAGAGAGCC	Human
Reverse E23a	TTTCGATTCTAGGTGGTG	Human
Forward E14	CAGGCAGATAGAAGTTCCTGTCA	Rat
Reverse E14	GTTTTGTAGCCTGTTCCCACTTTGC	Rat
Forward E14	GCAGGCAGATAGAAGTTCCTGTCAC	Human
Reverse E14	GTTCTACAAATTGAGTATTGGTATCAG	Human
Forward E23-2	GTTTGTACCAGGTGGTTAGC	Rat
Forward E23-2/E23a	TTTGTACCAGGCAACTTG	Rat
***Gap43* Forward**	CCGACAGGATGAGGGTAAAG	Rat
***Gap43* Reverse**	GCAGGAGAGACAGGGTTC	Rat
***Mmp3* Forward**	TGAAGATGACAGGGAAGCTGG	Rat
***Mmp3* Reverse**	GGCTTGTGCATCAGCTCCAT	Rat
***Dusp6* Forward**	TCTTTGGCTCCACTATACGCAA	Rat
***Dusp6* Reverse**	ATCCAGGCAATAGGTTTGCTTC	Rat
***Mbnl1* Forward**	ATGGCTGTTAGTGTCACACCA	Rat
***Mbnl1* Reverse**	CATGTTCTTCTGCTGAATCAA	Rat
***Mbnl2* Forward**	CAGGTTGAAAATGGAAGAGTAA	Rat
***Mbnl2* Reverse**	TTGAGCCCGGGACAGTGACCGG	Rat
***Celf3* Forward**	GACCGGAAGCTCTTTGTGGGG	Rat
***Celf3* Reverse**	AGAGTCCGGCTGCTGTGA	Rat
***Rpl19* Forward**	ATCGCCAATGCCAACTCT	Rat
***Rpl19* Reverse**	GAGAATCCGCTTGTTTTTGAA	Rat
***Rpl29* Forward**	ACAGAAATGGCATCAAGAAACCC	Rat
***Rpl29* Reverse**	TCTTGTTGTGCTTCTTGGCAA	Rat

Table 4: Primers used in the PCRs of the cDNA and the qPCR analysis to evaluate the skipping and differentiation levels across the different experimental conditions.

RNA-seq analysis

The RNA of PC12 cell cultures was collected in initial conditions (3h) and after 55h in presence or absence of NGF. Cells were treated with different PMOs

(PMO-Skp23a, PMO-Inc23a, PMO-Skp19). Biological triplicates were performed for each biological condition assayed.

Libraries, prepared starting from 200 ng of RNA/sample with the TruSeq stranded mRNA Illumina (automatically processed, PerkinElmer Sciclone NGS liquid handler) procedure, were quantified by the KAPA library quantitation kit for Illumina GA (on 7900-HT PCR system, Applied Biosystems) and the Agilent Bioanalyzer, and sequenced on the Illumina HiSeq 2000 platform with 2x100 reads and multiplexing 4 samples per lane.

Data Analysis

Sequencing data was quality trimmed with Trimmomatic v0.3 then processed with TopHat v 2.0.9, mapping with Bowtie2 against the rattus norvergicus reference genome Rnor 6.0. The reads overlapping every known gene were counted and the counts matrix was processed in R. Every sample was normalized by the median of counts. A list of differentially expressed genes was generated per batch selecting those genes with a FC > 2 or FC < 0.5 and the final list was defined as the intersection of the per-batch lists. Functional enrichment analysis was performed using DAVID and selecting the 3 Gene Ontology subsets and the KEGG pathways database. Heat map plots were generated with the gplots R package. Overlapping analysis of the different gene lists was also performed with R, with an in-house developed permutation analysis to determine the enrichment significance and generating the plots with the VennDiagram package.

Protein analysis

Protein extraction and quantification

RIPA Buffer composition:

RIPA Buffer (100ml). PH 8.0	
150 mM NaCl (1M) (Merck)	**15 mL**
1.0% IGEPAL® CA-630 (Sigma-Aldrich)	**1 mL**
0.5% deoxycholic acid (10%)	**5 mL**
0.1% SDS (10%) (Merck)	**1 mL**
50 mM Tris, pH 8.0 (1M) (Calbiochem)	**5 mL**
dH_2O	**73 mL**

Table 5: List of RIPA buffer components per 100ml at pH of 8.0.

Lysis Buffer composition:

Lysis Buffer	
3 mM DTT (1M)	**3µl**
Leupeptin (Sigma-Aldrich)	**10µl**
Aprotinin (Sigma-Aldrich)	**10µl**
1 mM PMSF (100mM)	**5µl**
1 mM Na_3VO_4(100mM)	**10µl**
5 mM NaF (500mM)	**10µl**
PhosSTOP™ (Sigma-Aldrich)	**10µl**

Table 6: Lysis Buffer composition per 1ml.

Procedure for plated cells: The cell medium was removed and cells were washed twice with cold 1X PBS. Complete RIPA buffer (**Table 5**) was prepared by adding protease inhibitors and phosphatase inhibitors freshly before use (**Table 6**). The appropriate amount of lysis buffer was added to each dish and incubated 5 minutes on ice. Finally, the cells were scraped vigorously and the lysate

transferred into a fresh eppendorf tube. Optionally, in case of cellular debris in the protein lysate, a spin of 16000 rpm for 15 min was done. All the protein samples were preserved at -20ºC.

Protein quantification: Quantification was done with Pierce™ BCA Protein Assay Kit (Thermo Scientific), following manufacturer's instructions. The absorbance was measured at 562 nm using a microplate reader (SPECTRAmax 340PC, Molecular Devices).

Western blot samples and reagents

Primary antibodies:

NF1		
NF1 Antibody	Bethyl laboratories	Dilution 1:1000
Neurofibromin (N): sc-68.	Santa Cruz Biotechnology	Dilution: 1:500
ERK 1/2		
P44/42 MAPK (Erk 1/2) (3A7) Mouse mAb	Cell Signalling	Dilution 1:2000
Anti-erk 1/2 (p44/42), Clone MK12	Millipore	Dilution: 1:1000
PKA α/ß		
Anti-pka Catalytic α/ß (pT^{197}) Phosphospecific Antibody, unconjugated	Invitrogen	Dilution: 1 μg/ml
PKA alpha + beta Antibody	Thermo Fisher scientific	Dilution: 1:500
Tubulin		
Monoclonal Anti-α Tubulin	Sigma-Aldrich	Dilution: 1:1000

Table 7: List of the primary antibodies (NF1, MAPK pathway, PKA pathway and tubulin) used in the western blot protocol and their corresponding working dilution.

Secondary Antibody:

Polyclonal Goat Anti-Rabbit Immunoglobulin/HRP. Dako Denmark. Dilution: 1:4000.

Polyclonal Goat Anti-mouse Immunoglobulin/HRP. Dako Denmark. Dilution: 1:4000.

Western blot solutions and reagents:

Membrane: PDVF Membrane; Western clear signal, Whatman.

Chemiluminescent substrate: Pierce ECL Western Blotting Substrate. Thermo Scientific.

Blocking buffer: 5% non-fat dry milk in PBS.

Membrane Stripping: R-Blot Plus Mild Solution (10x), Millipore.

Western experimental procedures

NF1 western blot: Protein samples (30μg) were separated by size on SDS-polyacrylamide gel (6% gel percentage), transferred into a PVDF membrane by electroblotting (3 hours at 70V), blocked with 5% non-fat dry milk and subjected to immunoblotting with the indicated NF1 antibodies (Neurofibromin-sc68 or NF1 Antibody Bethyl) (**Table 7**) overnight at 4ºC. Blot was exposed to Horse Radish Peroxidase-conjugated secondary antibody (1 hour room temperature) and detected with Pierce® ECL western Blotting Substrate. The levels of NF1 were normalized according to the α-tubulin signal.

Western blot ERK 1/2 and PKA: Protein samples (20μg) were separated by size on SDS-polyacrylamide gel (12% gel percentage), transferred into a PVDF membrane by electroblotting (1 hour at 360 mAMP), blocked with 5% non-fat dry milk and subjected to immunoblotting with the indicated P-ERK 1/2 or P-PKA

α/ß antibodies overnight (4ºC) (**Table 7**). Blot was exposed to Horse Radish Peroxidase-conjugated secondary antibody (1 hour room temperature) and detected with Pierce® ECL western Blotting Substrate. After that membranes were stripped with Re-Blot Plus Mild Solution (1X), in order to repeat the whole procedure using the other set of antibodies to detect total ERK 1/2 or PKA levels (**Table 7**). The levels of ERK 1/2 and P-ERK 1/2 were normalized according to the α-tubulin signal.

RAS Activation assay

The Ras Activation ELISA Assay Kit (Millipore) works on the principle that Ras only binds to its downstream kinase, Raf-1 (through the RAS-binding domain, RBD), when in its active-GTP-bound state. A recombinant c-Raf-RBD was provided with the kit, to capture activated Ras from the total protein sample. C-Raf-RBD binds to the wells of a 96-well glutathione-coated ELISA plate via a GST/glutathione interaction, thus capturing the active Ras and allowing the inactive/GDP-bound Ras to be washed away. The captured active Ras was detected and measured quantitatively through the addition of a monoclonal anti-Ras antibody. After, an HRP-conjugated secondary antibody was added for the signal detection. Following addition of the chemiluminescent substrate, signal was measured using a luminometer (Centro LB 960, berthold Technologies). Between 40-50 μg of total protein, was used for the assay following the manufacturer's instructions. Positive and negative controls were provided in the kit. Experiments were performed in triplicates for each experimental condition.

Immunofluorescence α-tubulin & Nerve Growth Factor Receptor (NGFR)

Primary Antibody:

Mouse anti-α-Tubulin Alexa 488. Invitrogen. Dilution 1:1000.

Nerve Growth Factor Receptor (p75). Mouse Monoclonal. Advanced Targeting Systems. Dilution 1:100.

Secondary Antibody:

Alexa Fluor 568 goat anti-rabbit IgG (H+L)(Invitrogen). Dilution 1:1000.

Procedure: Cells were fixed in 4% Paraformaldehyde (Merck) in PBS (15-20 min) and washed 3 times with PBS. Cells were permeabilized with 0.1% Triton X-100 for 10 minutes and blocked for 15 min in 10% of Fetal Bovine Serum (FBS) in PBS. All primary antibodies were diluted 1:100 in 1% FBS (1× PBS) and incubated 2 hours at room temperature (RT). Before secondary antibody application, the samples were washed three times in 1% FBS (1× PBS). Secondary antibody Alexa Fluor 568 goat anti-rabbit IgG (H+L)(Invitrogen) was used at 1:1000 in 10 % FBS (1× PBS) and incubated for 45 min at RT. Glass coverslips were mounted with VECTASHIELD mounting medium with DAPI H-1200 (Vector Laboratories). Images were taken in the confocal microscope Zeiss AxioObserver Z1, with the adquisition software ZEN black 2012 in the microscopy service from Institut Germans Trias i Pujol (IGTP).

In vitro functional assays

PMO design and treatment conditions

The 25-mer PMOs were designed, synthesized and purified by GeneTools (Philomath, OR, USA) (**Table 8**). Endo-Porter (GeneTools) was used to deliver PMOs into cells, according to the manufacturer's instructions. For the PMO treatment cells were seeded at 50% of confluency, in a six-well plate. The next day, culture medium was replaced with fresh medium containing the indicated concentrations of PMOs. Immediately after, Endo-Porter (6mM) was added and mixed. Three biological replicates were done for each condition to be studied.

PMO Name	Sequence 5'-3'	Target Position
PMO-SkpE23a	GTTGCCTACAGAACAGAGATGAGCA	**Exon 23a**
PMO-IncE23a	AAAAACAATGTTGGCTTGTACATAA	**Intron-Exon 23a**
PMO-Skp14	TCTTCCTACACAAAGACAACAAGCA	**Exon 14 Acceptor**
PMO-Skp14	TGTTTCCTGCAGTAGGGTGCTCAAT	**Exon 14 ESE**
PMO-CSRI	GTAACACAAATGGAACCAACAGAAA	**Intron-Exon 23a**
PMO-CSRIII	CACAGCACCGACTACATACAGCAAC	**Intron-Exon 23a**

Table 8: List of the different PMOs used in different processes in the thesis.

Cell proliferation and cell cycle analysis

Click-iT® EdU Assay: In order to asses the proliferation and the cell cycle status of our experimental conditions, we used the Click-iT® EdU Alexa Fluor® 488 Azide Flow Cytometry Assay Kit. It utilizes 5-ethynyl-2′-deoxyuridine (EdU) to

label newly synthesized DNA. Detection is based on a copper catalyzed covalent reaction between an azide and an alkyne.

Cells were with 20 μmol/L Edu for minimum 1h prior trypsinization. Harvested and washed 3 times with 1% BSA-FBS, fixed with 4% p-forrmaldehyde, permeabilized with a saponin-based buffer and a final incubation of 30 min with the Click-it Edu Reaction Cocktail (with Alexa Fluor® 488 Azide and $CuSO_4$). Cells were also stained with PI (15 mg/ml) in citrate buffer to detect DNA content. The stained cells were analyzed by flow cytometry using BD LSRFortessa™ cell analyzer, in the Cytometry service from the Institut Germans Trias i Pujol (IGTP). Experiments were performed in triplicates for each experimental condition.

Cell counting: The number of PC12 cells was determined using hemocytometer counting chamber to avoid cellular aggregation bias or by counting the number of cells per field using Hoesct staining (bisbenzimide Hoechst 33258) images obtained with LEICA-DMI 6000B (counting 10 fields at 20x or 40x for each biological replicate). Experiments were performed in triplicates for each experimental condition.

Cell death analysis

The analysis of apoptotic cells was done using Annexin-V-Alexa 568® antibody (Roche, Life technologies). Annexin-V is a cytoplasmatic protein that detects phosphatidylserine in the outer layer of apoptotic cell membranes. In order to differentiate necrotic from positive apoptotic cells, Annexin-V staining was performed in combination with a DNA staining (bisbenzimide Hoechst 33258) . The stained cells were analyzed by flow cytometry using BD LSRFortessa™ cell

analyzer in the Cytometry service from the Institut Germans Trias i Pujol (IGTP). The experiment was performed in triplicate.

Differentiation assays

Quantification of differentiated cells/neurite outgrowth: Analysis was performed on digitized images (10 fields at 20x) of live PC12 cells taken under phase contrast with a LEICA DMI 6000B inverted microscope. The **number of differentiated cells** was determined by counting cells counting (10 fields at 20x) that had at least one neurite with a length equal to the cell body diameter, and expressed as a percentage of the total cells in the field. The **neurite outgrowth** was determined by tracing the length of the neurites (20 neurites per field at 20x) using NeuronJ (Meijering E et al., 2004; Meijering E, 2010) an ImageJ plugin (http://www.imagescience.org/meijering/software/neuronj/).

NADH-dehydrogenase activity assay: The enzyme activity in PC12 cells was measured with a Cell Counting Kit-8 (Dojindo). This kit detects mitochondrial NADH-dehydrogenase activity in live cells by reduced reaction of a tetrazolium monosodium salt, producing a water-soluble formazan dye upon reduction in the presence of an electron mediator. The absorbance of 5 wells per condition was measured at 450 nm using a microplate reader (Spectra Max 340PC, Molecular Devices). The values were normalized with the total number of cells per experimental condition.

Statistical analysis: All the PMO experiments followed by different functional assays were repeated three times. For each biological dataset, mean and ±SEM was calculated and a paired Student's t-test assuming equal variances was applied. A P-value < 0.05 was considered to be significant. Statistical analysis was performed using PASW software (PASW statistics version 18.0).

RESULTS

Set up of a neuronal differentiation system based on PC12 cells

Nerve Growth Factor (NGF) induced neuronal differentiation of PC12 cells and *Nf1* alternative splicing of exon 23a

In order to investigate the role of the *Nf1* type II and I alternative splicing at physiological conditions during neuronal differentiation, we set up in our lab an already existing neuronal differentiation model system based on the use of PC12 cell line (CRL-1721). As mentioned in the introduction, PC12 cells were derived from a rat pheochromocytoma, a tumor from the adrenal gland. This cell line can be stimulated to differentiate into sympathetic-like neurons in the presence of neurotrophic factors like nerve growth factor (NGF) (Greene LA & Tischler AS, 1976) when plated on collagen type IV. In the presence of serum, PC12 cells acquire a round morphology and proliferate to high density. In contrast, in the presence of NGF, PC12 cells change the phenotype by stopping cell division, promoting extension of neurites, becoming electrically excitable (Das et al., 2004) and increasing the synthesis of several neurotransmitters. Due to these properties, numerous studies have used PC12 cells as a good experimental system for modelling the activity of sympathetic neurons.

We first tested PC12 differentiation in our hands. Cells were cultured with the aim to test NGF-mediated differentiation and examine the morphological changes and neurite extension associated to this process. As expected, in absence of NGF, no differentiation was observed and PC12 cells remained in their characteristic small and refringent form. In contrast, in the presence of NGF, the normally round cells started to extend neurites and increase the cell body size (**Figure 11**).

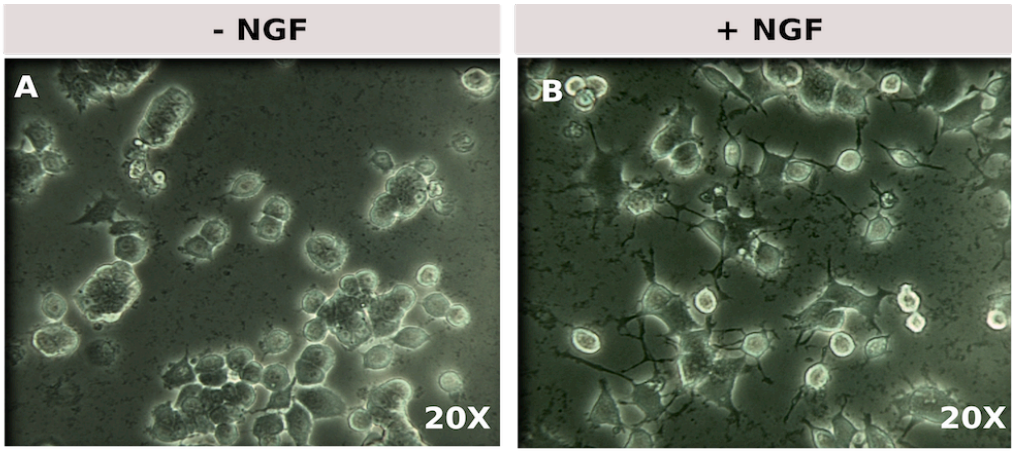

Figure 11: Phase contrast micrographs (20x) of PC12 cells on plated collagen IV-coated dishes in the absence (**A**) or presence (**B**) of NGF. The effect of NGF treatment (72h) on neurite outgrowth and cell morphology can be observed in image B.

In addition to the morphological and molecular changes reported during PC12 differentiation, it has been described that the process is associated with the alternative splicing of *Nf1* exon 23a (E23a) switching from the mainly expressed type II transcript (inclusion of E23a) to a partially expression of type II and I transcripts (exclusion or skipping E23a). PC12 cells were treated for up to three days with NGF to induce neuronal differentiation and the associated E23a skipping. The *Nf1* isoform expression was determined by a PCR of the cDNA, using a pair of primers flanking the region of E23a. Although significant changes in isoform expression during the first 24h were not detected, higher levels of expression of type I were detected around 48h after the NGF addition (**Figure 12**). As described in the introduction, E23a regulation is tissue-specific and it is conserved among vertebrates. We investigated the tissue-specific expression patterns of the two *Nf1* transcripts with the information available in the Database of Alternative Transcripts Expression (DBATE) (Bianchi V et al., 2013). As shown in **figure 13A** the canonical isoform type I (-E23a) was mainly expressed

in central nervous system (brain and peripheral brain), moreover we characterized the expression of the alternative transcripts in other human tissues and cell lines (**Figure 13B**). The different adult tissues or cell lines exhibited different patterns of *NF1* isoform predominance. To date, although the physiological role of *NF1* alternative splicing in neuronal differentiation has not been completely elucidate, the evidences of Costa RM and collaborators (Costa RM et al., 2001) suggest the possible balance of these two isoforms during neuronal differentiation.

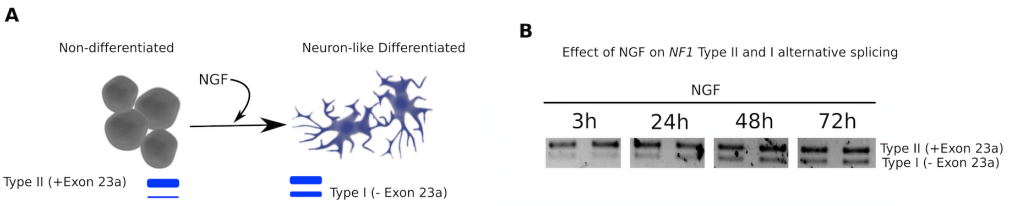

Figure 12: A) PC12 cell line can be stimulated to differentiate into sympatethic-like neurons in the presence of NGF. At the same time, the NGF treatment induces a switch of *Nf1* type II (+E23a) to I (-E23a). B) Time-dependent effects of NGF on *Nf1* type II and I alternative splicing in PC12 cell line.

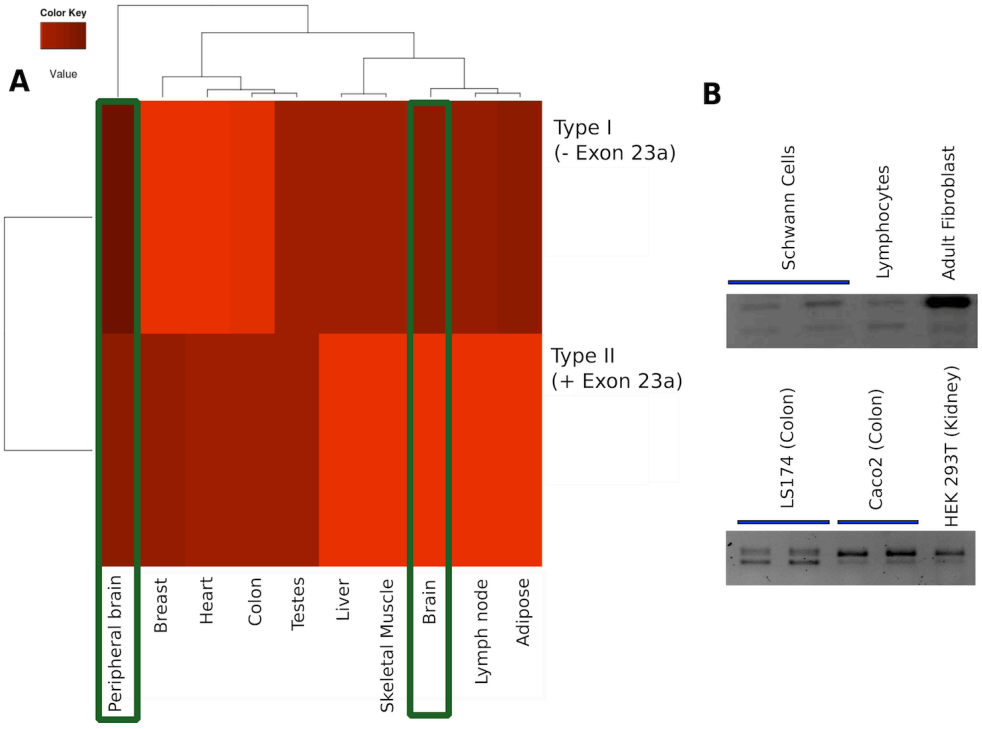

Figure 13: A) The heat map reports *NF1* gene isoform expression levels in different tissue samples. Central nervous system tissues with higher levels of isoform Type I (-E23a) expression are depicted in green. Expression levels dark red=high, light red=low. Data obtained from: Database of Alternative Transcripts Expression (DBATE). **B)** Expression of *NF1* type II and I transcripts in human tissues and cell lines.

Functional characterization of neuronal differentiation of PC12 cells: proliferation, differentiation, apoptosis and signaling

We planned to use Phosphorodiamidate Morpholino Oligomers (PMOs) to modulate *in vitro* the alternative splicing of E23a while preserving physiological expression conditions. In order to evaluate the functional impact of these PMOs in the physiology of PC12 cells, we set up a group of methodologies and functional assays to assess the proliferation, differentiation and cell signalling capacity. Differentiation of PC12 cells is usually measured with quantitative morphological

analysis that can include a determination of neurite length and their number per cell or the lag of time before acquiring a differentiation state. We set up two morphological analyses for PC12 cells. One relied on the double immunofluorescence staining with α-tubulin and Nerve Growth Factor Receptor (NGFR) to asses morphological changes, and the other was based on the determination of the neurite length and the percentage of differentiated cells. A differentiated cell was considered when neurites extended longer than the diameter of the cell body, and in this way the percentage of differentiated cells was detrmined. PC12 were maintained during 3 days in the presence or absence of NGF, during which the cells were observed with LEICA DMI 6000B fluorescence microscope. By analyzing phase-contrast pictures, the percentage of differentiated cells was determined as well as morphology adopted after the treatment with NGF (**Figure 14**).

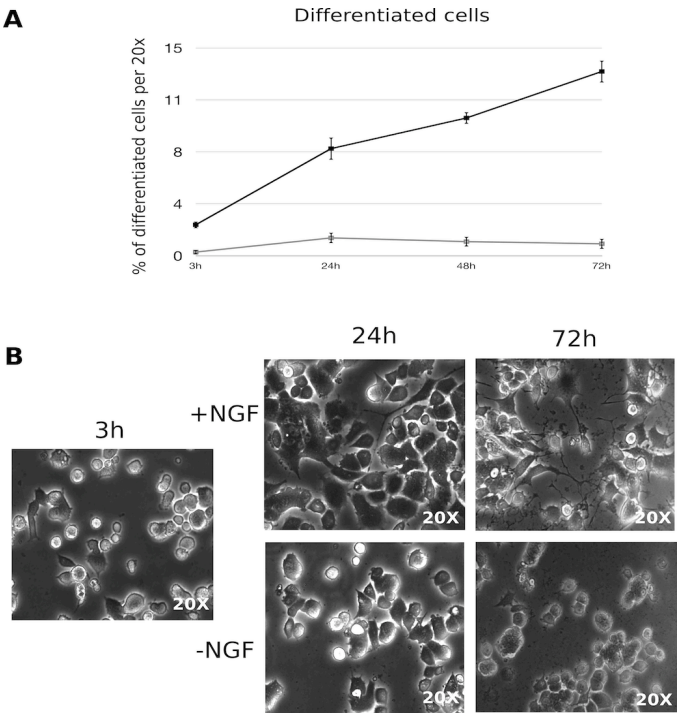

Figure 14: A) Percentage of PC12 cells bearing neurite outgrowths longer than the diameter of their cell body, in the presence (closed square) or absence (open square) of NGF during 72h. Error bars indicate ±SEM. **B)** Morphology of PC12 cells in the presence or absence of NGF at different time points.

Results

In addition to the morphological analysis we used other complementary ways of measuring neuronal differentiation, like the expression quantittation of neuronal markers or the analysis of metabolic enzyme activity. During NGF-induced PC12 differentiation or during neurogenesis in brain, mitochondrial NADH-dehydrogenase activity is incremented. In our model, NADH-dehydrogenase activity was examined using a specific cell counting kit (detailed in Material and methods section) and normalized with the total number of cells per condition. In addition, we designed a quantitative PCR (qPCR) screening of specific differentiation markers, in particular matrix metallopeptidase 3 gene (*Mmp3)*, the dual specificity protein phosphatase 6 gene (*Dusp6)* and the Growth-Associated Protein 43 gene (*Gap43)*. *Dusp6* is a member of the dual specificity protein phosphatase subfamily and inactivates ERK2, *Mmp3* is a member of the matrix metalloproteinase family of extracellular matrix-degrading enzymes that is involved in tissue remodeling, wound repair and tumor invasion and *Gap43* is highly expressed in neuronal growth cones during development and axonal regeneration. All three genes have been reported to be up-regulated upon NGF treatment of PC12 cells (Das KP et al., 2004; Dijkmans TF et al., 2008; Camps M et al., 2013). The relative expression levels of these markers were normalized against ribosomal proteins L19 and L29 (*Rpl19* and *Rpl29*) that are housekeeping genes previously described as suitable reference genes in normal or differentiated PC12 cells (Zhou L et al., 2010). As shown in **figure 15**, all differentiation markers interrogated were found to be up-regulated in the presence of NGF.

To monitor cell proliferation and cell cycle status, PC12 cells were both manually counted and examined with flow cytometry using Click-it Edu^{+}/ propidium iodide assay. The later assay allowed us to measure the capacity of the cells to synthesize new DNA (incorporation of EdU^{+}) and to check the cell cycle status. Click-iT

EdU$^+$ assay (Invitrogen) is based on the incorporation of 5-ethynyl-2'-deoxyuridine (EdU$^+$) into newly synthesized DNA and it is recognized by azide dyes via a copper mediated "click" reaction. These functional assays allowed us to study the proliferation capacity of cells in the presence or absence of NGF. As shown in **figure 16A & B**, after NGF treatment the number of total cells and EdU$^+$ cells was significativelly reduced in comparison to the non-treated cells. In addition, we observed that PC12 differentiated cells were mainly in G0/G1 phase after 72h, whereas cells not treated with NGF were accumulating in G2/M (**Figure 16C**).

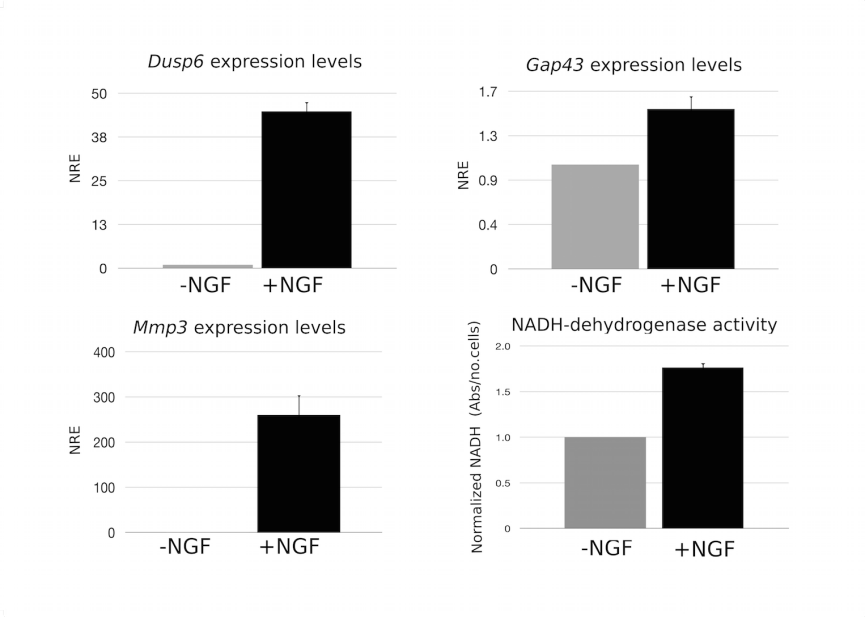

Figure 15: Relative expression of *Gap43*, *Dusp6* and *Mmp3* mRNA (error bars indicate ±SEM; normalized against *Rpl19* & *Rpl29*) after 72h with or without NGF. NADH activity was measured in the presence or absence of NGF after 72h (error bars indicate ±SEM; absorbance values normalized against number of cells per condition).

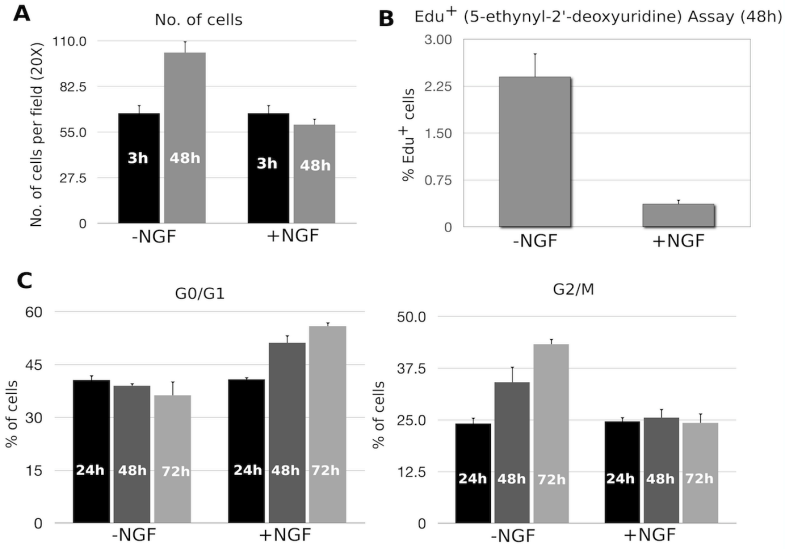

Figure 16: Proliferation and cell cycle functional assays set up for PC12 cells. **A)** Number of PC12 cells at different time points (3 and 48h) in the presence or absence of NGF. **B)** Percentage of EdU^+ cells at 48h in the presence or absence of NGF. **C)** Analysis of cell cycle status (GO/G1 and G2/M phase) in different time points (24,48 and 72h) in the presence or absence of NGF. Error bars indicate ±SEM.

In addition to analyze proliferation capacity and cell cycle characterization we also set up an assay to evaluate apoptosis and total cell death by flow cytometry. Apoptosis can be distinguished from necrosis by the characteristic morphological and biochemical changes of the cells undergoing these phenomena. In normal viable cells, phosphatidylserines (PS) are located on the cytoplasmic surface of the cell membrane. However, in apoptotic cells, PS can flip from the inner to the outer part of the cell membrane, exposing PS to the external cellular environment. In order to measure apoptosis we used an antibody against Annexin–V Alexa Fluor 568 conjugate, that is capable to bind to PS on apoptotic cell surfaces in the presence of Ca^{2+}.

Finally, we also wanted to characterize the state of two of the signaling pathways in which neurofibromin has been demonstrated to participate the RAS/MAPK pathway and cAMP/PKA pathway. On one hand, RAS/MAPK pathway status was analyzed using a western blot for determining the levels of ERK1/2 phosphorylation and a RAS-GTP ELISA activation assay (see material and methods section x), while cAMP/PKA pathway activity was assessed by a western blot of PKA α/β phosphorylation. In the case of PC12 cells, we detected an increase in the phosphorylation levels of ERK1/2 upon NGF treatment, with a maximum between 24-48h and a successive down regulation after 48h (**Figure 17**). These observations are in accordance with the results obtained by Yunoue S and collaborators (Yunoue S et al., 2003), that determined a time dependent increase in the relative Ras activity more than 10-fold upon NGF treatment, reaching a plateau around 24h and smother decreasing after that (24-72h).

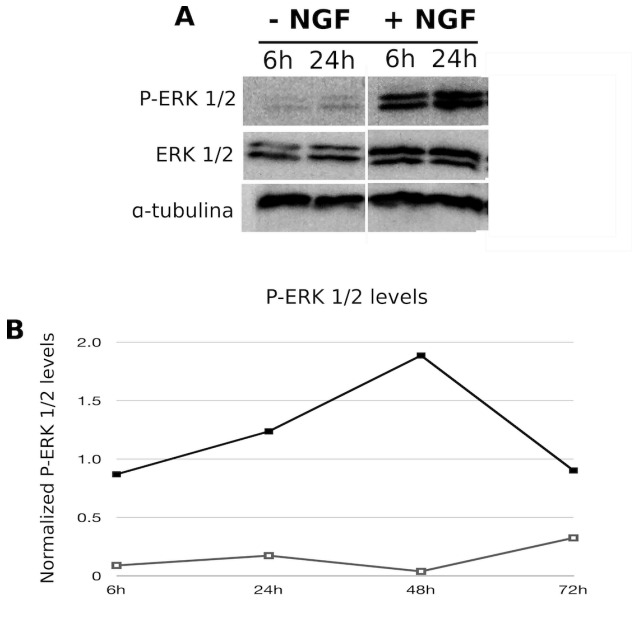

Figure 17: A) Time-dependent effects on ERK 1/2 phosphorilation levels of NGF treatment of PC12 cells at 6h and 24h. **B)** Phophorilation levels of ERK 1/2 in a time course (6h-72h) after addition at the indicated time points NGF. P-ERK 1/2 activity was quantified and normalized with total ERK 1/2 and α-tubulin in whole cell lysates.

Dissociating NGF-induced neuronal differentiation from the alternative splicing of exon 23a of the *Nf1* gene: forcing the expression of Type I isoform (E23a skipping)

Set up of a PMO-based system to induce the skipping of exon 23a

To better understand the role of alternative splicing associated with PC12 differentiation, we designed and tested *in vitro* antisense PMO to induce the skipping of E23a (PMO-SkpE23a) (**Figure 18A**). This PMO (25-mer) was designed to specifically bind to the acceptor-splicing site of E23a within the intron-exon junction. Before applying the PMO to PC12 cells we checked its efficiency in the HEK293T cell line since it has a high transfection efficiency. We tested different concentrations of PMO and successfully induced almost complete E23a skipping at low concentrations of PMO-SkpE23a (10 μM) in 24h (**Figure 18B**). After testing the efficacy of the designed PMO in inducing E23a skipping in HEK293T, we checked the efficacy and efficiency of the PMO in a dose response assay and time course experiments in PC12 cells (**Figure 18C**). In comparison to the HEK293T cell line, in PC12 cells the PMO was less efficient. However, using concentration of 20 μM during 48h, it was possible to achieve higher levels of skipping (**Figure 18C**). To better quantify skipping levels, we designed a qPCR assay using a pair of primers located in the boundary of exon 23-2 and 24 (forward primer specific for type I isoform, red arrow in **figure 18**) and in exon 25 (reverse primer). The isoform type I levels were normalized with total *Nf1* expression levels. The results indicated three times more isoform type I (-E23a) levels using PMO-SkpE23a than non-treated cells (in the absence of NGF) and also higher levels than the PC12 cells treated with NGF (**Figure 18D**).

One of the most important aspects of the use of PMO in this experimental set up was the intention to modify the alternative splicing of E23a while preserving the physiological expression conditions of the *Nf1* gene. To demonstrate that the expression of the *Nf1* gene was not modified with the use of PMO-SkpE23a was performed a qPCR analysis to quantify *Nf1* expression levels using a pair of primers located in exon 3 of the *Nf1* gene. By performing this qPCR it was determined that there were not significant alterations of gene expression, maintaining the *Nf1* mRNA levels in PC12 cells under physiological conditions (**Figure 19B**).

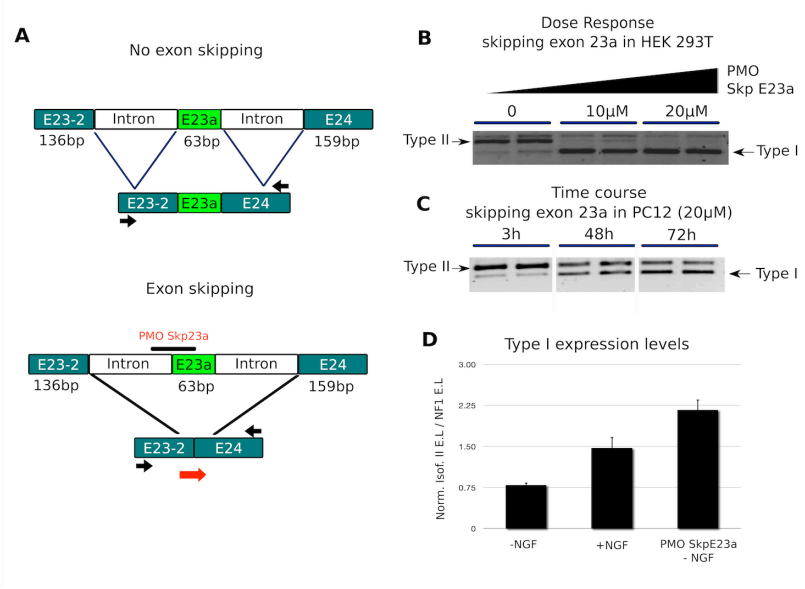

Figure 18: A) Schematic representation of E23a skipping strategy using a PMO targeting its acceptor splicing site. Black arrows indicate the position of the RT-PCR primers. B) Dose response analysis in HEK 293T cells to determine PMO concentration to efficiently induce the skipping of E23a (10 and 20 μM) of PMO SKpE23a. C) Time course experiment in PC12 cells to determine the levels of skipping induced by PMO-SkpE23a in different time points using a concentration of 20 μM (3, 48 and 72h). **D)** Normalized Isoform type I expression levels against total *Nf1* expression levels at 72h. In presence of NGF or with PMO-SkpE23a, the levels are higher than the control cells (-NGF). Error bars indicate ±SEM.

We tested the specificity of the designed PMO-SkpE23a by comparing it's skipping efficacy on E23a and it's influence on *Nf1* expression levels to that of an non-target PMO control. This PMO targets human beta-globin intron mutation that causes beta-thalassemia disease and was provided and designed by Gene Tools. We treated PC12 cells only with the PMO transfection agent (TA), the TA and the non-target PMO control or with the PMO-SkpE23a. The results indicated the specificity of E23a skipping by PMO-SkpE23a and that the physiological expression levels of *Nf1* gene were preserved (**Figure 19A & B**).

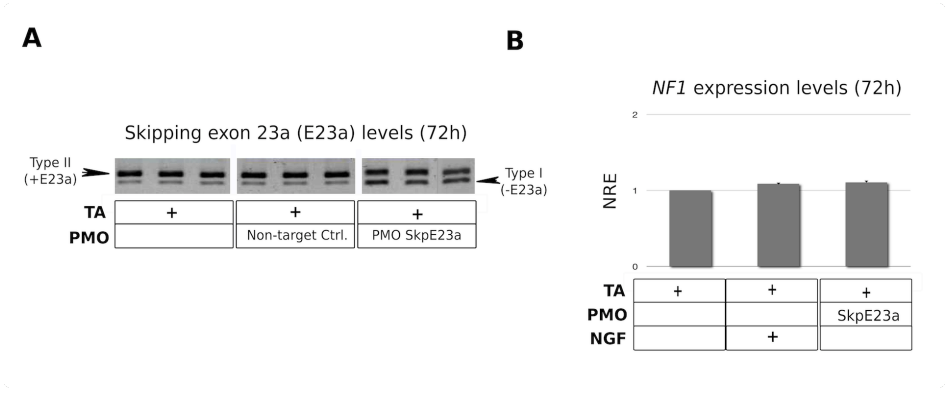

Figure 19: Effect of the non-target PMO control in our PC12 model system. **A)** Type I isoform levels at 72h. The non-target PMO control showed no effect in isoform type II and I expression as in cells only with transfection agent (TA). **B)** *Nf1* expression levels at 72h. There was no significant variation due to the use of a non-target PMO control. Error bars indicate ±SEM. TA: transfection agent

Functional characterization of neuronal differentiation of PC12 expressing *Nf1* Type I isoform (-E23a)

After setting up the use of PMO-SkpE23a and all the functional assays, we first wanted to test the effect of forcing E23a skipping in the absence or presence of NGF in the neuronal differentiation process of PC12 cells. As it was determined by the time-course experiment (**Figure 18C**), the effect of the PMO-SkpE23a on

the alternative splicing was already seen at 24h after treatment, and thus this PMO was actually shifting the alternative splicing 24h before than NGF treatment. There was 24h anticipation on the type II-I switch in comparison to NGF treatment alone. First, total mRNA of each experimental condition in triplicate was extracted after 72h and we determined the corresponding E23a skipping levels with the PCR of the cDNA (**Figure 20**).

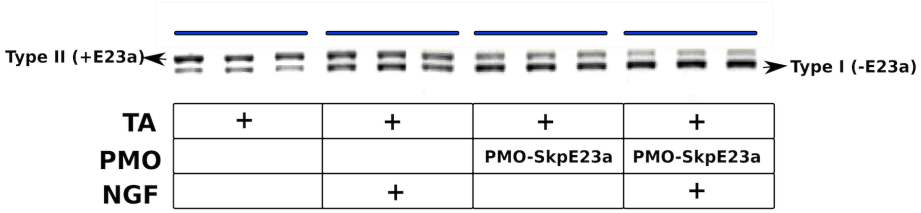

Figure 20: Analysis of *Nf1* mRNA around exon 23a for the different experimental conditions at 72h. The shorter transcript corresponds to the isoform type I (-E23a) and the longer one the isoform type II (+ E23a). TA: transfection agent.

Firstly, we observed that after the treatment with PMO-SkpE23a the proliferation capacity of PC12 cells was not altered. As shown in the **figure 21A** the number of cells treated only with PMO didn't differ from the control cells (-NGF). Moreover, cells treated with PMO and NGF shown also similar cell number to the ones treated only with NGF. A similar result was obtained when proliferation capacity was measured by the percentage of EdU^+ cells. As observed before, the number of cells after the treatment with PMO in presence or absence of NGF didn't change from their respective control (**Figure 21B**). Regarding the cell cycle, PC12 cells tend to accumulate in G2/M phase in their proliferative state (-NGF) and in G0/G1 phase in the differentiating state. The treatment with PMO-

SkpE23a didn't interfere with the PC12 cell cycle status when measured up to 72h (**Figure 22**). Taking into account this cell cycle analysis it can be considered that the skipping of E23a doesn't alter significatively the cell cycle arrest induced by NGF in PC12 cells.

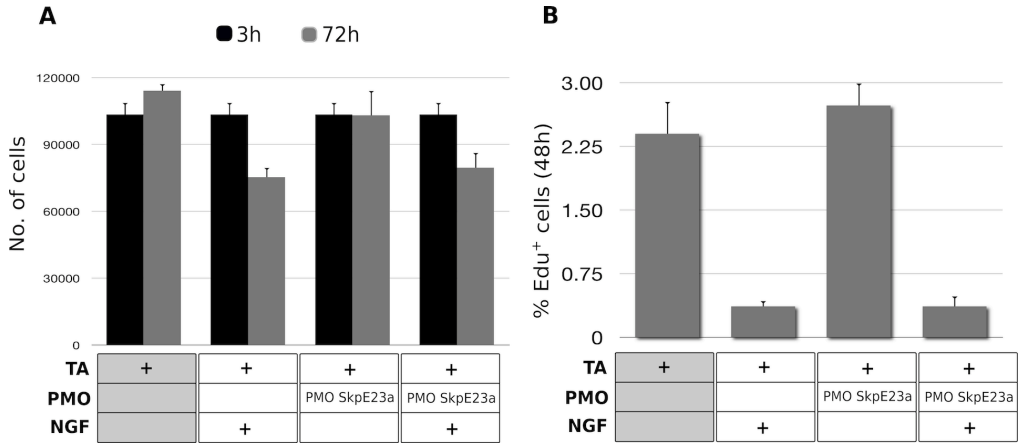

Figure 21: **A)** Cell number at 3h and 48h after NGF treatment. **B)** Percentage (%) of Edu$^+$ PC12 cells at 48h after treatment for the different experimental conditions. Error bars indicate ±SEM. No significant differences where detected in both assays.

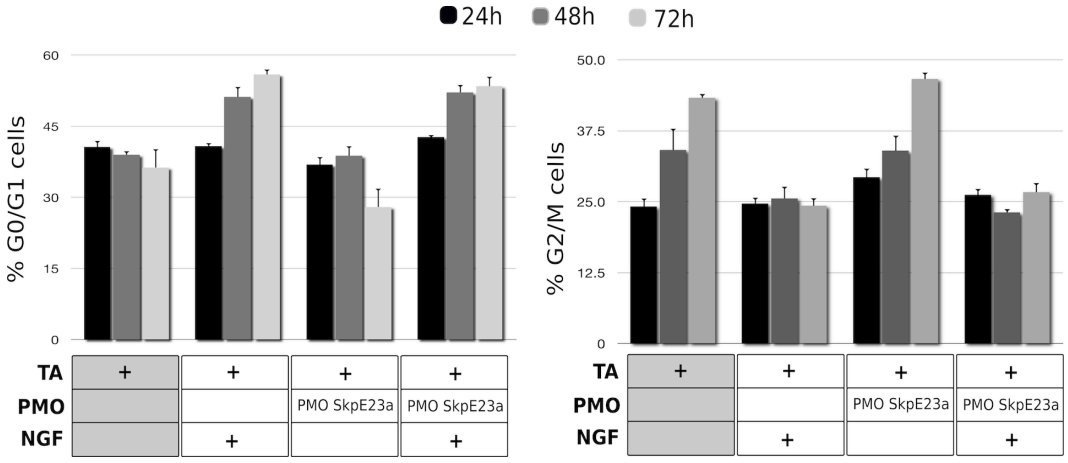

Figure 22: Cell cycle analysis of PC12 cells for the different experimental conditions. In the graphs we show the percentage of cells in G0/G1 phase and in G2/M. Error bars indicate ±SEM. No significant differences where detected in both assays.

After characterizing cell proliferation, we investigated the effect of E23a skipping in cell differentiation. We first characterized morphological changes in PC12 differentiation. We determined the number of differentiated cells with no NGF or after NGF treatment at different time points, 3, 24, 48 and 72h by contrast-photography with the inverted microscope (**Figure 23**). We also tested three differentiation markers (*Gap43*, *Mmp3* and *Dusp6*) by qPCR using RNA extracted at the final time point (72h). In addition, we measure the activity of NADH-dehydrogenase at the same time point. PC12 cells treated only with PMO-SkpE23a didn't show any increase in the expression of differentiation markers, in the enzymatic activity and also in the percentage of differentiated cells.

All together these results suggest that the change of isoform type II (+ E23a) to I (-E23a) using PMO-skpE23a is not sufficient to induce differentiation of PC12 cells in the absence of NGF. However, the results also demonstrate that after forcing E23a skipping with PMO in the presence of NGF there was a clear alteration in the correct neuronal differentiation process of PC12 cells, resulting in less differentiated cells (**Figure 23**), lower NADH-dehydrogenase activity (**Figure 24**) and a reduced expression of differentiation markers compared to cells treated only with NGF (**Figure 24**).

In order to better illustrate and characterize the altered phenotype, we performed an immunofluorescence with beta-tubulin and Nerve Growth Factor Receptor (NGFR). As before, we observed that PC12 cells treated with PMO and NGF had less neurites and percentage of differentiated cells (**Figure 25**).

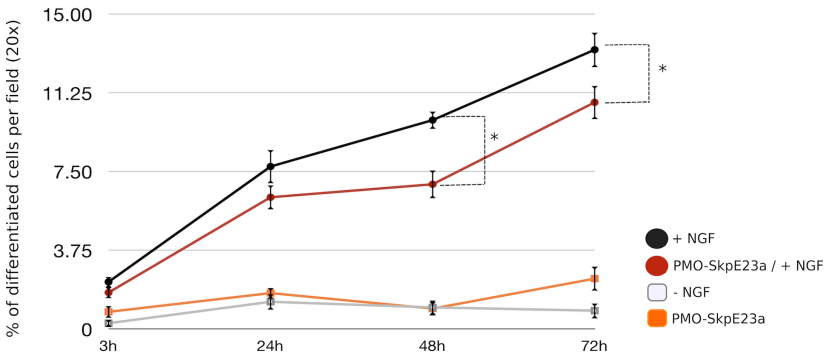

Figure 23: Percentage of differentiated cells per field (Phase-contrast, objective 20X) from the different experimental conditions at different time points (3,24,48,72h). Error bars indicate ±SEM. * $P < 0.05$ as evaluated by paired *t*-test vs cells treated only with NGF.

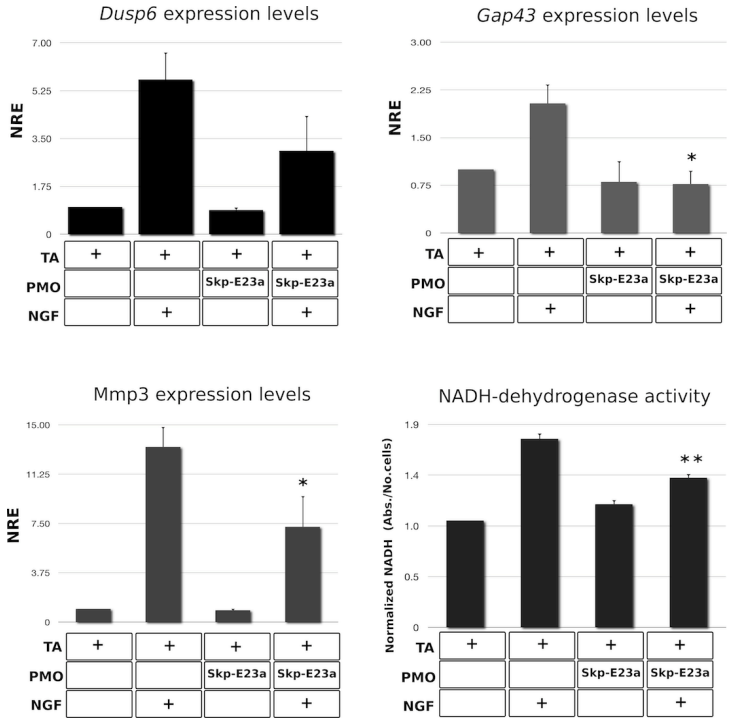

Figure 24: The effect of inducing exon skipping 23a (PMO-skpE23a) on NGF-triggered differntiation was measured, showing an interfere in the differentiation process. The graphs ilustrate the expression and the enzimatic activity of the differentiation markers (*Dusp6*, *Gap43*, *Mmp3* and NADH-dehydrogenase) for the different experimental conditions. Error bars indicate ±SEM. * $P < 0.05$, ** $P < 0.01$ as evaluated by paired *t*-test vs cells treated only with NGF.

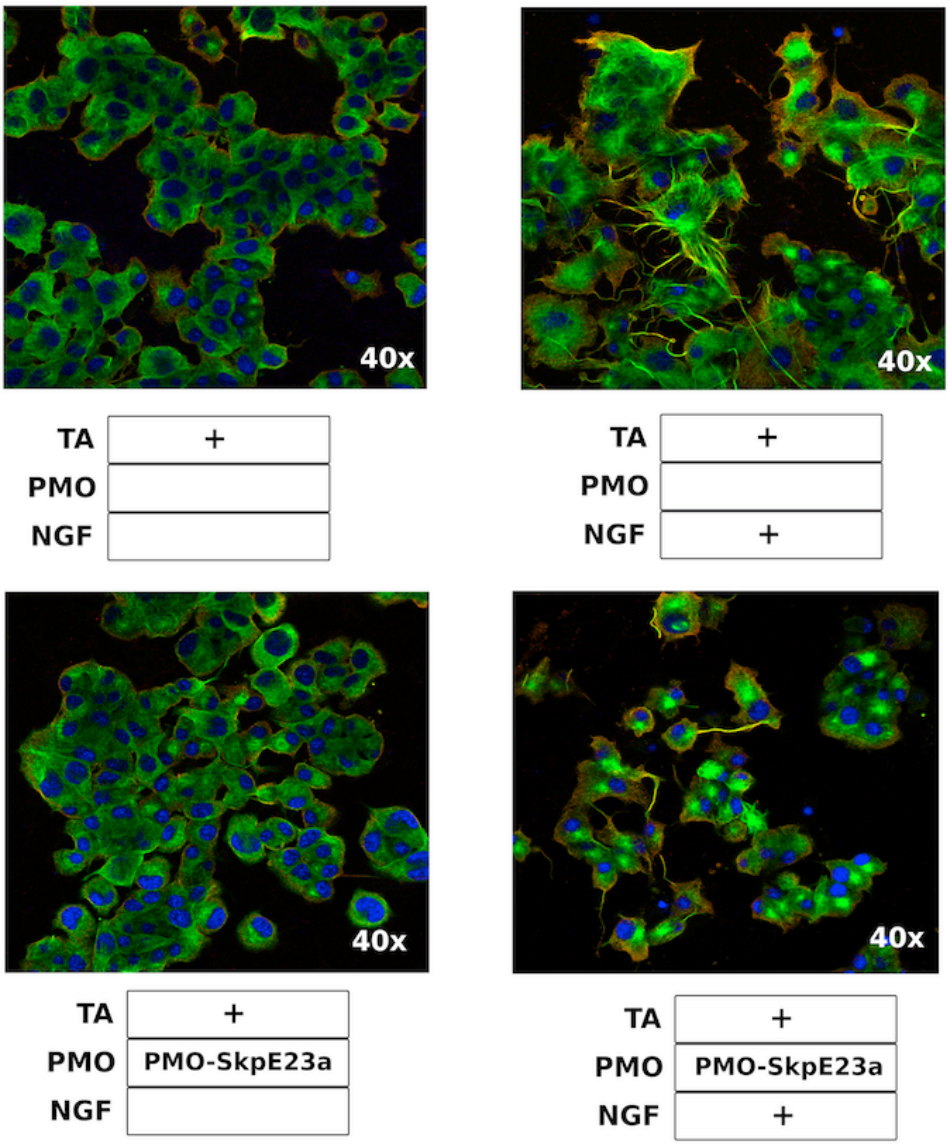

Figure 25: Double immunofluorescent staining of P75 (red) and α-tubulin (green) in PC12 cells for the different experimental conditions. DNA was stained with Hoescht (blue).

Results

Finally, the effect of forcing E23a skipping on the activation status of the Ras/MAPK pathway was also analyzed. Consistent with a higher RAS-GAP activity of Type I (-E23a) neurofibromin, we identified decreased levels of ERK 1/2 phosphorylation in cells treated with PMO-SkpE23a in both non-treated cells, and NGF treated cells after 72 h. (**Figure 26A**). The levels of active RAS in both conditions were also reduced after 48h compared to those in cells treated only with NGF (**Figure 26B**).

The levels of phospho-PKA increased in PC12 cells upon NGF treatment. However, in the presence of PMO-SkpE23a the levels of phospho-PKA were further elevated, and significatively increased when PMO-SkpE23a and NGF where added to PC12 cells (**Figure 26C**). Activation of cAMP/PKA signaling in neurons has been associated with the need of neurofibromin activity. However, this was the first time that the increase in cAMP/PKA signaling was associated to the type I isoform and just to the GAP activity of neurofibromin.

In summary, forcing E23a skipping was not sufficient to induce PC12 differentiation in the absence of NGF. The skipping didn't alter the proliferation capacity of PC12 cells, neither the cell cycle arrest produced by NGF treatment. However, E23a skipping singnificatively altered the NGF-triggered differentiation of PC12 while decreasing the RAS/MAPK signaling and increasing the cAMP/PKA signaling.

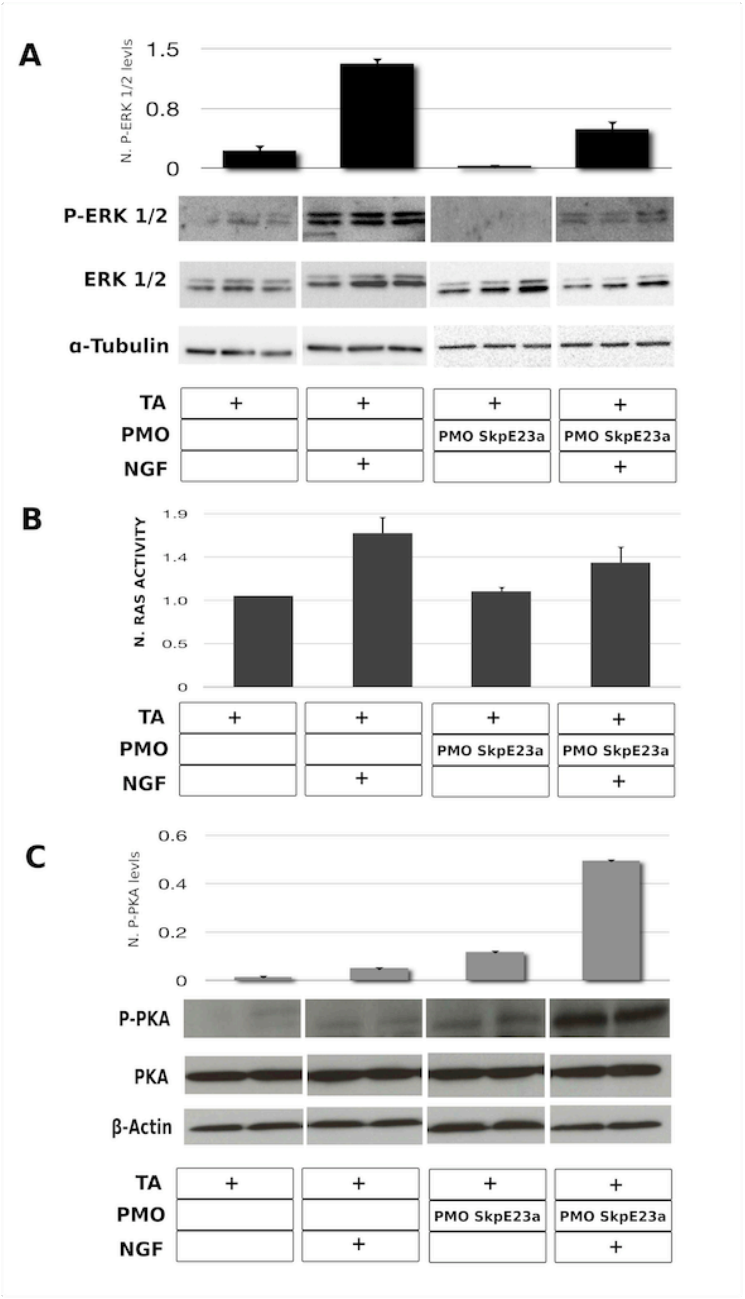

Figure 26: A) Western blot analysis of phospho-ERK1/2 and total ERK1/2 (42/44 kDa) in lysates from the different experimental conditions at 72h. The loading control was α-tubulin (50 kDa). **B)** RAS ELISA activation assay for the different experimental conditions at 48h. **C)** Western blot analysis of phospho-PKA and total PKA (40 kDa) in lysates from the different experimental conditions at 48h. The loading control was β-actin (42 kDa).

NGF-induced neuronal differentiation after forcing the expression of isoform type I (-E23a) or in the absence of neurofibromin

As it has been mentioned before, time course experiments to monitor the effect of PMO-SkpE23a indicated that at 24h the levels of isoform type I (-E23a) were similar to that exhibited by NGF treated PC12 cells at 48h. So adding PMO-SkpE23a at the same time of NGF treatment was actually shifting the switch from type II to type I isoform at least 24h earlier (**Figure 27**). This fact, together with the interference in the differentiation process and the RAS/MAPK and cAMP/PKA signaling by PMO-SkpE23a treatment, seemed to indicate the importance of the time-dependent regulation of these pathways by the type II-I isoform switch for a proper neuronal differentiation.

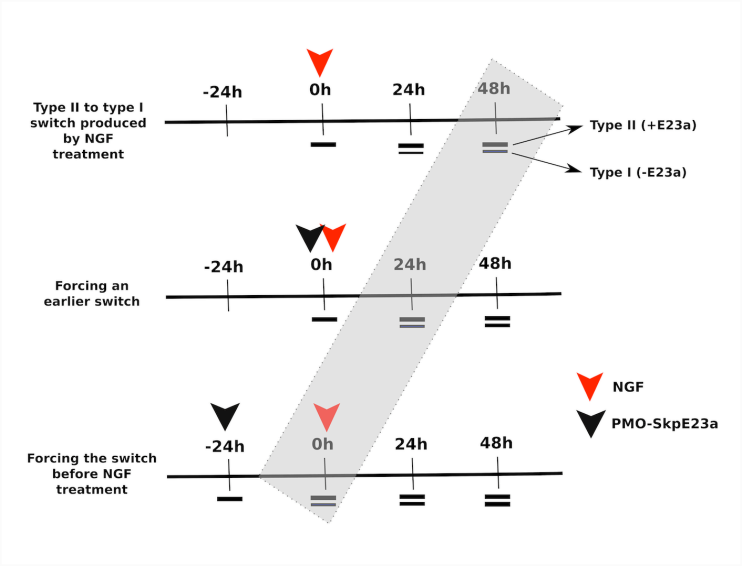

Figure 27: Schematic representation of the different experimental conditions regarding E23a skipping. NGF induces a progressive switch from isoform type II to I during 48h. When PMO-SkpE23a was added at the same time that NGF, at 24h the levels of isoform type I (-E23a) were similar to that exhibited by NGF treatment at 48h. This levels where reached before NGF treatment, when PMO-SkpE23a was added 24h before.

We wanted to further investigated on this time-dependent regulation of type II-I isoform switch by inducing NGF-differentiation after forcing the switch from type II to I. To do that we decided to treat PC12 cells with PMO-SkpE23a 24h before NGF treatment and thus analyze the differentiation process once alternative splicing had already taken place. At the same time, we wanted to compare the effect of the increase in type I isoform, with the greatest RAS-GAP capacity, with the total loss of neurofibromin activity and thus the absence of RAS-GAP regulation.

We decided to abrogate neurofibromin activity using the same PMO system, by forcing the skipping of an out-of-frame exon (exon 14) generating an *Nf1* mRNA bearing a STOP codon that would be degraded by Non-sense Mediated Decay (NMD) machinery or in any case, generating a truncated and non-functional neurofibromin. Two PMOs were designed to target the intron-exon boundary of exon 14 (E14) acceptor site and a specific sequence that acts as an enhancer-splicing element in its exonic region (**Figure 28**). To determine and localize this ESE sequence and achieve a more efficient skipping, we analyzed the sequence of exon 14 using the bioinformatic tool human splicing finder (HSF) (Desmet FO et al., 2009). This tool is useful to predict the effects of mutations on the splicing signals or for identifying splicing motifs in any human sequence.

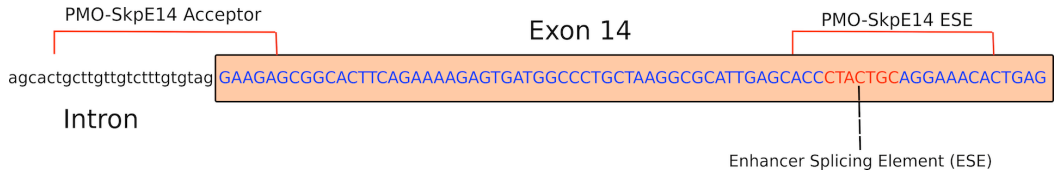

Figure 28: Position PMOs in exon 14. One PMO is located in the acceptor site of exon 14 (PMO-Skp14 Acceptor) and the other one located inside an enhancer-splicing element (PMO-SkpE14 ESE).

Results

The effectiveness of these new PMO designs (**Figure 29A**) was analyzed by checking the expression levels of *Nf1* mRNA, the absence of neurofibromin by western blot and the activation of cAMP/PKA pathway, activated in neuronal differentiation processes only in the presence of neurofibromin (**Figure 29C**). To simplify, we will mention from now on the combined treatment of the two PMOs for exon 14 as PMO-SkpE14. To obtain and visualize total levels of E14 skipping, PC12 cells were treated with puromycin a NMD inhibitor in the presence of PMO-SkpE14. The PCR of the cDNA results obtained showed approximately 50% of E14 skipping (**Figure 29B**). However, the knock down of NF1 protein (neurofibromin) detected by western blot was proportionally lower than the relative mRNA values. We think that this discrepancy could be explained if the effect of puromycin was not complete and some *Nf1* transcripts were anyway degraded by the NMD.

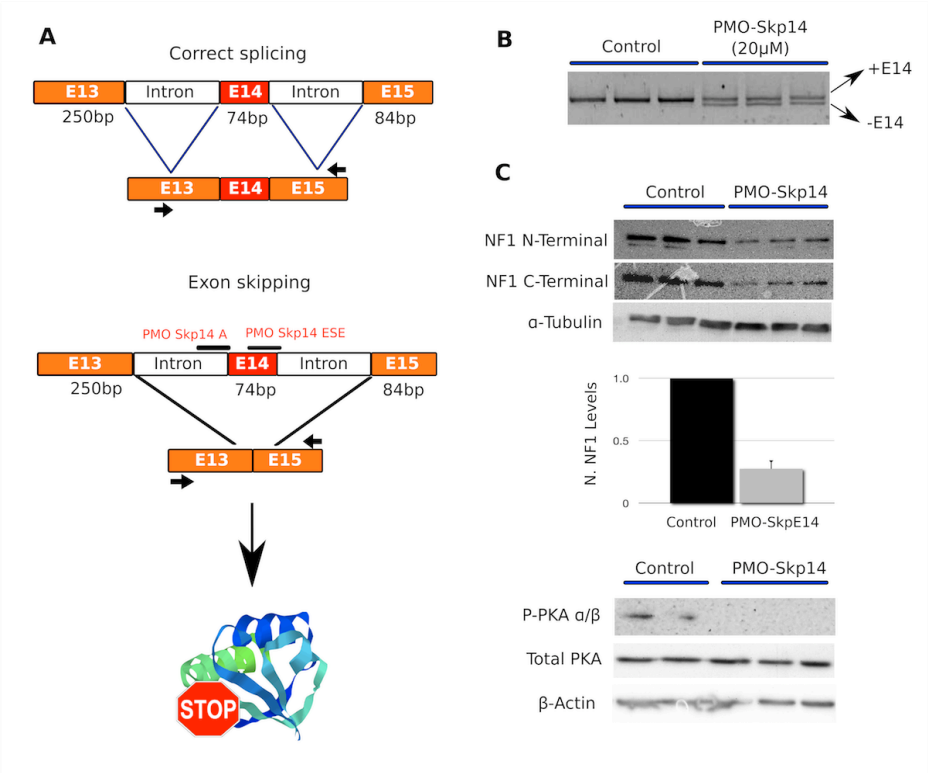

Figure 29: A) Schematic representation of exon 14 (E14) skipping using two specific PMOs. The PMO-SkpeE14A for the acceptor site region and the PMO-SkpE14 ESE for enhance splicing element (ESE) located in the exonic region. The skipping of E14 produces a shift in the reading frame, a premature stop-codon and generates a truncated form of NF1 protein. Black arrows indicate the position of the RT-PCR primers. **B)** RT-PCR of PC12 cells treated with or without PMO-SkpE14. The two-band pattern indicates RNA with (+E14) or without (- E14) exon 14 of the *Nf1* gene. **C)** The top figure shows a significant reduction in neurofibromin levels detected with two different antibodies (N and C-Terminal). Bottom figure shows a western blot of phosphorylated PKA and total PKA. Absence of phosphorylated PKA indicates the loss of neurofibromin activity.

Thus, we performed a new experiment to further investigate the response to NGF treatment after forcing previously the type II/I switch or knocking down the neurofibromin levels. First, the effect of different PMOs on exon skipping was monitored (**Figure 30**). When PMO-SkpE23a was used 24h before adding NGF the switch from type II (+E23a) to type I (-E23a) isoform was already produced.

Results

Time course experiments of E14 skipping indicated that the maximum efficiency of PMO-SkpE14 was at 48h. Therefore we decided to also add PMO-SkpE14 24h before NGF treatment. Doing so, neurofibromin depletion and NGF-triggered differentiation were performed parallelly, reaching significant neurofibromin depletion levels, at least 24h after initiating PC12 differentiation. All subsequent experiments using this PMO were performed in the same way.

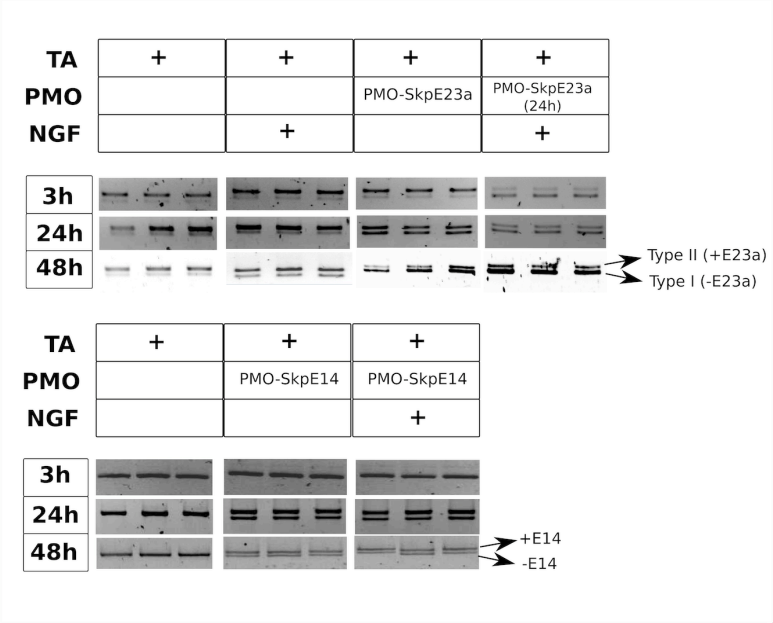

Figure 30: RT-PCR analysis of *Nf1* mRNA to monitor E23a and E14 skipping in the different experimental conditions at 3, 24 and 72h. It can be observed that at 3h the levels of E23a skipping were much higher in the condition where PMO-SkpE23a was added 24h before NGF compared to the condition where PMO-SkpE23a and NGF were added at the same time. TA: Transfection agent.

The interference of different PMO treatment on cell proliferation and NGF-induced arrest was analyzed by cell counting at 3 and 48h after NGF addition to PC12 cells. There was no significant alteration in the proliferation capacity or interference of the NGF-induced arrest capacity in the different conditions tested

(**Figure 31**). However, in conditions using PMO-SkpE14 a slight level of cell death was observed at 48h, a phenomenon that was greatly enhanced when cells were monitored for longer period of times (data not shown). This observation made us measure the percentage of apoptotic cells after PMO treatments in the presence or absence of NGF specially focusing in an early apoptotic phase (when cells can still preserve cellular integrity), since the cell death previously observed was a slow phenomena (**Figure 32**). This assay allowed the detection of a significant increase of PC12 cells at early apoptosis when neurofibromin levels were highly reduced by PMO-SkpE14 treatment. However, NGF treatment that induces the arrest of PC12 cells significantly reduced this phenomenon, preventing most PMO-SkpE14 treated cells to undergo apoptosis. In fact, a cell cycle analysis of these cells at 48 and 72h revealed no differences with control NGF treated cells, although at these time points only cells that didn't undergo apoptosis were actually being measured (data not shown).

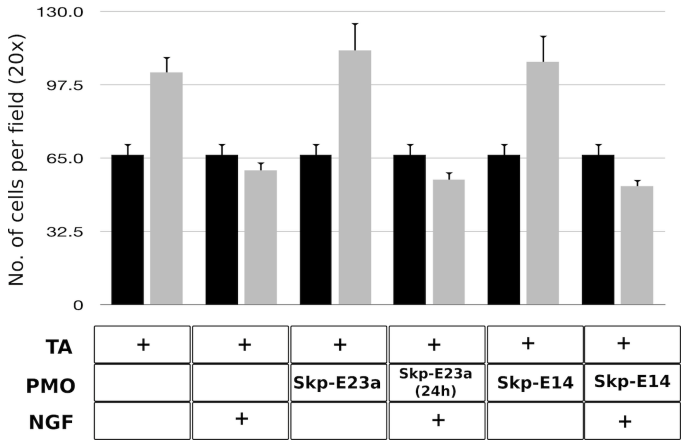

Figure 31: Cell number per field (20x) for the different experimental conditions at two different time points 3 and 48h. Error bars indicate ±SEM. No significant differences where detected. TA: Transfection agent.

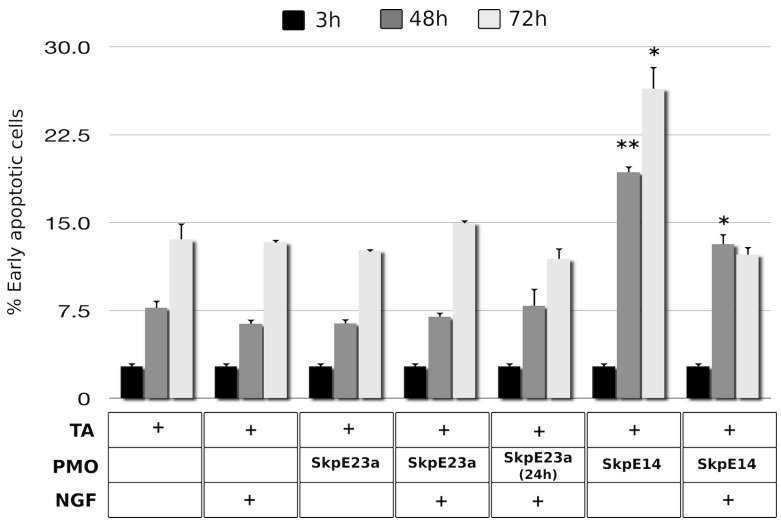

Figure 32: Percentatge of early apoptotic cells for the different experimental conditions at three time points (3,48 and 72h). Error bars indicate ±SEM. * $P < 0.05$, ** $P < 0.01$ as evaluated by paired *t*-test vs control cells only with transfection agent (TA). TA: Transfection agent.

Then we tested the effect of these new PMO treatments on the differentiation capacity of PC12 cells. Similar to our previous observations, the induction of type I isoform (-E23a) 24h before NGF treatment interfered with a correct differentiation process, with less number of differentiated cells (**Figure 33**) and reduced expression of differentiation markers (**Figure 35**). Moreover, in the case of cells treated with PMO-SkpE14 (with a significantly reduced neurofibromin levels) and NGF, the abnormal differentiation phenotype was even more extreme, and characterized by a reduction in the number of differentiated cells (**Figure 33**), abnormal extension of neurites (**Figure 34A**), the appearance of unknown thickness in the form of bubbles in the neurite extensions (**Figure 34B**) and reduced expression of differentiation markers (**Figure 35**).

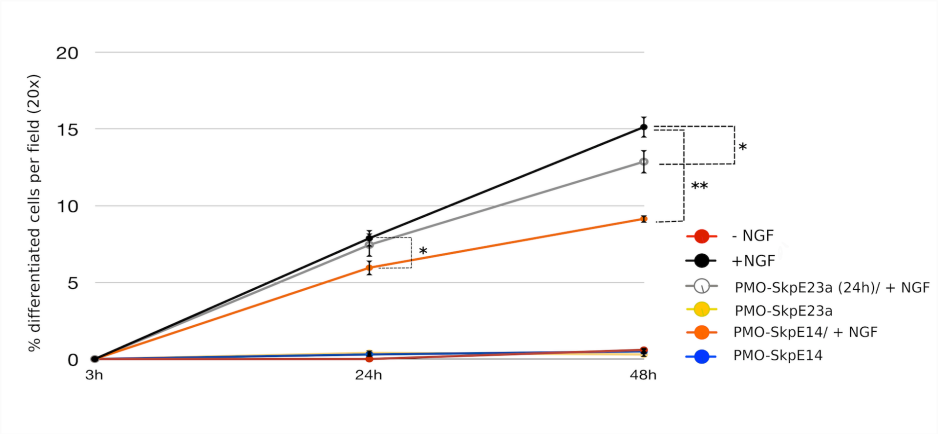

Figure 33: Percentage of differentiated cells per field (Phase-contrast, objective 20X) from the different experimental conditions at different time points (3, 24, 48h). Data are presented as the ±SEM. * $P < 0.05$, ** $P < 0.01$ as evaluated by paired *t*-test vs cells treated with NGF only.

Specifically, we got significant differences with two of the three differentiation markers (*Gap43* & *Dusp6*) for both conditions, the cells treated with PMO-SkpE23a (24h) and PMO-SkpE13 with NGF. In the case of *Mmp3,* due to the variability in the qPCR values we just observed a non-significative reduction in the case of cells treated with PMO-SkpE23a (24h) and higher levels for the cells treated with PMO-SkpE14 and NGF (**Figure 35**). In the literature, it has been reported that *Mmp3* is up-regulated in PC12 cells *NF1* knockdown (siNF1) after NGF treatment (Hirayama M et al., 2013). Enzymatic activity measured as NADH-dehydrogenase, was also reduced when PMO-SkpE23a was added to the cells 24h before NGF treatment (**Figure 35**). This assay was not performed in the case of NF1 knockdown conditions (PMO-SkpE14) due to the interference produced by the increase in apoptotic cells. To characterize in more detail these two altered phenotypes, we performed an immunofluorescence with α-tubulin and NGFR showing the abnormal formation of neurite extensions in both conditions (**Figure 36**).

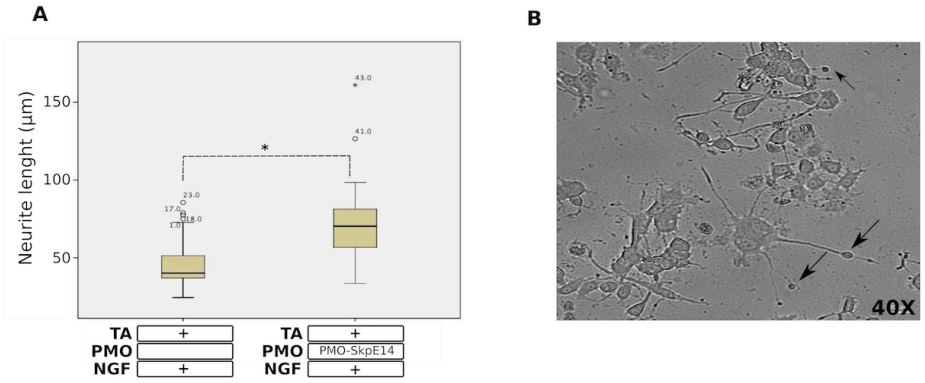

Figure 34: A) Box plot representation of the neurite length of PC12 cells treated with NGF or with the PMO-SkpE14 and NGF. Neurite length was determined with NeuronJ plugin for ImageJ. * $P < 0.05$ as evaluated by paired *t*-test. **B)** The black arrows indicate the unknown expansions in the neurite body when PC12 cells are treated simultaniously with PMO-SkpE14 and NGF.

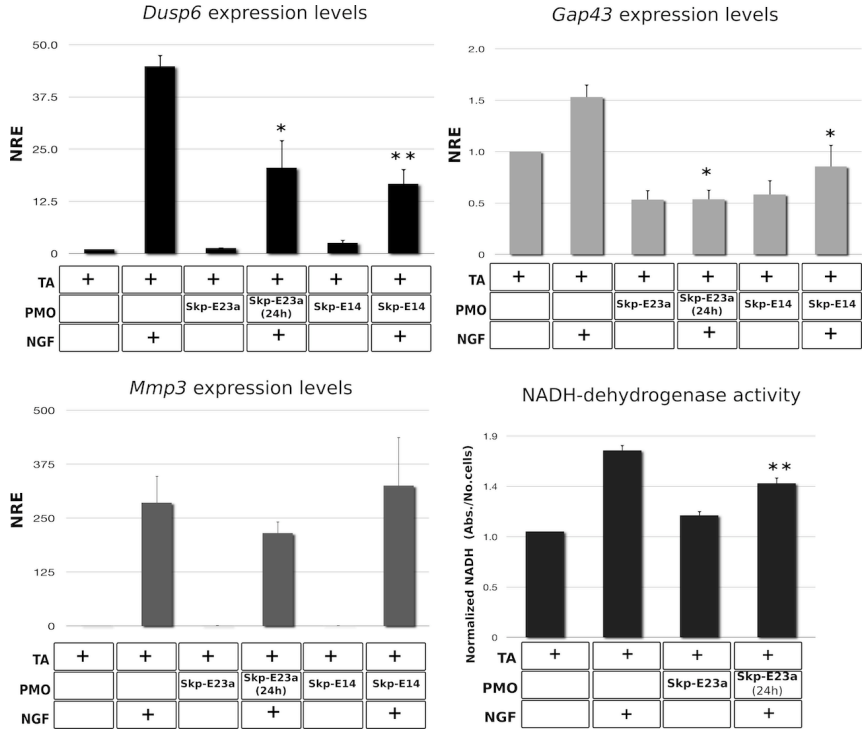

Figure 35: Both PMO treatments (PMO-SkpE23a 24h earlier and PMO-SkpE14 truncating NF1) altered the expression of neuronal differentiation markers upon NGF treatment. The graphs ilustrate the expression and of the differentiation markers (*Dusp6*, *Gap43*, *Mmp3*) and the enzymatic activity of NADH-dehydrogenase for different experimental conditions. Error bars indicate ±SEM. * $P < 0.05$, ** $P < 0.01$ as evaluated by paired *t*-test vs cells treated with NGF only. NRE: Normalized relative expression, TA: Transfection agent.

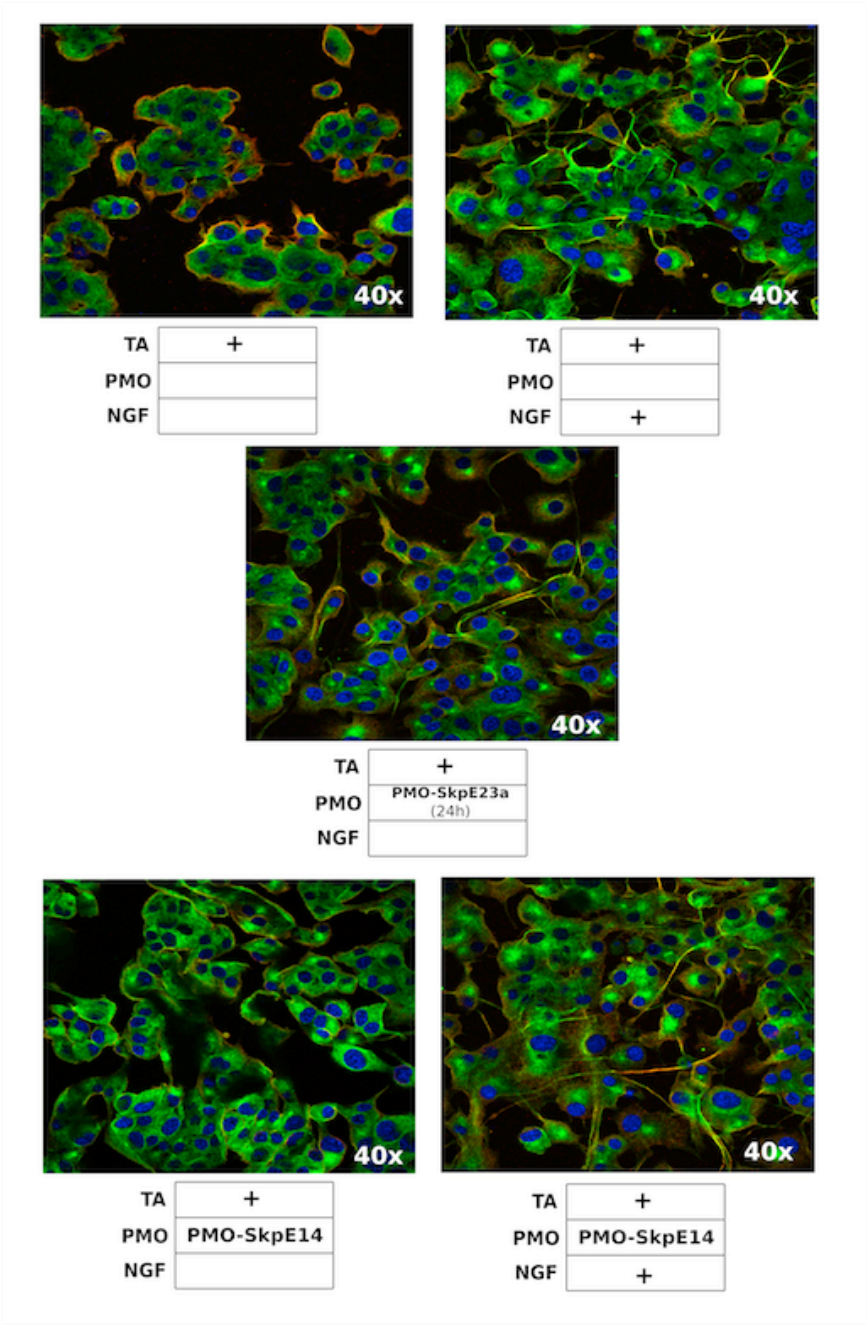

Figure 36: Double immunofluorescent staining of NGFR (red), α-tubulin (green) in PC12 cells in different experimental conditions. DNA was stained with Hoescht (Blue).

Results

Finally, the RAS/MAPK and the cAMP/PKA pathways were investigated. For this experiment we also included a condition in which PMO-SkpE23a was added at the same time as NGF treatment. Furthermore, in order to better monitor MAPK activation, a time course of phosphor-ERK was performed (**Figure 37A**). As shown before, a progressive increase in ERKs phosphorylation was observed after NGF treatment of PC12 cells. ERK phosphorylation levels were significantly reduced when PMO-SkpE23a was added at the same time as NGF, consistent with an increase proportion of type I neurofibromin, containing 10 times more GAP activity towards RAS. Surprisingly, in conditions where NGF was added after forcing the type II – I switch (PMO-SkpE23a 24h before) the levels of ERK phosphorylation were higher than control cells treated with NGF, reaching levels similar to those exhibited in PC12 cells treated with PMO-SkpE14 (neurofibromin knockdown). Furthermore, this pattern was also evidenced when measuring PKA phosphorylation levels at 48h after NGF treatment. Again, the induction of type II – I switch before NGF treatment (PMO-SkpE23a 24h) abolished the activation of cAMP/PKA pathway similarly and even more enhanced to conditions in which neurofibromin was depleted (PMO-SkpE14) (**Figure 37C**). These results concerning ERK and PKA phosphorylation seemed to indicate that when type II – I switch was induced by PMO before NGF treatment, upon induction of PC12 cell differentiation, neurofibromin function was apparently lost, since results were very similar to conditions in which neurofibromin was depleted (PMO-SkpE14).

However, when we looked directly to the levels of RAS-GTP (**Figure 37B**), we didn't observed an increase in RAS activity in these two conditions (PMO-SkpE23a 24h before and PMO-SkpE14), indicating an apparent decoupling between RAS activity and ERK phosphorylation, result that needs to be further investigated.

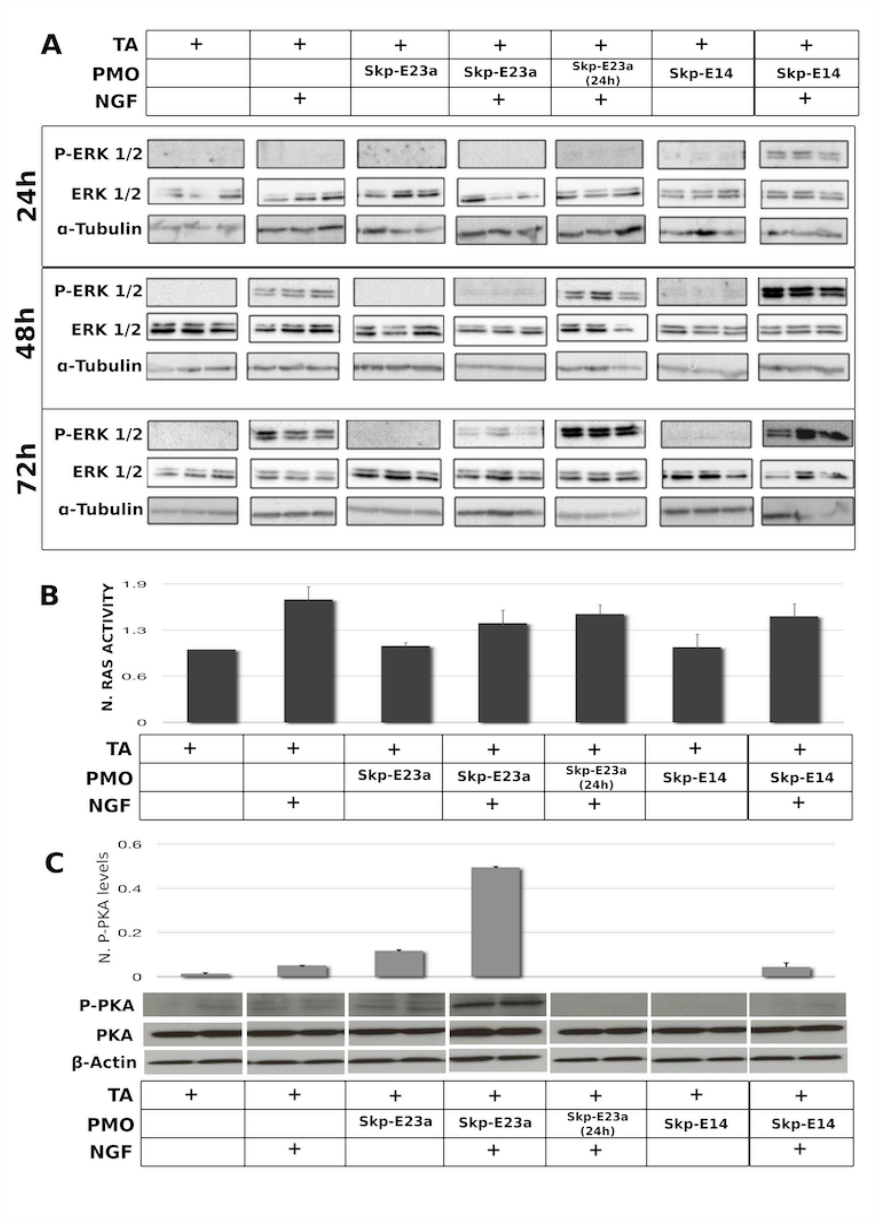

Figure 37: A) Time course analysis showing phospho-ERK 1/2 (42/44 kDa), total ERK 1/2 in lysates for the different experimental conditions and time points (24, 48 & 72h). The loading control was α-tubulin. **B)** RAS ELISA activation assay for the different experimental conditions at 48h. **C)** Western blot analysis of phospho-PKA and total PKA (40 kDa) in lysates from the different experimental conditions at 48h. The loading control was β-actin (42 kDa).

Results

The phosphorylation status of ERK 1/2 and PKA when PC12 cells treated 24h before with PMO-SkpE23a where induced to differentiate into neurons upon NGF addition was similar to the activation status of these kinases when PC12 cells were treated with SkpE14 and NGF. Thus, these results seemed to indicate that when type II/I switch was induced by PMO 24h before NGF addition to PC12 culture, neurofibromin function was apparently lost right after NGF differentiation induction. We hypothesized that a possible negative feedback was acting directly or indirectly on neurofibromin to suppress the abnormal high NF1-GAP activity, and downstream effects on signalling, in PC12 cells when neuronal differentiation was induced by NGF.

To better understand the biological status of PC12 24h after treatment with PMO-Skp23a, we used transcriptional information from an RNASeq analysis that we performed to understand the effect of the different PMOs (PMO-SkpE23a; PMO-Inc23a, PMO-skpE14) on PC12 cells in the presence or absence of NGF and at initial conditions (3h) or after 55h of NGF treatment (see material and methods). We compared the transcriptional profiles of PC12 cells treated for 24h with PMO-SkpE23a and control cells with no NGF, at initial conditions, and detected a signature of 57 genes that were differentially expressed by two-fold or greater between both conditions (**Figure 38**). We used this signature to compare these two conditions together with cells treated only with PMO-SkpE23a for 55h. This comparison revealed that this gene signature represented a transient transcriptional activation response due to PMO-SkpE23a treatment (forcing Type II / I switch and increasing NF1-GAP activity) that was present at 24h but recovered to a normal control state at 55h, although skipping of E23a was still present and even more enhanced (**Figure 38A**). Among the genes differentially expressed after forcing Type II / I switch before NGF treatment two of them were

highly over expressed and recovered to normal levels after 55h (marked in green in **A**, **B** of **Figure 38**). These two genes, *Egr1* and *Fosl1*, are related to an NGF early response (DeFranco C et al., 1993; Ito E et al., 1990). It has been described constitutive expression of *Fosl1* in PC12 cells results in pronounced inhibition of NGF-induced differentiation (Ito E et al., 1990). We also found a group of genes, that didn't return to the original levels of expression after 55h (marked in orange and purple in **figure 38 A, B**). Then the expression pattern of these differentially expressed genes was applied to the whole RNA-Seq experiment (**Figure 39**). We detected four different clusters (1A, 1B, 2A and 2B), where gene enrichment was performed using DAVID functional annotation tool (Huang DW et al., 2009a; Huang DW et al., 2009b) although no gene enrichments were found for these clusters. However, most of the genes contained in these clusters were transcriptionally regulated in the same manner that NGF treatment produced in PC12 cells. In fact, some of these genes have been shown to be implicated in NGF-triggered differentiation, like the transcriptional repressor *Nab2* (Houston P et al., 2001; Qu Z et al., 1998).

The transient overexpression profile identified after 24h of treatment with PMO-SkpE23a that partially overlap with NGF-response genes, in one hand enhances the importance of NF1-E23a alternative splicing in the NGF-triggered neuronal differentiation, and in the other, supports the hypothesis that the biological state of PC12 cells after 24h of PMO-SkpE23a treatment (consistent with the new and transient transcriptional status) facilitates a negative feed-back triggered by NGF treatment that acts suppressing neurofibromin function.

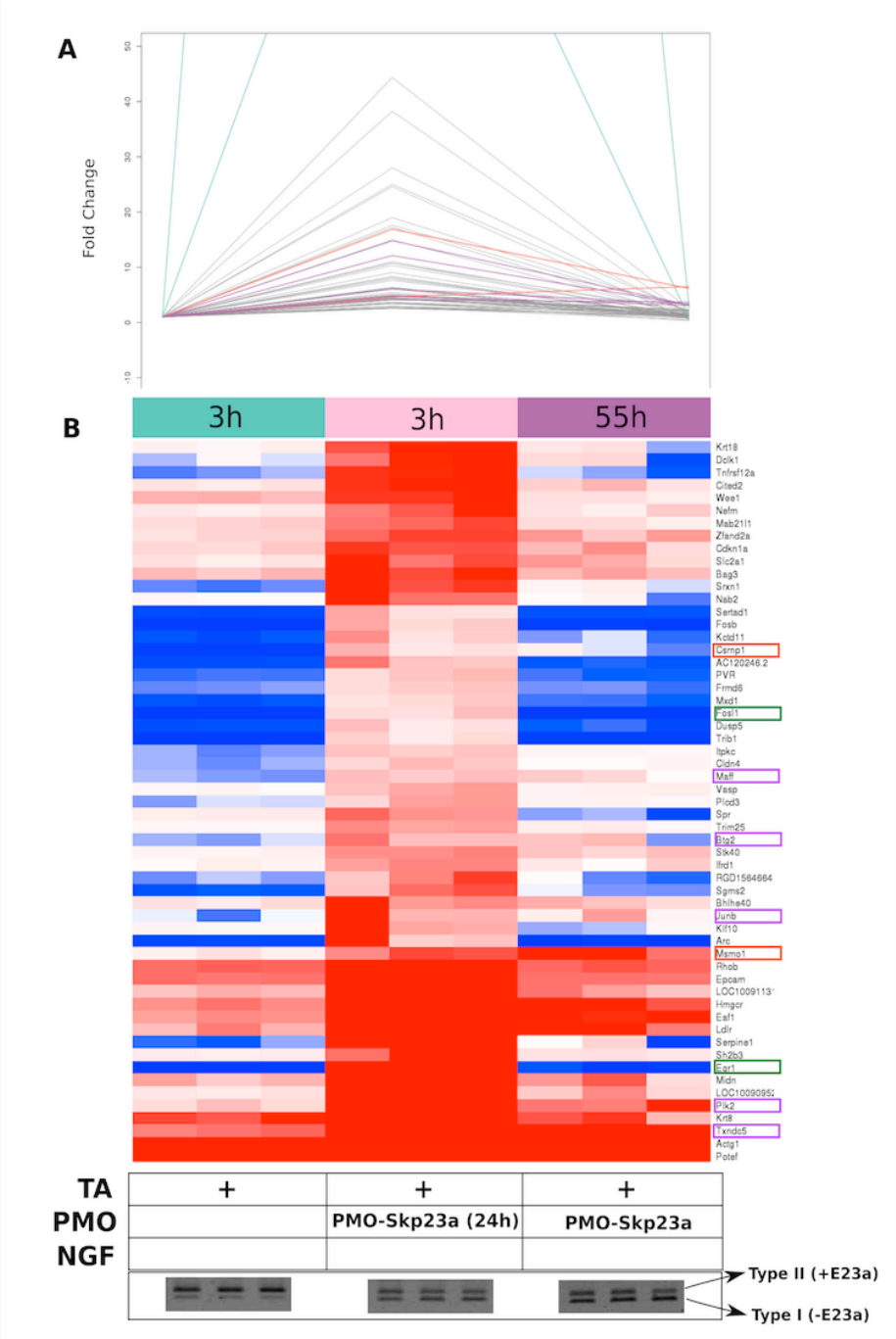

Figure 38: A) Expression patterns (represented by fold change) for the different experimental conditions at 3h and 55h. Genes which were up regulated at 3h and returned to original levels at 55h are marked in green lines, genes up regulated at 3h but that don't return to the original levels at 55h are marked in orange and purple lines. **B)** Heat map of differentially expressed genes (FC >2) in the presence or absence of PMO-SkpE23a at 3h and at 55h. Genes referred in A are marked with the same code of colors.

TA	+	+	+	+	+	+	+	+	+	+	+
PMO		PMO-Skp23a (24h)		PMO-Inc23a	PMO-Skp14	PMO-Skp23a		PMO-Inc23a	PMO-Skp14	PMO-Skp23a (24h)	PMO-Skp23a
NGF							+	+	+	+	+

Figure 39: Heat map of differentially expressed genes in the presence or absence of PMO-SkpE23a 24h before NGF at 3h for all the experimental conditions. Clusters are marked with black and yellow squares

Dissociating NGF-induced neuronal differentiation from the alternative splicing of Exon23a of the *Nf1* gene: forcing the expression of Type II isoform (E23a inclusion).

Correct neuronal differentiation of PC12 cells seemed to be produced by an accurate time dependent regulation of RAS/MAPK signaling (and probably also of the cAMP/PKA pathway), that in turn was dependent on the correct temporal regulation of alternative splicing of E23a of the *Nf1* gene. At the same time, the knockdown of neurofibromin levels by PMO-SkpE14 also altered the correct neuronal differentiation phenotype and the adequate RAS/MAPK signaling.

To further investigate on the relationship of the regulation of the alternative splicing of E23a and the function of neurofibromin on PC12 neuronal differentiation we decided to analyze PC12 differentiation by forcing the expression of type II isoform, that is, inhibiting the skipping of E23a upon NGF treatment (switch from type II to I isoforms), while preserving the correct splicing of the exons and the *Nf1* gene. Although at experimental level it is relatively easy to use PMOs to trigger the skipping of an exon, inducing the inclusion of an exon during natural skipping conditions of an alternatively spliced exon had not been reported before by using PMOs.

In silico analysis of exon 23a alternative splicing regulation and expression analysis of splicing factors CELF3 and MBNL1/2

As mentioned in the introduction, it has been established that exon 23a (E23a) is differentially spliced and predominantly skipped in neurons (Gutmann D et al., 1999). The intronic sequences surrounding E23a are highly enriched in AU-rich & UG-rich sequences, which have been shown to be the binding sites of Hu and

CELF proteins (E23a skipping promoters) (Barron V et al., 2009) and TIA-1/R or MBNL proteins (E23a inclusion promoters) (Fleming V et al., 2012). Although it is still not fully understood how conserved intronic sequences contribute to splicing regulation, it is known and accepted that alternative exons are under the regulation of different combinations of splicing factors. Moreover, significant number of alternative exons identified to be regulated in brain or muscle, have been associated with conserved adjacent intronic sequences (Sugnet CW et al., 2006). Intronic conservation has been described around several *Nf1* alternatively spliced exons (9br, 10a-2, 23a, 23b and 48a), with E23a having the largest intronic regions with high sequence identity (Kaufmann D et al., 2004). In light of these studies, we corroborated this information by comparing the conservation of E23a flanking introns with the surrounding constitutive exons, using conservation data of 100 vertebrates displayed by the University of California Santa Cruz (UCSC) genome browser (Kent WJ et al., 2002) (**Figure 40**).

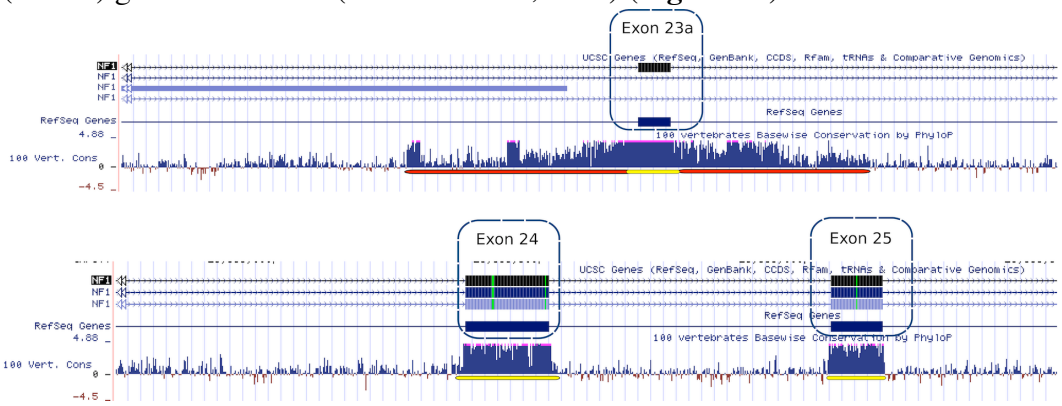

Figure 40: High conservation levels (100 vertebrates data) in flanking intronic sequences (red band) of exon 23a (yellow band). In contrast, non-intronic conservation was not detected flanking other constitutive exons (yellow band E24 and E25) around E23a. Data displayed in UCSC genome browser (Kent WJ et al., 2002).

Next, to better characterize the regulation of this alternatively spliced exon in PC12 cells, we studied the expression of splicing factors that were known to regulate E23a inclusion or exclusion. For this purpose a qPCR assay was designed to analyze the expression of *Celf3* a factor that promotes E23a skipping (Zhu H et al., 2008; Barron VA et al., 2010) and of *Mbnl1* and *Mbnl2* (Fleming VA et al., 2012) two factors that promote E23a inclusion. The relative expression levels were normalized against ribosomal proteins (*Rpl19* & *Rpl29*). We observed an opposite expression of these splicing factors depending on the differentiation state of PC12 and E23a skipping levels. In the case of C*elf3*, the expression was increased from 24h to 48h, as expected for a E23a skipping promotor (**Figure 41**). It has been described by others that over-expression of *Celf3* results in high levels of E23a skipping (Barron V et al., 2009). Regarding splicing factors *Mbnl1* and *Mbnl2*, the expression was down-regulated from 24 to 72h (**Figure 41**).

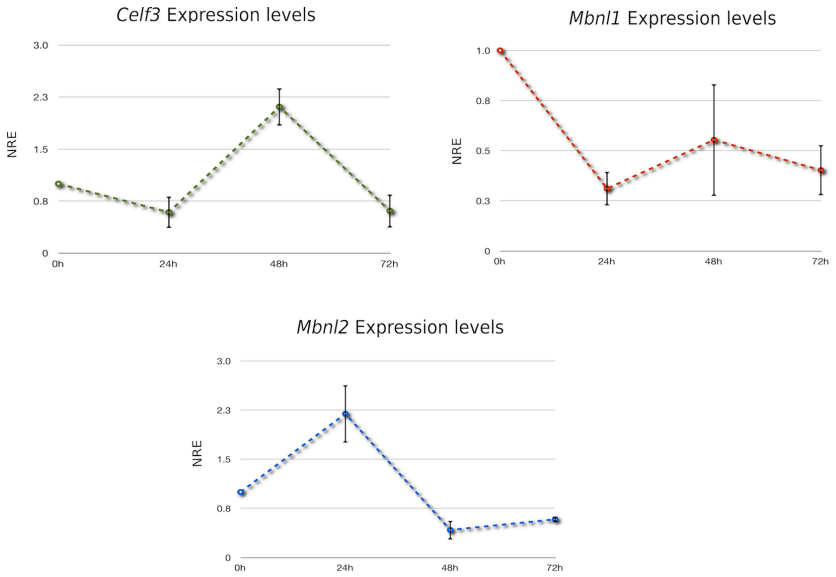

Figure 41: Relative expression of splicing factors *Celf3*, *Mbnl1* and *Mbnl2* (± SEM; normalized against *Rpl19* and *Rpl29*) in a time course of 72h of PC12 NGF-induced differentiation.

Set up of a PMO-based system for inducing the inclusion of exon 23a

Using *in silico* approaches we determined the potential binding sites for splicing factors surrounding E23a genomic region. Splice Aid2 (Piva F et al., 2011) is a bioinformatic tool that allows the assessment of the target RNA sequences that are bound by splicing proteins in humans. Although this tool was designed only for human sequences, the high levels of conservation in intronic and exonic sequences observed in the E23a region in different species made us assume that the molecular mechanisms and the splicing factors were highly conserved between human and rat and thus potentially also function in PC12 cells. With this data, information from literature and the results obtained with the qPCR expression analysis of the splicing factors (*Mbnl1/2* and *Celf3)* in PC12 cells, we identified the potential intron sequences with E23a regulatory skipping capacity. We were able to establish three different regions within the intronic sequence 5' to E23a (**Figure 42**), which bind most of the factors that promote its exclusion (mainly protein families Hu and CELF). These regions of interest were called Conserved Splicing Regions (CSR).

We designed and tested three PMOs in order to block and restrict the access of proteins promoting E23a skipping in the presence of NGF. We checked their functioning in PC12 cells (+NGF) using a concentration of 20 μM during 72h. As shown in **figure 43A**, we were able to stop NGF-triggered E23a skipping using a PMO targeting CSR II region. We termed this PMO-IncE23a and we discarded PMOs for CSR III and CSRI regions because they were not able to stop the skipping associated with NGF differentiation. PMO for CSRIII had even a higher efficiency in inducing E23a skipping compared with control cells (+NGF). This high levels of E23a skipping were also detected when PC12 were treated with the

combination of three PMOs (**Figure 43**). Thus blocking the intronic region CSR III had a dominant effect in E23a skipping over the effect of the other PMOs.

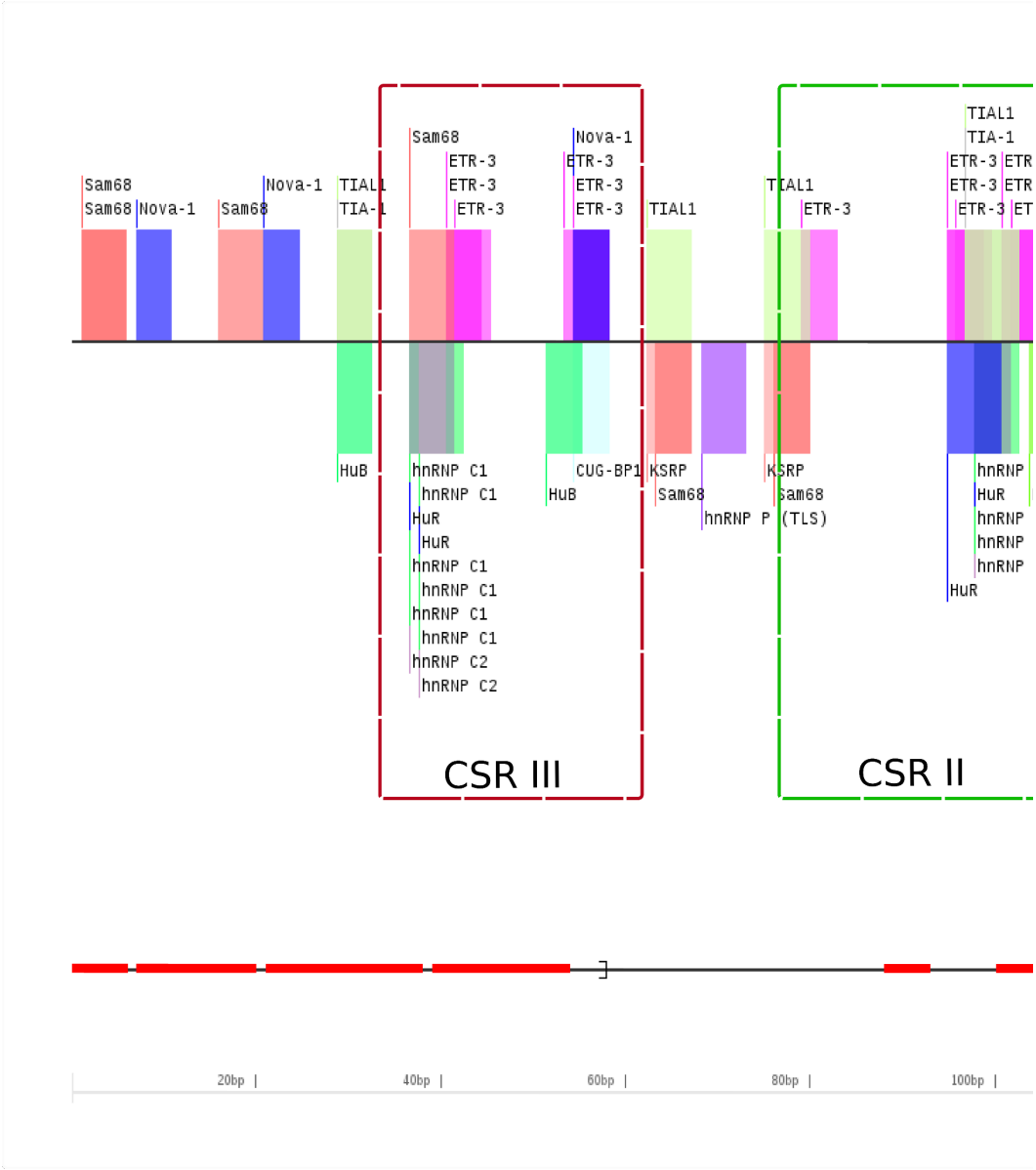

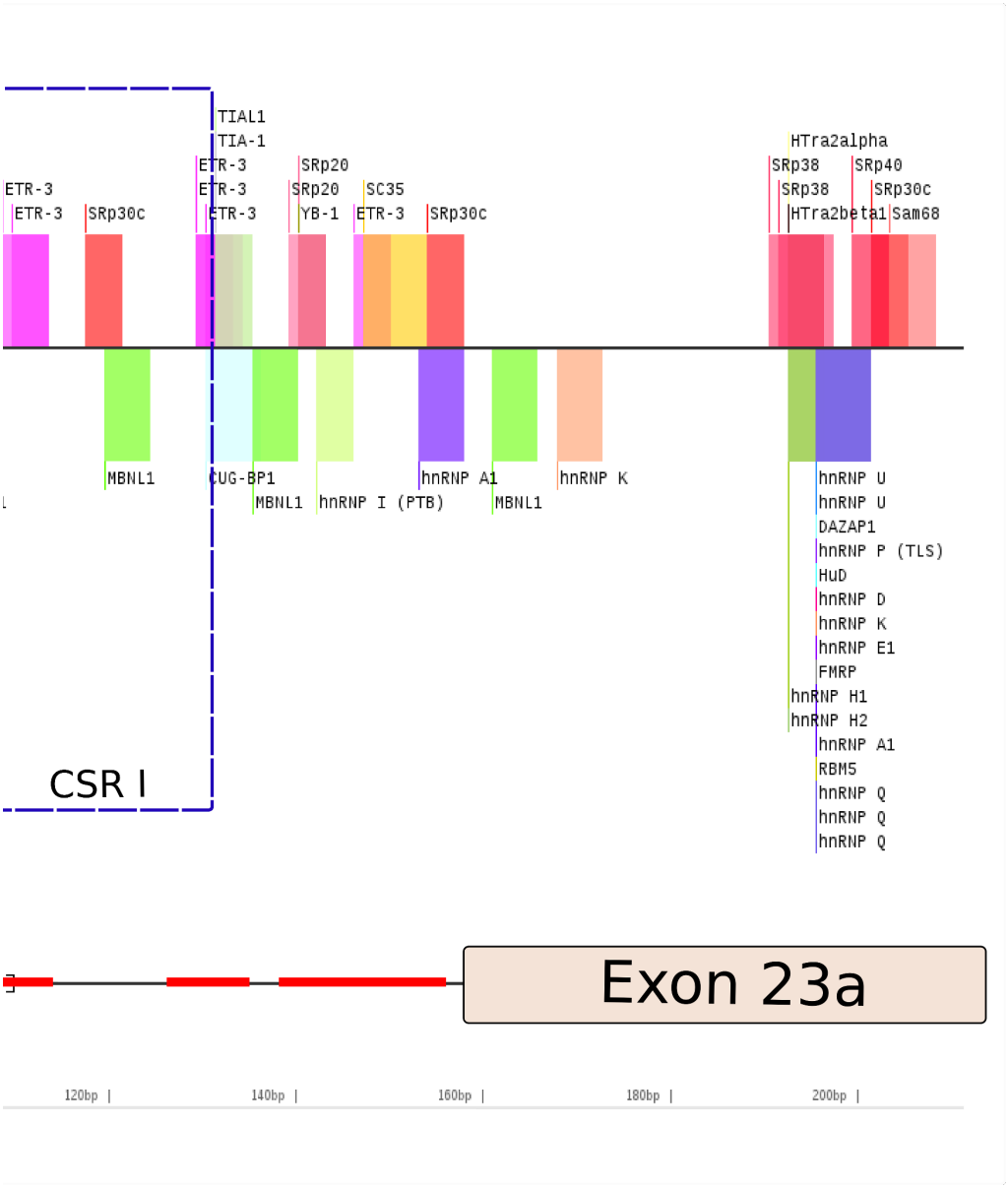

Figure 42: Highly conserved intronic regions 5' of E23a and the splicing factors predicted to bind to them, using Splice Aid2. The boxes represent the three regions that we selected in order to block with a specific PMO. CSR: Conserved Splicing Region.

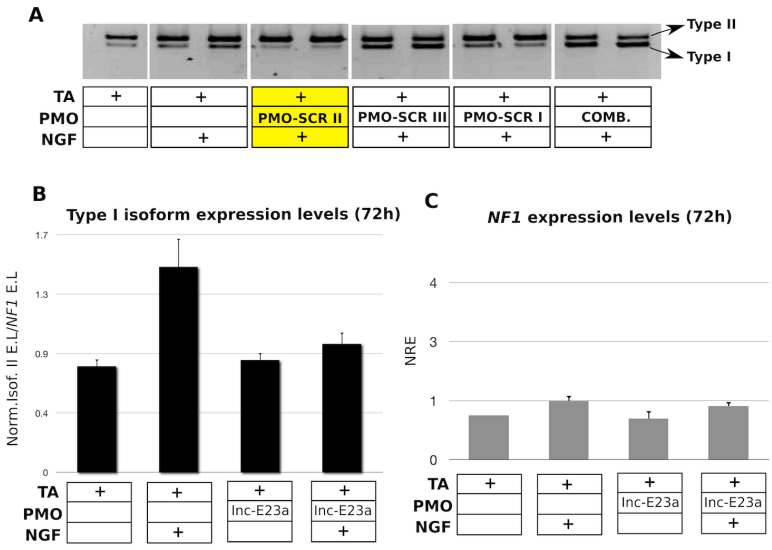

Figure 43: **A)** Analysis of *Nf1* mRNA of E23a splicing using three types of blocking PMOs (CSR I, II & III) and their combination (COMB) at 72h after NGF treatment. **B)** Normalized type I expression levels against total *Nf1* expression levels. Error bars represent ±SEM. **C)** *Nf1* expression levels at 72h. There is no significant variation with the use of the PMO-IncE23a. Error bars represent ±SEM.

Once the PMO for inducing E23a inclusion was selected (PMO-IncE23a), we tested its efficiency by measuring the levels of isoform type I using the previously designed qPCR analysis (see Results section 2). Isoform type I levels were normalized against total *Nf1* expression levels. When we treated PC12 with or without NGF for 72h in the presence of the PMO-IncE23a, we obtained the same levels of isoform type I expression as control cells (-NGF) and reduced with respect to PC12 cells treated with NGF (**Figure 43B**). In addition, we wanted to analyze whether the expression of *Nf1* gene was modified or not by the use of PMO-IncE23a. In this regard, no significant variation of *Nf1* gene expression was detected when analyzing total expression of the *Nf1* gene by qPCR (**Figure 43C**).

Functional characterization of neuronal differentiation of PC12 cells expressing *Nf1* Type II isoform

In order to study the neuronal differentiation process when forcing the expression of isoform type II (+ E23a, low activity RAS-GAP), PC12 cells were treated with and without PMO-IncE23a in the presence or absence of NGF for 72h. After 72h, PC12 where collected, RNA extracted and an RT-PCR was performed to evaluate the NF1 alternative splicing of E23a. As expected, in the cells treated with PMO-IncE23a the levels of isoform type I were like in the control (-NGF) and we detected elevated levels of this isoform only in the cells treated with NGF (**Figure 44**).

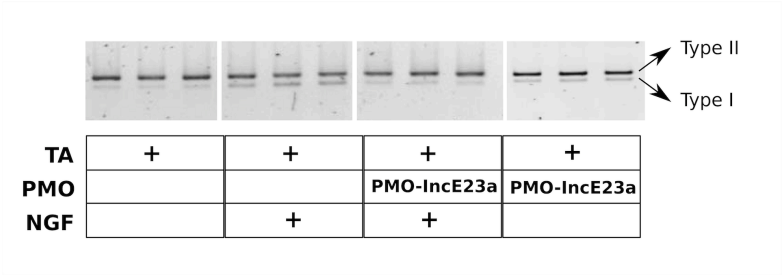

Figure 44: RT-PCR analysis of *Nf1* mRNA of E23a splicing for the different experimental conditions at 72h. The shorter transcript corresponds to the isoform type I (-E23a) and the longer one to isoform type II (+ E23a).

At the proliferation level, no differences in the number of cells was observed when PC12 cells were treated or not with PMO-IncE23a (**Figure 45**). In addition, there was no difference in the NGF-triggered cell cycle arrest in PC12 cells treated or not with PMO-IncE23a (**Figure 45**). However, certain level of cell death was observed in cells treated with PMO-IncE23a. To better measure this cell death phenomenon we determined the percentage of early apoptotic cells as before. For comparative purposes we also added conditions with PMO-SkpE14, forcing a knockdown in neurofibromin levels. In contrast to cells treated with

PMO-SkpE14 we observed a significant percentage of early apoptotic cells in PMO-incE23a treated cells only when NGF was not added. When in PMO-IncE23a treated cells NGF was added, cells arrested and no early apoptosis was detected (**Figure 46**).

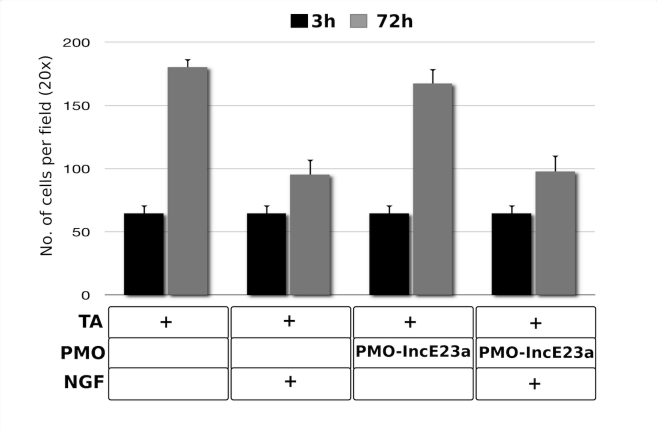

Figure 45: Cell number per field (20x) for the different experimental conditions at two different time points 3 and 72h. Error bars indicate ±SEM. No significant differences where detected.

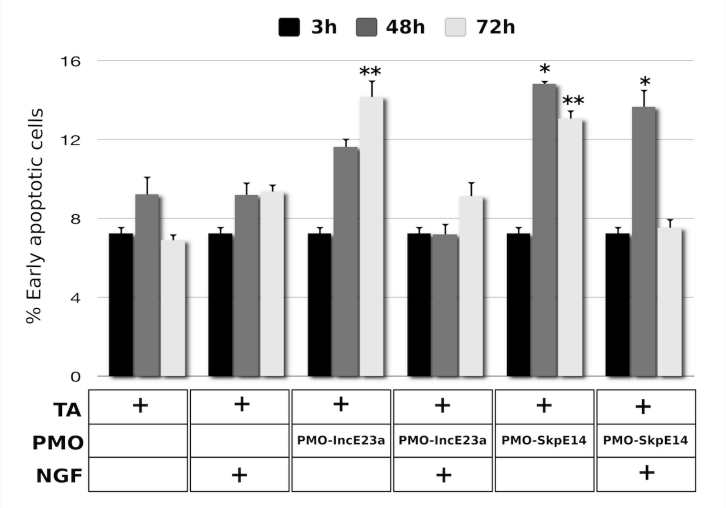

Figure 46: Percentatge of early apoptotic cells for the different experimental conditions at three time points (3,48 and 72h). Error bars indicate ±SEM. * $P < 0.05$, ** $P < 0.01$ as evaluated by paired *t*-test vs control cells only with transfection agent (TA).

Inhibiting the switch from type II to type I isoform upon NGF treatment (by forcing the inclusion of E23a) didn't alter the proportion of PC12 cells that extended neurites compared to the cells treated only with NGF (**Figure 47**). However we detected a clear reduction in the complexity and thickness of the neurites (**Figure 49**) and also a reduction in the expression of neuronal differentiation markers (**Figure 48**). Particularly, we got significant differences with two of the three differentiation markers, *Gap43* and *Mmp3*. To better characterize this phenotype we performed an immunofluorescence staining using ß-tubulin and NGFR antibodies. We observed that cells treated with NGF and PMO-IncE23a had a reduced thickness of the neurite and diffuse ß-tubulin pattern in the neurite body (**Figure 49**).

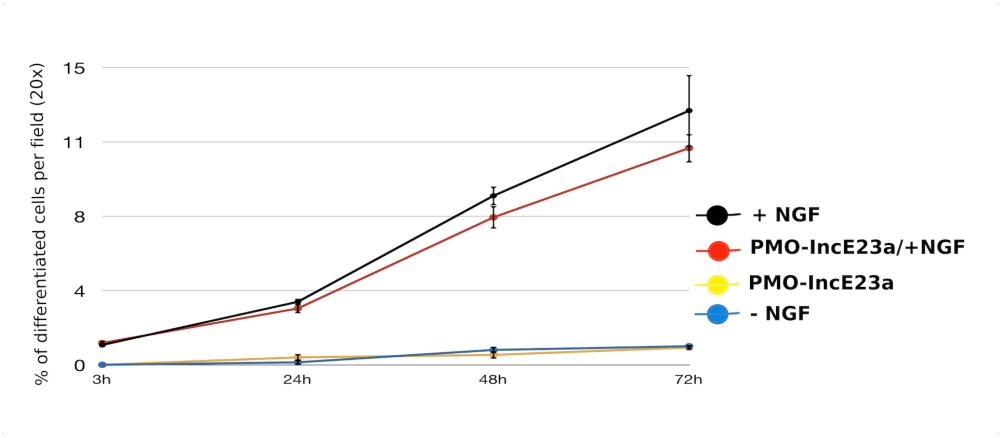

Figure 47: Percentage of differentiated cells per field (Phase contrast, objective 20x) from the different experimental conditions at different time points (3, 24, 48 and 72h). No significant differences were observed between cells treated with NGF only and cells with PMO-IncE23a in the presence of NGF.

Therefore, not only modifying the time-dependent regulation of the alternative splicing by forcing an earlier switch from type II (+E23a) to I (-E23a) isoform was interfering in the proper differentiation process but also this aberrant differentiation was produced by impeding the switch upon NGF treatment.

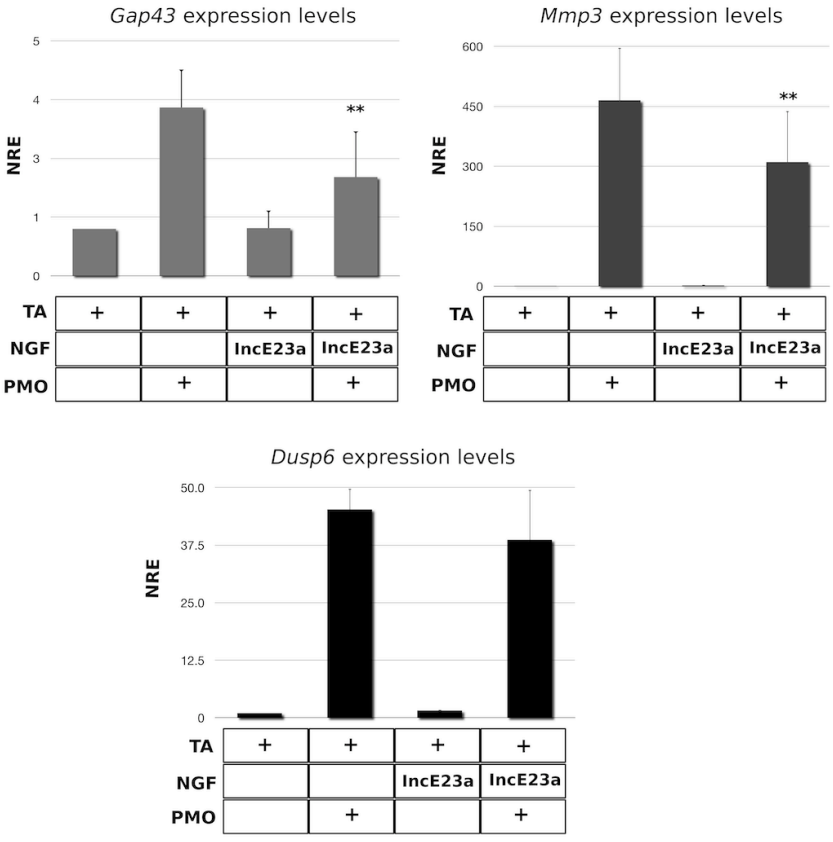

Figure 48: Cells in which expression of isoform type II was forced, showed an altered differentiation process. The graphs illustrate the expression of the differentiation markers *Dusp6*, *Gap43* and *Mmp3* for different experimental conditions. Error bars indicate ±SEM. * $P < 0.05$, ** $P < 0.01$ as evaluated by paired *t*-test against cells treated with NGF only. NRE: Normalized relative expression, TA: Transfection agent.

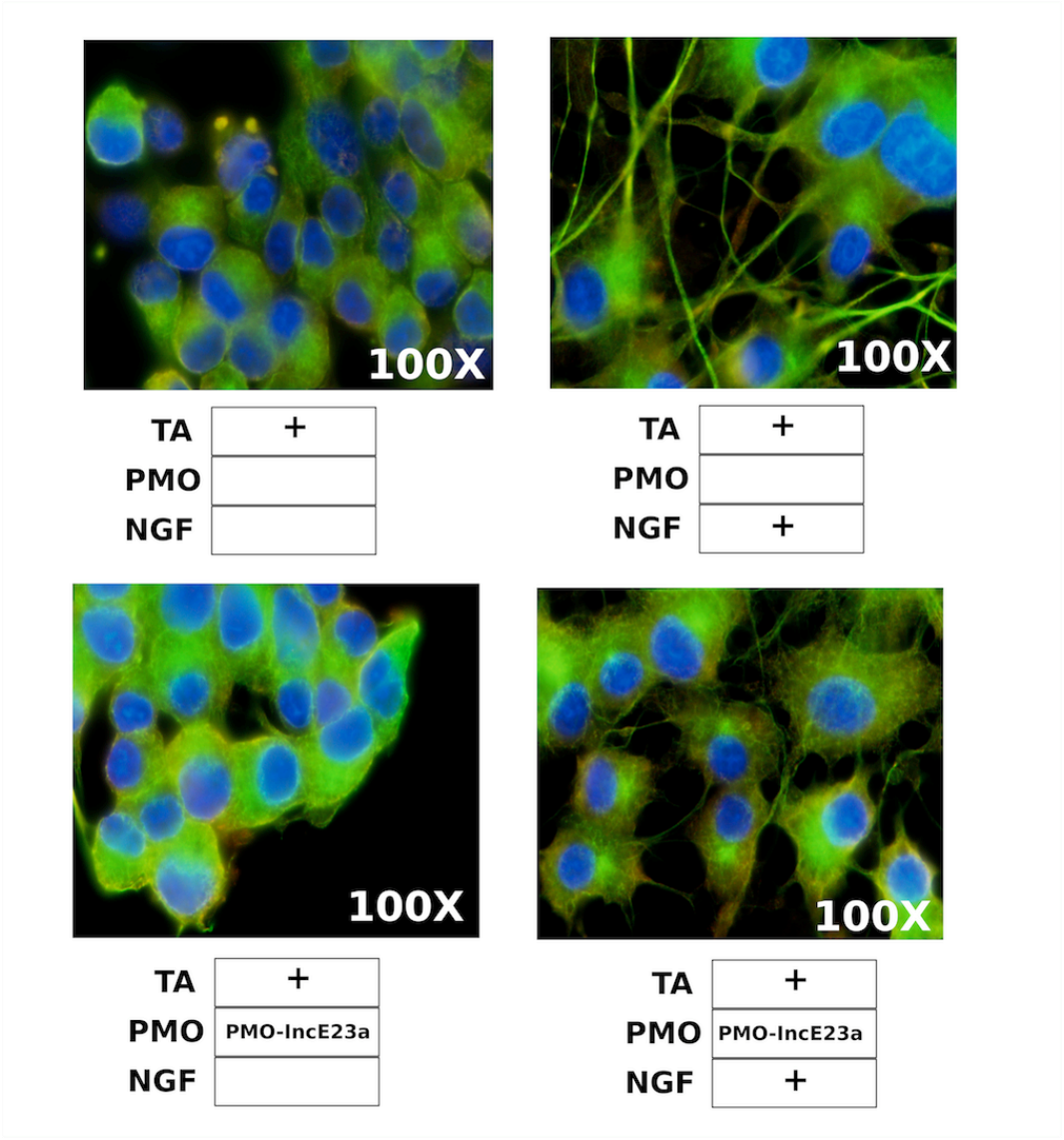

Figure 49: Double immunofluorescence staining of NGFR (red), α-tubulin (green) in PC12 cells in different experimental conditions. A reduction in neurite complexity and thickness can be observed in PC12 cells treated with PMO-IncE23a and NGF, compared to NGF alone. DNA was stained with Hoescht (blue).

Results

We also analyzed the activation of the RAS/MAPK and cAMP/PKA pathways in these conditions (**Figure 50**). We didn't observed at 72h after NGF treatment any change in the levels of ERK phosphorylation or RAS activation when comparing PMO-IncE23a treated cells plus NGF and PC12 cells treated only with NGF. At 48-72h there was no apparent differences, despite type II isoform preserve a decreased GAP activity compared to type I isoform. In contrast we indeed detected a high decrease in the phosphorylation levels of PKA in cells treated with PMO-IncE23a and NGF, compared to NGF alone. This result was consistent with the ones obtained for PMO-SkpE23a, and reinforced the link between the GAP activity of neurofibromin and the regulation of the cAMP/PKA pathway.

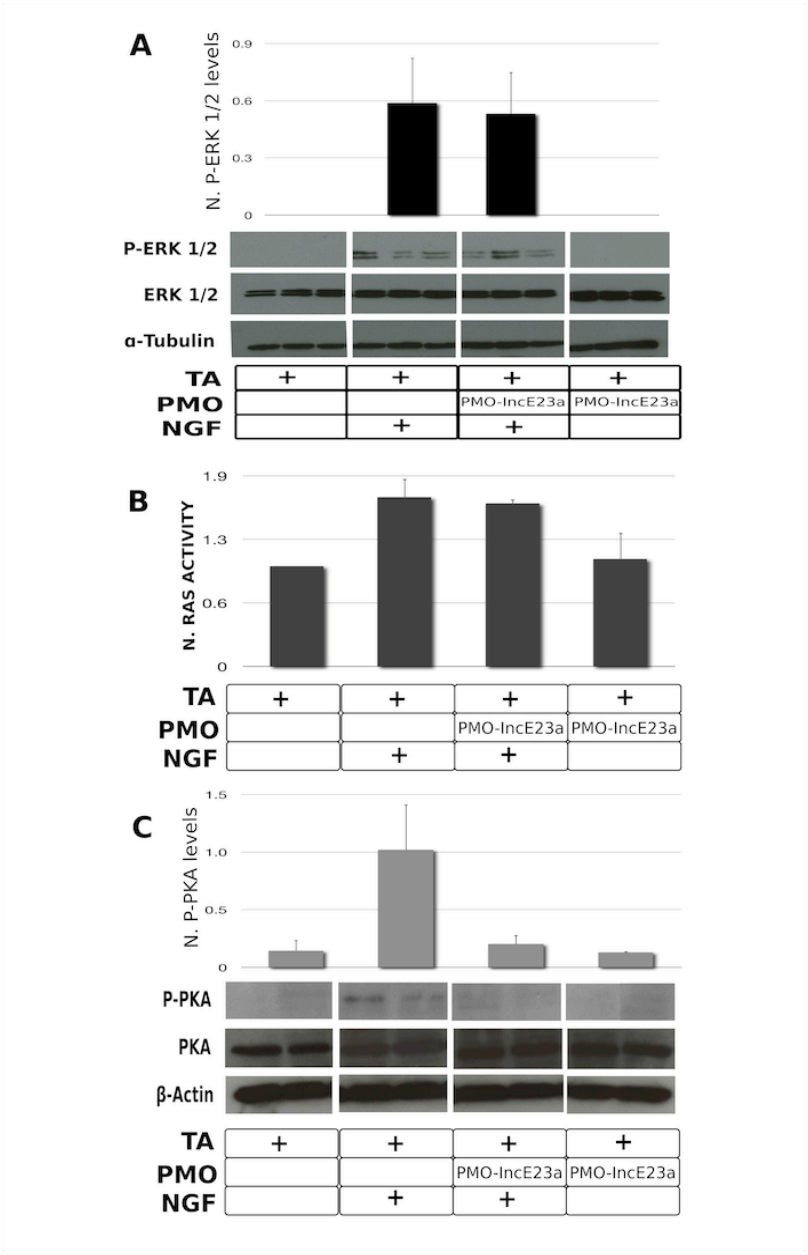

Figure 50: A) Western blot analysis of phospho-ERK1/2 and total ERK1/2 (42/44 kDa) in lysates from the different experimental conditions at 72h. The loading control was α-tubulin (50 kDa) **B)** RAS ELISA activation assay for the different experimental conditions at 48h. **C)** Western blot analysis of phospho-PKA and total PKA (40 kDa) in lysates from the different experimental conditions at 48h. The loading control was β-actin (42 kDa). Error bars indicate ±SEM.

Modulation of Exon23a alternative splicing in other differentiation model systems

Set up of a neuronal differentiation model system based on hippocampal H19-7 cell line

To assess whether the results obtained were restricted to the PC12 neuronal differentiation model used, we decided to investigate the modulation of alternative splicing of exon 23a through the use of PMOS in another model of neuronal differentiation and determine whether the observed phenotypes were specific to PC12 cells or a more general phenomenon. The H19-7 cell line (CRL-2526) was derived from a rat hippocampal cells and was conditionally immortalized with a temperature-sensitive SV40 large T antigen. Like PC12 cells, H19-7 cells respond differentially to Epidermal Growth Factor (EGF) and Fibroblast Growth Factor (FGF). At a permissive temperature (33ºC), EGF treatment induces proliferation, whereas at the non-permissive temperature (39ºC), addition of basic Fibroblast Growth Factor (bFGF) induces differentiation (Akchice N et al., 2010). We first characterized the effects of bFGF-mediated differentiation in H19-7 and examined the morphological changes associated with this process. As expected, in the absence of bFGF at 33ºC, no differentiation was observed and H19-7 cells remained in their characteristic fibroblastic morphology. In contrast, in the presence of bFGF at 39ºC, cells started to extend neurites and increase the cell body size (**Figure 51A**).

It has been described that bFGF activate high expression levels of ERK 1/2 after induction of differentiation similar to the prolonged activation of MAPK reported in PC12 cells (Akchice N et al., 2010; Kuo WL et al., 1996). We first analysed the expression of *NF1* mRNA isoforms by RT-PCR at non-differentiated (-bFGF at

33ºC) and differentiated (+bFGF at 39ºC) conditions. As shown in **figure 51B**, at 39ºC the switch from type II to type I was already observed at 24h after bFGF-triggered differentiation.

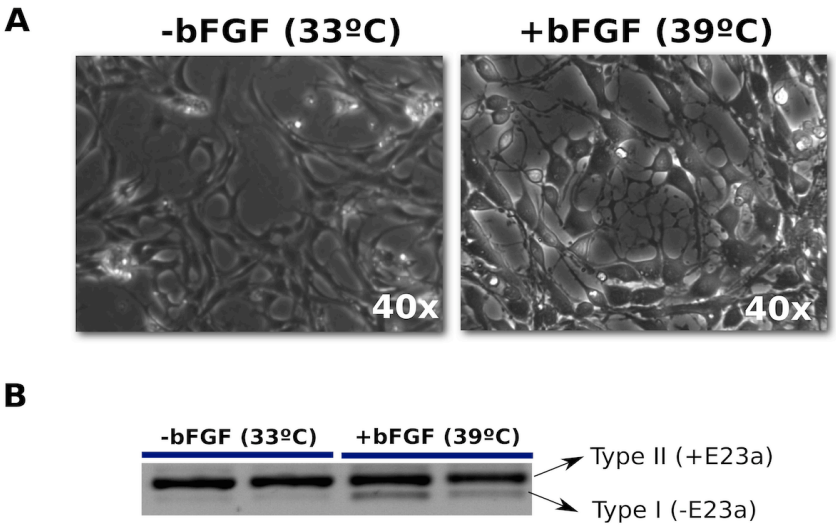

Figure 51: A) Phase contrast micrographs (40x) of hippocampal H19-7/IGF-IR cells in absence (33ºC) or presence (39ºC) of bFGF at 24h. **B)** In H19-7, the bFGF treatment at 39ºC induces a switch of *NF1* isoform I (+E23a) to II (-E23a) at 24h**.**

We then set up specific proliferation and differentiation assays adjusted to this neuronal differentiation model. In particular differentiation was assessed with a quantitative PCR (qPCR) analyzing the specific differentiation marker Dual Specificity Phosphatase 6 (*Dusp6*). Morphological changes of differentiating H19-7 cells were evaluated by performing α-Tubulin immunofluorescence staining that was monitored using LEICA-DMI 6000B fluorescence microscope. Cell proliferation was determined by automatic particle counting (ImageJ) with Hoescth nuclei staining (images at 20x field).

Functional characterization of neuronal differentiation in H19-7 forcing the expression of *Nf1* Type II or Type I isoforms

Using the H19-7 neuronal differentiation model we tested the effect of forcing the two *Nf1* alternatively spliced isoforms together with the knockdown of neurofibromin, using PMOs. The H19-7 cells were treated with 20μM of the different PMOs (Skp-E23a, Inc-E23a and Skp-E14). After 30h of bFGF-induced differentiation, total RNA was extracted in order to determine exon E23a skipping or inclusion levels for all the different PMOs treatments. As shown in figure 49, PMO-SkpE23a and PMO-Skp14 were highly efficient in the induction of exon skipping (E23a and E14 respectively). PMO-IncE23a was not as efficient as for PC12 cells in promoting E23a inclusion. However, this PMO was also useful for partially preventing the skipping of E23a upon bFGF-triggered differentiation of H19-7 cells (**Figure 52**).

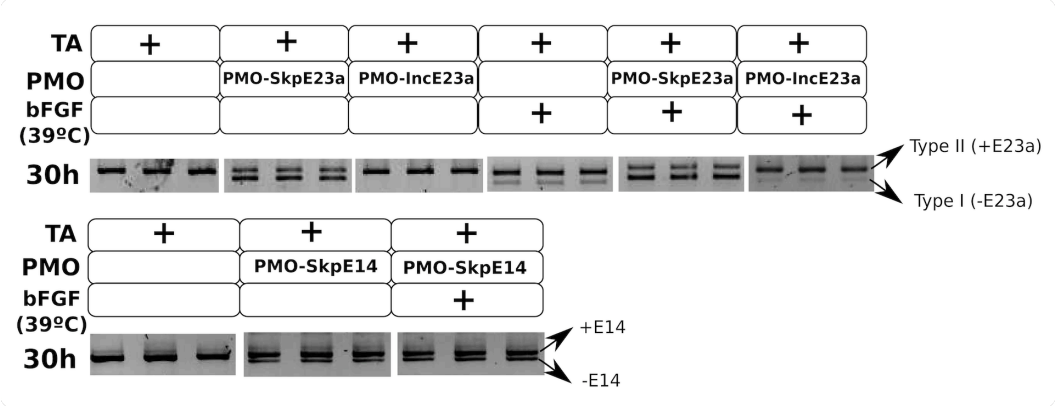

Figure 52: Analysis of *Nf1* mRNA E23a splicing and E14 skipping for the different experimental conditions at 72h. In the upper image, the shorter transcript corresponds to the type I isoform (-E23a) and the longer one to the type II isoform (+ E23a). In the lower image the shorter transcript corresponds to the lack of E14 and the longer to the addition of E14. TA; Transfection agent.

We then analyzed the effect of the different PMOs on the viability and differentiation capacity of H19-7 cells. As illustrated in **figure 53**, after 24h of treatment with bFGF at 39ºC we observed a strong reduction in the viability (decrease in cell number) for all the experimental conditions. It has been reported in the literature that after 24h of bFGF-mediated differentiation the cell death in H19-7 cells is around 60% and almost 80% after 48h (Akchice N et al., 2010; Sun Y et al., 2010). We also reported a decrease in cell viability associated to the differentiation process. However, in the case of PMO-SkpE14 treated-cells, the levels of cell death were higher than the ones treated only bFGF, consistent with results obtained after forcing E14 skipping (reduced neurofibromin levels) in PC12 cells.

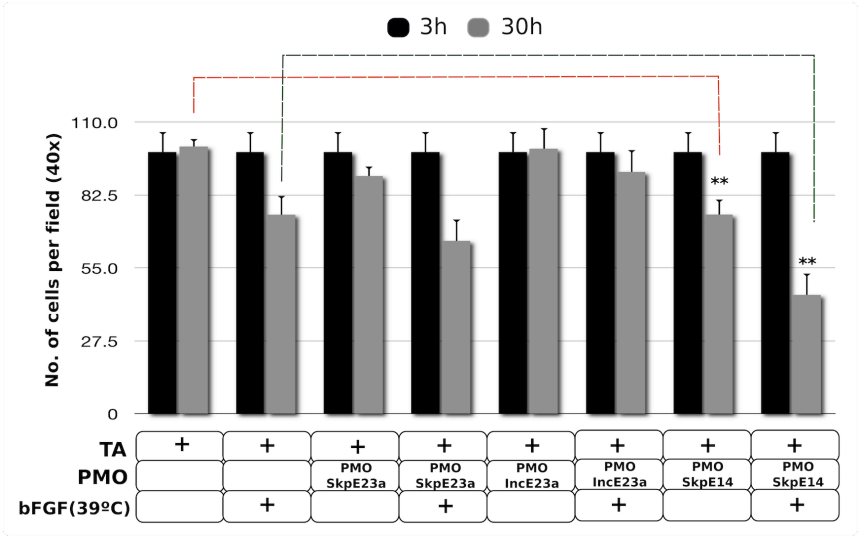

Figure 53: Decreased viability of H19-7 cells in the different experimental conditions after induction of their differntiation (24h). Error bars represent ±SEM. ** $P < 0.01$.

Results

We investigated the effects of the different PMOs on the differentiation capacity. Based on a morphological characterization and analogous to the findings in PC12 cells, forcing solely the switch from type II to type I isoforms did not result in any differentiation phenotype in the absence of differentiation conditions (data not shown). However, all PMO tested interfered with the proper differentiation of H19-7 cells upon bFGF treatment as measured by the levels of *Dusp6* differentiation marker, that was lower in all the treatments compared to control cells with transffection agent (TA)(**Figure 54**). Furthermore, α-tubulin immunofluorescence of H19-7 cells in the different experimental conditions showed a morphological alteration of the differentiation phenotype (**Figure 56)**. This phenomenon was more evident in the cells treated with the PMO-SkpE23a or with PMO-SkpE14, were cells acquired a characteristically fibroblastic morphology in contrast to the trapezoidal morphology of the differentiated cells only with bFGF. Moreover, we observed in PMO-SkpE14 treatment with bFGF the appearance of unknown thickness in the form of bubbles in the neurite extensions (**Figure 55**), like the ones observed previously in PC12 cells after knocking down neurofibromin in the presence of NGF. However, in cells treated with PMO-IncE23a we didn't detect any significant morphological change after inducing differentiation (**Figure 56**), although the qPCR analysis revealed a decrease in the expression of *Dusp6* levels (**Figure 54**). This can be partially explained by the fact that PMO-IncE23a was quite inefficient in forcing E23a inclusion (**Figure 52**).

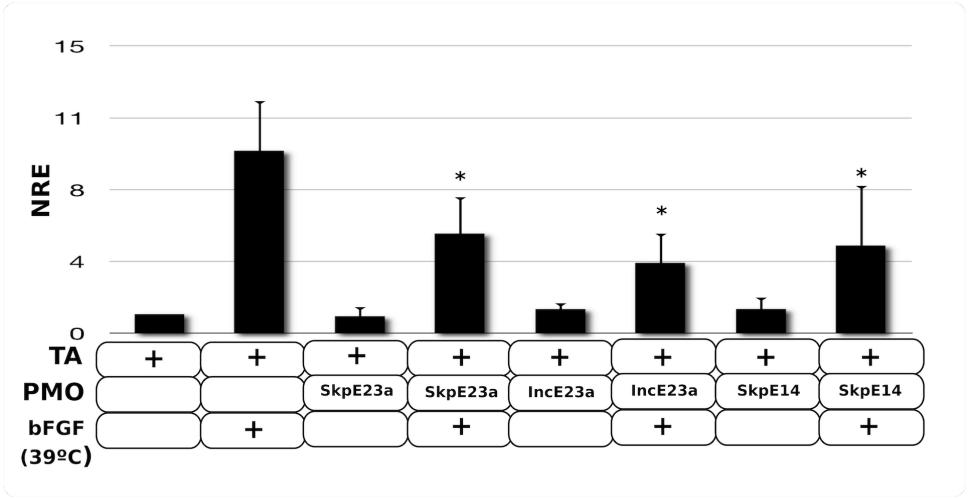

Figure 54: The graph illustrates the expression of *Dusp6* for different experimental conditions. Error bars represent as ±SEM. * $P < 0.05$, as evaluated by paired *t*-test vs cells treated only with bFGF. NRE: Normalized relative expression, TA: Transfection agent.

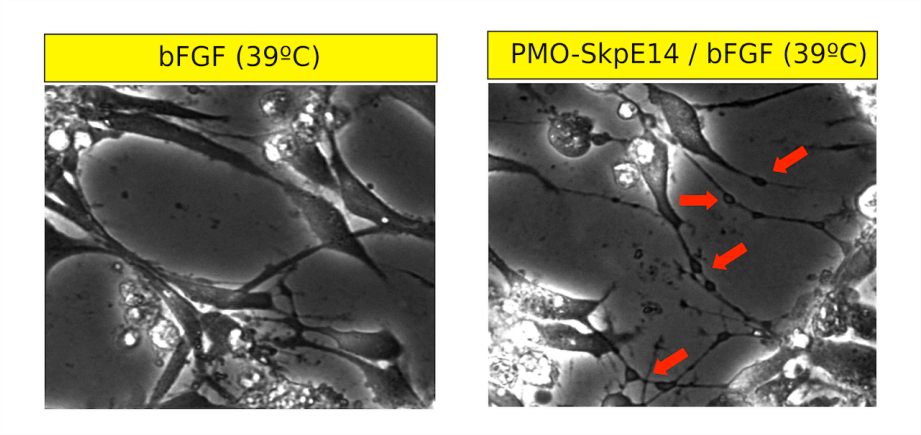

Figure 55: Differences in neurite morphology between H19-7 cells treated with or without PMO-SkpE14 in presence of bFGF. Red arrows indicate the characteristic bubble like thikening of neurite extension similar to the ones obvserved in PC12 in the same experimental conditions.

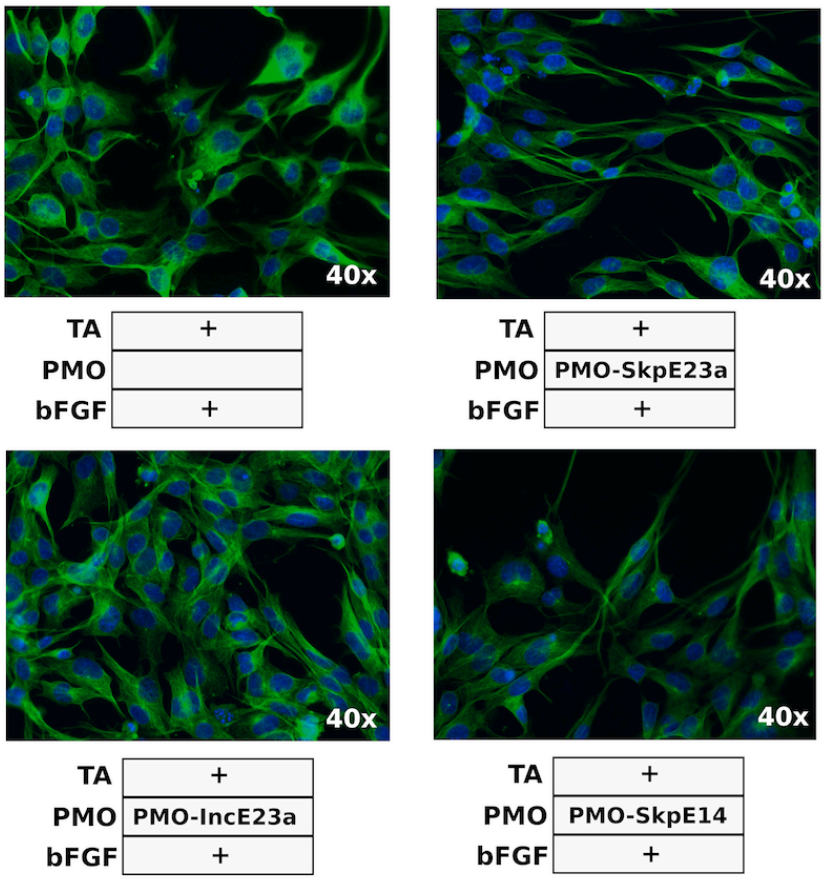

Figure 56: Immunofluorescence staining of α-tubulin (green) in hippocampal H19-7/IGF-IR cell line in different experimental conditions. DNA was stained with Hoescht (blue).

Analysis of E23a alternative splicing during *NF1* Schwann cell differentiation

After corroborating that the modulation of E23a alternative splicing by PMO was interfering with the sympathetic neuron-like PC12 differentiation and also with the differentiation of H19-7 hippocampal cells both models of the Central Nervous System (CNS), we wanted to further explore this alternative splicing in a different cellular system. We used primary *NF1* (+/-) Schwann cells derived from the peripheral nerve of an NF1 patient. Primary Schwann cells (SCs) previously isolated in our lab from a nerve biopsy were cultured and expanded, and their differentiation toward myelinizating SCs was performed by exposing this cells to constant forskolin (an elevator of cAMP) for 5 days (see materials and methods) (**Figure 57A**). Purity assessment of primary Schwann cell cultures was performed using a specific antibody for the protein S100, specific of SCs in the PNS. Our primary cultures were highly pure and presented more than 95% of SCs (**Figure 57B**). Total RNA was extracted in proliferation and differentiation conditions and the status of E23a alternative transcripts was determined. As shown in **figure 57C** upon Schwann cell differentiation we observed a slightly increase in type II isoform expression in contrast to the type II-I switch triggered by NGF differentiation in PC12 cells. These results are in accordance with the observations of Gutmman and collaborators (Gutmann D et al., 1993) were SCs differentiation was associated with a switch from type I to type II isoform an opposite regulation than in neuronal differentiation. In addition, we cultured *NF1* (-/-) SCs derived from a plexiform neurofibroma. In these SCs lacking neurofibromin we also made the stricking observation of the appearance of thickening in the form of bubbles in the SCs extensions (**Figure 58**), a phenotype that closely resembled the same phenomena identified in PC12 and H19-7 neurites (**Figures 34 & 55**).

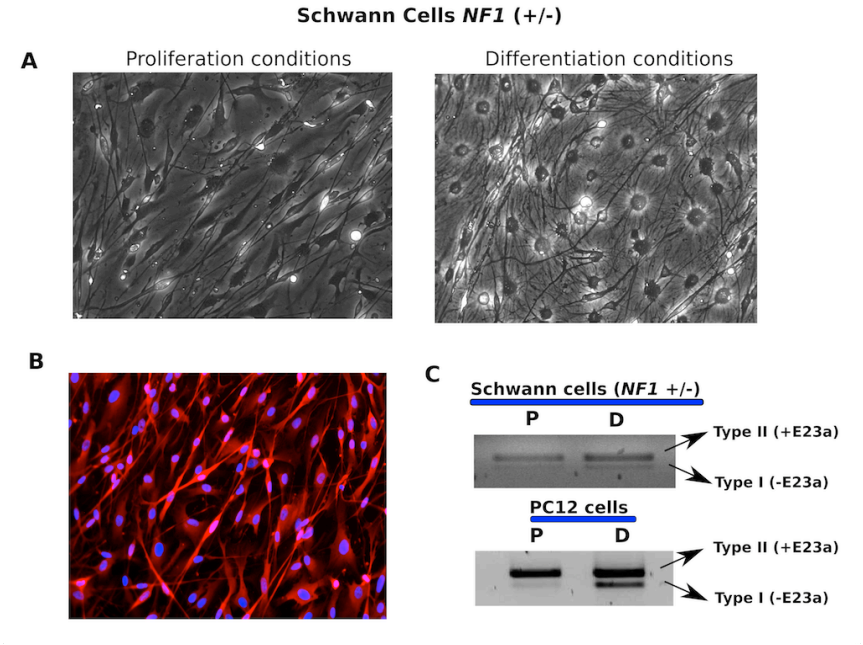

Figure 57: **A)** Phase contrast photographs (20x) of *NF1* (+/-) Schwann cell (SCs) proliferating (left) and differentiating (right). **B)** S100 immunofluorescence staining to determine SCs purity. C) The upper image shows an increase in type II (+E23a) expression associated to the SC differentiation process. In the lower image, switch from type II to I isoform during PC12 differentiation.

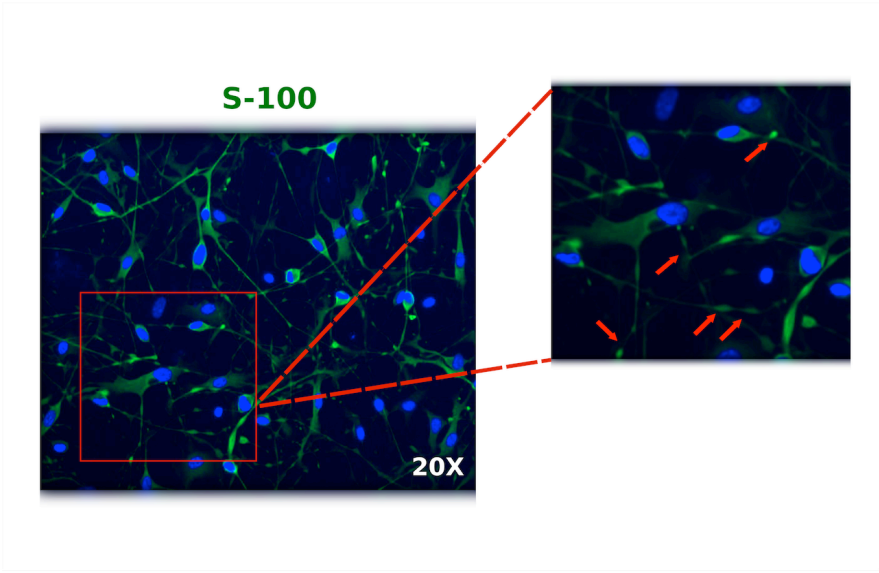

Figure 58: S100 immunofluorescence staining of SCs culture. Red arrows indicate the unknown bubble like thickening in the cell body of SCs cells.

To characterize the functional effect of alternative splicing of E23a in SCs and compare it with the one in PC12, we analyzed phosphor-ERK 1/2 levels during proliferation and differentiation in both cellular models. As shown in **figure 59**, SCs that were proliferating showed higher levels of phosphorylation of ERK1/2 than in differentiated SCs, the opposite effect than in PC12 cells.

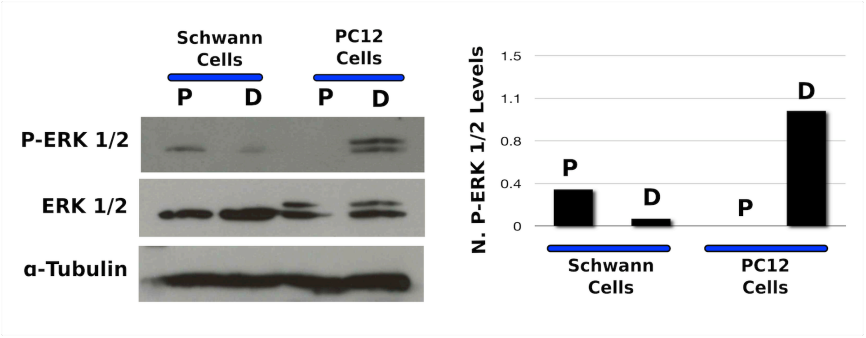

Figure 59: Western blot analysis showing phosphor-ERK 1/2 and total ERK1/2 (42/44 kDa) in lysates from proliferative (P) and differentiated (D) Schwann and PC12 cells. Graph represents normalized P-ERK 1/2 levels. The loading control was α- tubulin.

All together these results suggested that the functional implication and regulation of E23a alternative splicing during neuronal differentiation was a general process, rather than a process restricted to the PC12 differentiation model system. These results also pointed out to the different regulation of alternative splicing of E23a in the distinct differentiation processes depending on the cell type (e.g: neurons vs. Schwann cells).

Comparison of the aberrant differentiation phenotypes produced by forcing an earlier switch from type II/I, no switch and neurofibromin knockdown

During neuronal differentiation, PC12 cells change their phenotype by stopping cell division, promoting neurite extension and increasing the synthesis of several neurotransmitters. Neurite outgrowth can be seen as a two-step process (Burry R 2001), in which in an earlier phase, neurite outgrowth initiates and in a later phase, neurites elongate and form ramifications creating a complex network. During this process the switch from *NF1* Type II to Type I transcript takes place as a result of a transcriptional response to NGF treatment, and thus, the functional impact of the increase in neurofibromin GAP activity can be considered as a late phase event in this differentiation process. The use of the designed PMOs to modify at will E23a splicing and neurofibromin knockdown permitted to test different experimental conditions: forcing an earlier Type II to Type I switch; forcing the switch before NGF treatment; forcing the absence of a switch; and forcing neurofibromin knockdown. In all cases, PC12 neuronal differentiation was altered in different ways as summarized and compared in **figure 60**.

After forcing an earlier switch by PMO-SkpE23a there was an alteration in the correct neuronal differentiation process, were PC12 cells showed a reduced percentage of differentiated cells (between 48-72h after NGF treatment) and a clear reduction of neurite ramifications resulting in a less complex neuronal network established among differentiated PC12 cells. However, neurite length was not altered. At the molecular level, after forcing an earlier switch there was a reduction in the expression of differentiation markers (*Gap43*, *Mmp3* and *Dusp6*) and also in the enzymatic activity of NADH-dehydrogenase. Similar results

concerning a reduction in the percentage of differentiated cells were observed after forcing Type II - Type I switch before NGF treatment (PMO-SkpE23a 24h before NGF). However, in this condition neurite complexity was further reduced compared to PMO-SkpE23a treatment, and it was observed an increase in neurite thickness and straightness. The differentiation markers and the NADH-dehydrogenase activity were significantly reduced. Forcing the inclusion of E23a (inhibiting the switch type II/I) by PMO-IncE23a in the presence of NGF also altered the correct neuronal differentiation process. In this experimental condition the percentage of differentiated cells and the neurite length were not altered in comparison with cells treated with NGF only, but we observed a clear reduction in the neurite thickness and a fragile appearance. Differentiation markers were also reduced. Finally, the more severe phenotype was observed after the knockdown of neurofibromin levels. In PC12 treated with the PMO-SkpE14 and NGF, cells showed an aberrant differentiation in which the percentage of differentiated cells was reduced and neurites were less complex and abnormally extended. As observed in cells treated with PMO-SkpE23a 24h before adding NGF, there was an increase in neurite thickness and straightness, but this time with an even more extreme phenotype. At a morphological level there was also observed the presence of unknown thickness in the form of bubbles along neurite extensions, a phenotype also present in H19-7 cells with a neurofibromin knockdown (**Figure 55**) or in Schwann cells *NF1*(-/-) (**Figure 58**). Differentiation markers were also significantly reduced.

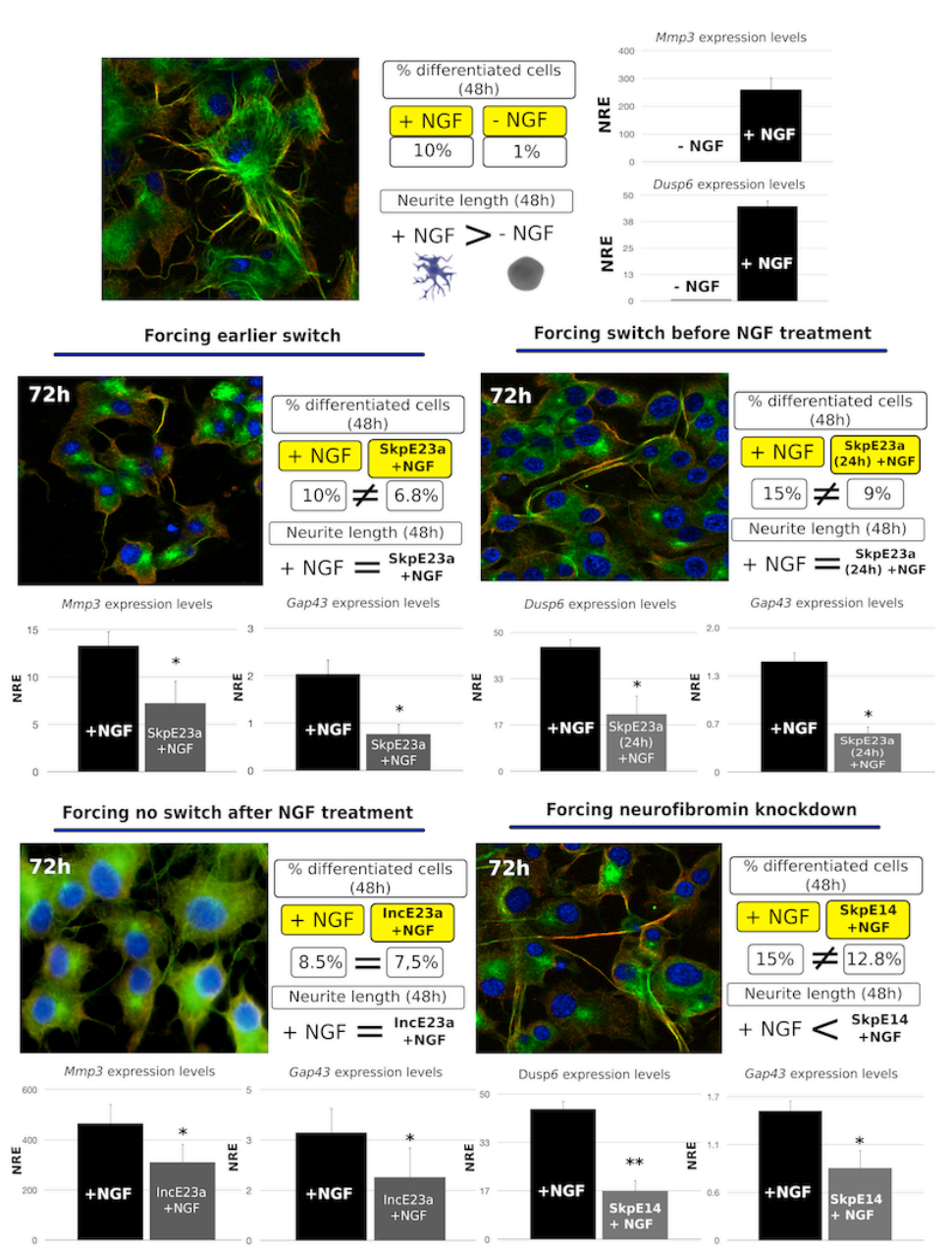

Figure 60: Schematic comparison between differentiated phenotypes for all the PMO associated conditions (earlier switch, switch before NGF treatment, no switch and neurofibromin knockdown).

Type II/I switch is regulated by a transcriptional response to NGF-triggered differentiation, progressively increased along the neuronal differentiation process and reaching a maximum at the late phase of differentiation. We wanted to investigate whether the different alterations in the proper PC12 neuronal differentiation process due to the different PMO treatments were also correlated with an alteration in the NGF-dependent global transcriptional response, at a late phase of differentiation. To do that, we performed an RNA-Seq analysis of the different PMO treatments of PC12 cells, using biological triplicates of each condition, in the presence or absence of NGF at 55h. The experimental design is summarized in material and methods pp. 44-45.

Among the 12126 genes above the minimum expression threshold of 500 reds taking into account the whole set of experimental conditions, 186 genes were found to be differentially expressed by two-fold or greater after NGF treatment, in comparison to control cells (-NGF) at 55h. The expression patterns of these 186 genes along the whole experiment can be seen at **Figure 61**. We observed that NGF exerted a wide transcriptional response on PC12 cells and that the effect on this transcriptional profile by the different PMO treatments was, in comparison, small. Biological triplicates introduced a significant experimental batch effect that made difficult to detect any difference associated to the presence of different PMOs. However, we identified 4 clusters of genes (1A, 1B, 2A and 2B, marked in black and yellow respectively in **Figure 61**) that were down and up-regulated in conditions where PMOs were added in the absence of NGF. Importantly, when compared to non-NGF treated controls, these genes were modified in the same way as NGF was eliciting to PC12 cells. Since PMOs were only modifying neurofibromin activity, we reasoned that this group of genes could be those influenced by pathways (in which neurofibromin was involved) important during NGF-triggered PC12 neuronal differentiation (**Table 9**). For these transcription

clusters, gene enrichment was performed using DAVID functional annotation tool (Huang DW et al., 2009a; Huang DW et al., 2009b). Clusters 1A and 1B were related with cell cycle, mitotic division, DNA replication and cytoskeletal/ microtubule reorganization (**Table 10**), and some genes were found to be important in the process of neurite formation and outgrowth like the *Iqgap3, Tpx2* and *Tacc3* (Caro-Gonzalez HY et al., 2012; Mori D et al., 2009; Sadek CM et al., 2003; Wang S et al., 2007). The enrichment analysis of clusters 2A and 2B, showed only a clear association with genes related to metabolic processes (cholesterol and sterol activity). Interestingly, among these 186 genes we found a significant number of genes (16), that overlapped with the differentially expressed genes between the presence or absence of PMO-SkpE23a added 24h before NGF and at initial time points (3h; **Figure 62**). As shown before, these genes are only transiently expressed, and accordingly, we found that only two of these genes (*Ldlr* and *Zfand2a*) overlapped with the genes present in the four selected clusters in PMO-treated conditions at 55h. All together, these results reinforce the idea that neurofibromin function, especially its GAP activity, participates in pathways influencing transcriptional responses associated to NGF-triggered neuronal differentiation.

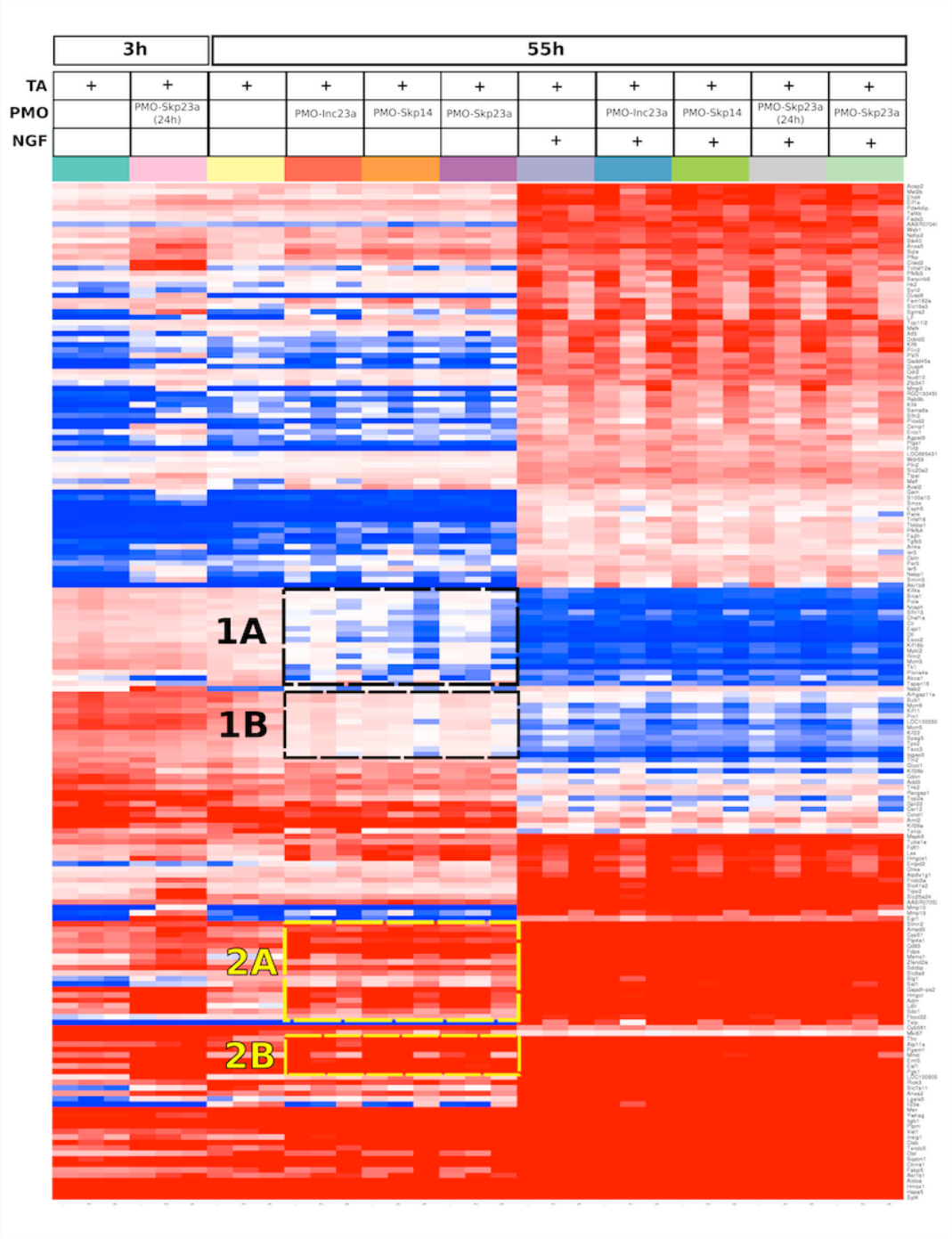

Figure 61: Heat map of differentially expressed genes (FC >2) in the presence or absence of NGF at 55h for all the experimental conditions. Clusters are marked with black and yellow square

Cluster 1A	Kif4a, Brca1, Pole, Ncaph, Slfn13, Chaf1a, Cit, Espl1, Dtl, Esco2, Kif18b, Mybl2, Rrm2, Mcm3, Tk1, Plxna4a, Abca1, Tspan18
Cluster 1B	Arhgap11a, Bub1, Mcm6, Kif11, Prc1, LOC10035953, Mcm5, Kif22, Spag5, **Tpx2**, **Tacc3**, **Iqgap3**
Cluster 2A	Stmn2, Ampd3, Cyp51, Ptp4a1, Cd63, Fdps, Msmo1, Zfand2a, Sdcbp, Slc6a8, Btg1, Sat1, Gapdh-ps2, Hmgcr, Adm, Ldlr, Sdc1, Fbxo32
Cluster 2B	Tfrc, Atp11a, Pgam1, Mmd, Eml5, Eaf1, Pgk1

Table 9: List of genes within the four clusters. Examples of genes related with neurite outgrowth and formation, are marked in bold.

Cluster	Name	Type	Adj. P-value
1A	Chromosome segregation	**GO-BP**	8.2E-4
1A	DNA metabolic process	**GO-BP**	6.0E-4
1A	DNA replication	**GO-BP**	5.8E-4
1A	DNA replication	**GO-BP**	5.8E-4
1A	cell cycle process	**GO-BP**	8.9E-3
1A	sister chromatid segregation	**GO-BP**	7.4E-3
1A	mitotic sister chromatid segregation	**GO-BP**	7.4E-3
1A	Pyrimidine metabolism	**KEGG**	6.7E-2
1A	mitotic cell cycle	**GO-BP**	2.6E-2
1A	cell cycle phase	**GO-BP**	2.5E-2
1A	cell cycle	**GO-BP**	1.6E-2
1B	microtubule cytoskeleton	**GO-CC**	6.6E-4
1B	spindle	**GO-CC**	6.2E-4
1B	Cell cycle	**KEGG**	7.4E-3
1B	cytoskeletal part	**GO-CC**	4.9E-3
1B	DNA replication	**KEGG**	4.6E-2
1B	ATP binding	**GO-MF**	3.8E-2
1B	nucleotide binding	**GO-MF**	2.3E-2
1B	microtubule	**GO-CC**	2.2E-2
1B	adenyl ribonucleotide binding	**GO-MF**	2.0E-2
1B	adenyl nucleotide binding	**GO-MF**	1.7E-2
1B	purine ribonucleotide binding	**GO-MF**	1.5E-2
1B	purine nucleoside binding	**GO-MF**	1.4E-2
1B	ribonucleotide binding	**GO-MF**	1.3E-2
1B	purine nucleotide binding	**GO-MF**	1.3E-2
1B	cytoskeleton	**GO-CC**	1.2E-2
1B	non-membrane-bounded organelle	**GO-CC**	1.2E-2
1B	intracellular non-membrane-bounded organelle	**GO-CC**	1.2E-2
1B	nucleoside binding	**GO-MF**	1.1E-2
2A	cholesterol biosynthetic process	**GO-BP**	4.8E-2
2A	Cholesterol metabolic process	**GO-BP**	3.0E-2
2A	sterol metabolic process	**GO-BP**	1.9E-2

Table 10: Gene enrichment results obtained using DAVID functional annotation tool for the different clusters. Annotated terms: GO-Biological Process (GO-BP), GO-Molecular function (GO-MF), GO-Cellular Compartment (GO-CC) and KEGG pathways (KEGG).

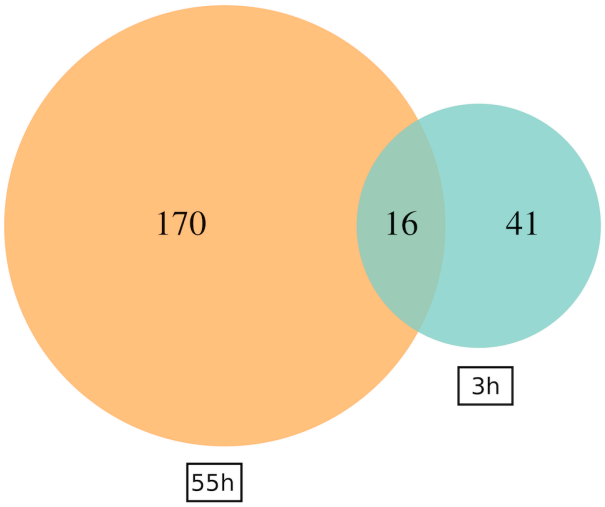

Figure 62: Venn diagrams of the differentially expressed genes between the presence or absence of PMO-Skp23a (24h before NGF) at the initial time point (blue circle) and the genes of cells treated with or without NGF at 55h (brown circle).

DISCUSSION

The importance of the alternative splicing of exon 23a of the *NF1* gene has previously been studied in different experimental systems: different established cell lines, genetically modified mouse, primary tumors or ES cells, to mention some. The results generated in this thesis highlight the importance of a correct regulation of E23a alternative splicing during the whole neuronal differentiation process in a time dependent manner. Some of these results are new, some are consistent and others discordant with previous results. We think that two of the major factors that could explain some of the discrepancies found are, in one hand, that the use of PMOs allows preserving physiological conditions regarding expression of the *NF1* gene, and on the other hand, the fact that we have studied the process of neuronal differentiation as a dynamic and time-dependent process, while some other works study differentiation as an end point. We think this thesis provides a nice example of how an alternative splicing of a single gene can influence cell fate by the fine, coordinated, integrated and time-dependent regulation of two different signaling pathways.

A PMO-based method for modifying, at will, alternative splicing

The use of the antisense technology to modulate splicing events has been reported for various hereditary diseases in order to correct or change to less deleterious forms. Among these diseases are Cystic Fibrosis, Duschenne Muscular Dystrophy (DMD), NF1, NF2 and Hutchinson-Gilfrod (Castellanos E et al., 2012; Fernandez-Rodriguez J et al., 2012; McClorey et al., 2006; Popplewell L, 2012; Pros E et al., 2009; Wang Q et al., 2010). However, the use of this technology to modulate alternatively spliced exons is rare and few examples can be found in the literature (Schnerwitzki D et al., 2014; Shieh JJ et al., 2009). In this study, we designed and generated PMOs to hybridize specifically to intronic

splicing regulatory elements (canonical splice sites and *cis*-elements) that modulate NF1 exon 23a exclusion and inclusion. We consider this PMO strategy a unique tool that has not been used before to explore alternative splicing in physiological conditions of the cell.

Our decision to use PMOs was based on previous studies demonstrating their high-targeting specificity, stability, low toxicity and resistance to nucleases (Sazani P et al., 2001) in comparison to other antisense technologies. In general, PMO backbone has no significant ionic charge at neutral pH, in comparison to the polyanionic phosphodiester backbone of a natural nucleic acid. This favors the interaction of PMOs with nucleic acids, and because PMOs are uncharged, they have no strong electrostatic interactions with proteins. In contrast, interactions of anionic phosphorothioate oligos with proteins cause multiple physiological, no side effects (Lebedeva I, Stein CA. 2001). In addition, this thesis project extends previous reports that PMOs are powerful and versatile tools for exploring normal pre-mRNA splicing regulation in a natural physiological context.

Previous experience in our group in the use of PMOs helped us in the setting up of the reported system. Our laboratory has used PMOs to revert the inclusion of cryptic exons, due to deep-intronic mutations, in fibroblasts and lymphocytes from NF1 and NF2 patients (Castellanos E et al., 2012; Pros et al., 2009; Fernandez-Rodriguez et al., 2011). The efficiency of PMOs used in this project was satisfactory. In the case of PMOs designed to force exon skipping (PMO-SkpE23a and PMO-SkpE14) we got more than 50% of skipping in PC12 and H19-7. Skipping of E23a (PMO-SkpE23a) was visible 24h after the treatment, while the effect of PMO-SkpE14 was delayed 48h. In terms of exon inclusion, PMO-IncE23a was really efficient in PC12 cells, and was able to stop almost all

the expression of isoform type I associated to NGF differentiation. However, in H19-7 the efficiency of PMO-IncE23a was reduced, but was still useful to partially prevent the skipping of E23a upon bFGF-triggered differentiation. Technically, the inclusion of an exon during natural skipping conditions of an alternatively spliced exon is difficult and previous knowledge about splicing regulatory aspects is necessary. In case of PMO-IncE23a we blocked a conserved splicing sequence at the 5' of E23a regulated by factors that promote splicing. The use of PMOs to force exon inclusion has been reported previously in a few number of works, however, most studies have been based in the correction of aberrant exon skipping, like in Spinal Muscular Atrophy, *FGFR1* gene (Bruno I et al., 2004; Zhou H et al., 2013) or the inclusion of specific viral exons important for infection (Guan W et al., 2011).

The specificity of our PMOs was demonstrated by the initial use of a non-target control PMO provided by Gene Tools, that didn't have any effect in the skipping and inclusion of E23a. In order to minimize possible side effects of a non-target PMO on the different readouts, we decided to use only the transfection agent (Endo-Porter) as a control for the different experimental assays, since transfection is the process in which the physiological status of the cells can be compromised. Another advantage of PMOs is the low toxicity associated to the transfection agent Endo-Porter (ethoxylated polyenthylenimine, EPEI) in comparison to the classical delivery systems, a weak-base amphiphilic peptide, designed to deliver PMOs into the cytosol and nuclear compartment by endocytosis-mediated process, preventing the damage in to the cell membrane (Morcos PA, 2001; Summerton JE, 2005). We didn't detect any morphological or molecular alteration in PC12 or H19-7 cells associated to the use of Endo-Porter.

Moreover, using PMOs we successfully modulated E23a splicing without altering

the physiological levels of *Nf1* mRNA as measured by qPCR analysis. Thus, PMOs provided us the confidence of obtaining reliable and physiologically sound results. Other methodologies and experimental set ups have been used to study the role of alternative splicing of exon 23a. For example, using a specific human splicing reporter system for generating derived neurons containing or missing a constitutive *Nf1* E23a in mouse embryonic stem cells (Hinman M et al., 2014), and the construction and use of over-expression plasmids carrying both Type I and II isoforms in PC12 cells (Yunoue S et al., 2003). In our understanding, both approximations are valid, although we think that the use of PMOs better preserves the expression levels of neurofibromin and the general physiological status of the cells.

We used the developed PMO system in different cell types and cell models, like PC12, H19-7 and HEK293T cells. We think that this system can be applied to other NF1 *in vitro* models to better understand the role of alternative E23a splicing while preserving physiological conditions. Furthermore, following the same or similar *in silico* and *in vitro* analyses to design and test the use of PMOs to modulate alternative splicing, this methodology can be applied to other genes with similar alternative splicing examples.

The E23a splicing regulation: The role of splicing factors and conserved intronic regions

Alternative splicing is highly regulated by both cis- sequences and trans- acting factors, some of them being tissue specific. We have studied the sequence conservation of intronic regions adjacent to exon 23a across several species that provided information on the different splicing factors regulating E23a alternative

splicing. In addition, we have studied the expression of few of them during PC12 cell differentiation. All these results provided information to better understand the regulation of E23a alternative splicing during neuronal differentiation.

The E23a is highly regulated at developmental level and in tissue-specific manner by at least two families of proteins: a) Hu proteins and CUG-BP1/ETR-3 like factors which promote its skipping; b) MBNL1/2 and TIA-1/R proteins which are positive regulators. Taking into account this information, we studied for the first time considering the splicing regulation of the *Nf1* gene the expression of some of these splicing factors (*Celf3*, *Mbnl1* and *Mbnl2*) in PC12 cells and characterized their expression changes during NGF-triggered differentiation. We detected that *Celf3* was overexpressed 48h after NGF treatment in PC12 cells, which is in accordance with results obtained by Barron V & Lou H (Barron V & Lou H, 2012) where over-expression of *Celf3* in CA77 cell line strongly promoted E23a skipping. Furthermore, overexpression of *Mbnl1/2* in CA77 cell line was found to promote E23a inclusion (Flemming VA et al., 2012). In PC12 cells we observed a down regulation of these two genes upon NGF treatment. These results support and clarify the antagonistic role of different splicing factors in E23a splicing regulation.

In addition, we detected a high degree of sequence conservation in intronic regions adjacent to E23a that were not present in other constitutive exons of the *Nf1* gene. This degree of intronic sequence conservation has also been identified in several other alternatively spliced exons in genes such as *CTFR*, *PER3*, *CARS* and *SYT7* (Kaufmann D et al., 2003). To date, we don't have a clear picture of how conserved sequences in these introns contribute to alternative splicing. The length of these conserved regions usually exceeds 50 bp, while binding sites for splicing proteins are relatively short. Therefore, this implies that the conserved

regions in introns could serve as binding sites for several different splicing factors, thus contributing to alternative splicing regulation (Sorek R & Ast G, 2003). Sugnet C and collaborators (Sugnet C et al., 2006) studied a group of 171 exons whose inclusion or skipping was different in brain or muscle compared to other tissues. A subset of them was clearly associated with unusual blocks of intron sequence conservation, like for E23a. In the nervous system factors regulating alternative splicing are highly enriched, especially CELF proteins (Ladd A, 2013). Most of these factors bind to UG-Rich sequences that form part of these intronic conserved sequences (Barron V & Lou H, 2012). This strongly suggests that these regions are important target sequences for specific splicing factors that regulate E23a in a tissue-specific manner.

Dissociating alternative splicing of E23a from NGF treatment in neuronal differentiation of PC12

This work provides significant evidences that modulation of alternatively spliced E23a plays an important role in the neuronal differentiation process associated with PC12 and H19-7 cells. In both cases we observed that either forcing the abnormal skipping or inclusion of E23a interfered with a correct neuronal differentiation process, altering the proper signaling of Ras/MAPK and cAMP/PKA pathways and the expression of differentiation markers, resulting in an altered aberrant phenotype, Specifically, at a morphological level, forcing an earlier type I (-E23a) isoform in PC12 cells, resulted in a reduction of the percentage and complexity of differentiated cells, whereas forcing type II isoform (+E23a) resulted in a reduction of neurite thickness (summarized in Results pp.116 -117).

When type II/I switch was induced by PMO-SkpE23a treatment, PC12 cells did not differentiate into sympathetic-like neurons, in the absence of NGF. However, after 24h of PMO-SkpE23a treatment we observed a transient up-regulation of a transcriptional profile that partially overlaps with NGF-response genes. Furthermore, the different PMOs used to interfere with neurofibromin function, also altered a signature of genes in a similar way to the NGF-triggered transcriptional response. All together this results indicate that, despite type II/I switch is not enough to induce differentiation, pathways functionally regulated by this switch impact on the NGF-induced transcriptional response, necessary for a correct neuronal differentiation.

The function of E23a has been studied by its deletion in a mouse model (Costa RM et al., 2001). These experiments provided first important evidences regarding the impact of E23a exclusion on mouse behavioral impairments, similar to those observed in patients with NF1, such as learning and motor deficits. This phenotype closely resembled that of *Nf1* (+/-) mice (Li Y et al., 2005; Silva AJ et al., 1997) and hinted the possible biological role of *NF1*-E23a in neuronal differentiation and/or signaling. Results obtained in this thesis could favor the idea that E23a would be important for a proper neuronal development, although experiments using the developed PMOs in WT mice would provide information also on its possible implication in the correct neuronal signaling *in vivo*.

Furthermore, Hinman M and collaborators (Hinman M et al., 2014) generated mouse embryonic stem (ES) cells with a constitutive *Nf1* exon 23a inclusion (23aIN/23aIN) or deletion (23aΔ/23aΔ). Upon differentiation of these ES cells to neurons, they examined the expression of the neuronal marker β-tubulin III (by western blot and immunofluorescence), and characterized neurite length. No differences were found in 23aΔ/23aΔ and 23aIN/23aIN in ES-derived neurons.

Our results and those of others seem to be contradictory with these ones. We think that a possible explanation for this discrepancy is the limited characterization of neuronal differentiation, especially at a quantitative and time-dependent manner. Another aspect to consider could be a possible buffer effect exerted by the cell as a response to the lack of E23a, in a similar, but not identical, way as we observed the desensitization of neurofibromin function when PC12 cells were treated with the PMO-SkpE23a 24h before NGF treatment.

Neuronal differentiation of PC12: a dynamic process that needs fine regulation of E23a alternative splicing in a quantitative and time-dependent manner

The RAS/MAPK pathway is highly conserved and plays an important role in different cellular processes including cell proliferation, differentiation and survival. To date, many studies have reported the importance of the spatiotemporal control of this signaling pathway as key factor to regulate specific cellular responses (Ref Nat Cell Biol). In PC12 cells NGF induces sustained activation of ERKs and promotes cell differentiation into sympathetic-like neurons (Kao S et al., 2001; Marshall CJ. 1995). Moreover, cAMP had also been involved in the regulation of cell proliferation and differentiation in PC12 cells, suggesting a possible crosstalk between these two pathways (Stork PJ, Schmitt JM. 2002) during neuronal differentiation.

Several time-course experiments studying the dynamics of the RAS/MAPK signaling during neuronal differentiation have been performed (REF). Upon NGF treatment of PC12 cells, and after a first brief peak of activation, RAS/MAPK activity gradually increases up to 10-fold, reaching a plateau around 24h-48h and

successively decreasing over time (Yunoue S et al., 2003). It has also been reported in PC12 cells, a time-dependent increase in the GAP activity of neurofibromin after NGF treatment that correlates with an increasing type II/I switch, reaching also significant levels between 24-48h after NGF-triggered differentiation (Yunoue S et al., 2003). In accordance with these observations we detected an increase in the phosphorylation levels of ERK1/2 upon NGF treatment, with a maximum between 24-48h, followed by a successive down regulation after 48h. When we altered this temporal dynamics by forcing type II/I switch with PMO-SkpE23a 24h or 48h earlier, we detected also an altered RAS/MAPK signaling over time, resulting in an aberrant differentiation process. These results highlight the importance of a proper regulation of RAS/MAPK signaling not only quantitatively but also in a time-dependent manner for an adequate PC12 differentiation.

The cAMP/PKA pathway had also been associated with PC12 differentiation, where cAMP activates Rap1 a mediator of sustained ERK activity in a time-dependent manner (Herbst KJ et al., 2011). Although we studied the activation of the cAMP/PKA pathway upon NGF treatment and its alteration by using different PMOs, we only measured this signaling pathway at 48h. A time-course experiment would be required to understand also the relationship with the dynamics of type II/I switch.

Understanding the possible dissociation between RAS and phosphorylated ERK levels.

High levels of RAS and MAPK activation either in neurons or PC12 cells have been observed in conditions where neurofibromin has been knockdown or when type II neurofibromin (reduced GAP activity) has been expressed (Hinman M et al., 2014; Yunoue S et al., 2003). In our experiments, when using PMO-SkpE14

to knockdown neurofibromin or PMO-IncE23a to decrease neurofibromin GAP activity, we detected a certain decoupling between RAS and ERKs activation. This discrepancy in the linearity of the RAS/MAPK activation has also been observed in many other works (e.g.: Kriegsheim A et al., 2009; Yunoue S et al., 2003). There exist different possible explanations to this dissociation, like the existence of negative feedbacks or the crosstalk of the RAS/MAPK with other pathways. For instance, it has been reported that ERK activation can inhibit RAS and RAF1 in PC12 and other cellular systems (Dhillon AS et al., 2007; Dougherty MK et al., 2005) and that a crosstalk between RAS/MAPK and cAMP pathways influencing the overall ERK activation status (Dumaz N, Marais R. 2005; Stork PJ, Schmitt JM. 2002). However, despite the existence of all these evidences, we think that in addition to our results, it is necessary to measure RAS activity in a different way to reach a robust and consistent result considering this apparent decoupling between RAS and ERK activation status.

A negative feed-back regulating neurofibromin GAP activity?

When NGF was added after forcing type II/I switch by PMO-SkpE23a 24h before, we expected a reduced activation level of ERKs similar to conditions in which NGF and PMO-SkpE23a were added simultaneously. Surprisingly, the levels of ERK phosphorylation were higher than in control cells treated with NGF, reaching levels similar to those exhibited in PC12 cells in which neurofibromin was knockdown by PMO-SkpE14 (**Figure 37**). Similarly, when PMO-SkpE23a was added 24h before NGF, PKA activation was also reduced, as in PMO-SkpE14-treated cells, upon NGF differentiation. In addition, at a morphological level, PC12 cells treated with PMO-SkpE14 and NGF, exhibited an aberrant differentiation pattern in which the percentage of differentiated cells

was reduced and neurites were less complex and abnormally extended. PC12 cells treated with PMO-SkpE23a 24h before adding NGF also reproduced this phenotype. All these results seemed to point to an apparent loss of neurofibromin function in these later conditions, triggered either by the PMO treatment or by the PMO treatment and NGF-induced differentiation. These results made us hypothesize with the possible existence of a negative feedback on neurofibromin function, due to the excess of GAP activity of type I isoform. Consistent with hypothesis, we identified a transient over-expression profile in PC12 cells after 24h of treatment with PMO-SkpE23a compared to non-treated control cells.

We are currently working to determine whether this apparent loss of NF1 activity is caused by a direct degradation of neurofibromin, by the ubiquitin-proteosome pathway (Cichowski K et al., 2003), using western blot analysis. Additionally, we are interested in determining whether type I and type II neurofibromin isoforms have a different stability at a cellular level.

Neurofibromin depletion during neuronal differentiation: aberrant differentiation and apoptosis. Too much ERK activation?

We observed that a significant proportion of PC12 cells in which neurofibromin was depleted by PMO-SkpE14 treatment underwent apoptosis after 48h. When PMO-SkpE14 and NGF were added simultaneously, a proportion of this cells arrested, differentiated, and were protected from cell death. However, the differentiation process was aberrant, with PC12 cells exhibiting less complex neurites and abnormally extended, together with the presence of unknown thickness in the form of bubbles along neurite extensions. Supporting these observations, it has been reported that PC12 cells treated with an *Nf1*-siRNA did

not differentiate correctly upon NGF treatment, and were characterized by a partial inhibition of neurite growth (Hirayama M et al., 2013; Kriegsheim A et al., 2009). Furthermore, it was observed in PC12 cells carrying different *Nf1*-GAP mutants (R1276K & R1276A/R1391K) a clear reduction in the percentage of differentiated cells after 48h of NGF treatment (Yunoue S et al., 2003).

We do not completely understand why some of the PC12 cells treated with PMO-SkpE14 and NGF arrest and differentiate and others undergo cell death through apoptosis. However, one possibility would be the different position in the cell cycle when NGF triggers arrest of PC12 cells. Another issue would be the mechanism driving apoptosis in these cells. In this regard, we observed that either in the presence or absence of NGF the levels of ERK phosphorylation of PMO-SkpE14-treated cells were significatively higher in comparison to their respective controls (PC12 in presence or absence of NGF). It has been suggested the important role of ERK1/2 in promoting neuronal cell death. For example, in the hippocampal cell line HT-22, a sustained activation of ERK1/2 after 6h of glutamate treatment, induced cell death (Subramaniam S, Unsicker K. 2009). However, in PC12 cells a sustained high activation of ERK1/2 not always promote cell death (Greene L, 1978; Klesse JL et al., 1999) and thus it is possible that additional factors would be required for inducing it. Other reports have also associated depletion in *NF1* with cell death. For instance, in *Nf1* knock down (*Nf1*-KD) PC12 cells treated with NGF an overexpression of pro-apoptotic proteins like CASP1 and CASP12 were detected (Hirayama M et al., 2013). Cell death also has been reported to be associated with the NF1 (+/-) hippocampal cells (Brown J et al., 2010).

Unknown thickness in form of bubbles in the absence of neurofibromin

One finding recurrently appearing in *NF1* knock down (PMO-SkpE14)

differentiating PC12 or H19-7 cells or even in *NF1*(-/-) Schwann cells under differentiation conditions was the appearance of unknown thickness in the form of bubbles of neurite extensions. These formations were similar to the characteristic varicosities structures that commonly form in the neurite body of PC12 cells, but in a much higher frequency. It has been described that the GAP-related domain of neurofibromin interacts with the amyloid precursor protein and that, in turn, this protein has been proposed to function as a vesicle cargo receptor for the motor protein kinesin-1 in neurons (De Schepper et al., 2006). In fact, in differentiated PC12 cells treated with amyloid–β-peptide, it has been reported an increase of varicosities structures (Vaisid T et al., 2008) like the ones observed in NF1 depleted cells. A possible hypothesis would be that the lack of neurofibromin facilitates the accumulation of amyloid–β-peptide and other proteins transported by vesicles during the formation of neurites.

Neurofibromin's GAP activity regulates PKA activation

The cAMP/PKA together with RAS/MAPK pathways are related with the regulation of differentiation in PC12 cells. The cAMP/PKA is important for the sustained activation of ERK 1/2 in PC12 cells upon NGF treatment *in vivo* and *in vitro* (Herbst KJ et al., 2011; Yao H et al., 1998; York RD et al., 1998). Moreover, it is widely accepted that in PC12 cells the activation of RAF/MEK/ERK cascade is regulated by the two cAMP effectors, PKA and the exchange protein directly activated by cAMP (Epac) (Dumaz N, Marais R. 2005; Stork PJ, Schmitt JM. 2002). Furthermore in neurons, their activity and depolarization induces changes in synaptic plasticity that requires both pathways cAMP/PKA and RAS/MAPK (Patterson SL et al., 2001; Stork PJ, Schmitt JM. 2002). Taking together all these studies a crosstalk between these two pathways

is well supported by experimental evidences, although the specific mechanisms of crosstalk and regulation are not fully understood.

Our results show that the levels of phospho-PKA in PC12 cells were moderately elevated upon NGF treatment. However, the levels of phospho-PKA were highly increased upon NGF and PMO-SkpE23a addition, or on the contrary, reduced when PC12 cells were treated with PMO-IncE23a and NGF. These results suggest that the GAP activity of neurofibromin (directly or indirectly) in addition to regulate the RAS/MAPK pathway, also regulates the activation of PKA in the process of PC12 neuronal differentiation. In fact it has been proposed a mechanism in which neurofibromin regulates the cAMP pathway by activating an atypical PKC through a RAS dependent mechanism (Anastasaki C, Gutmann DH. 2014). However, our results seem to be in favour of a more direct regulation. When we compared control PC12 cells with PC12 cells treated with PMO-SkpE23a (high GAP activity), the levels of ERK activation were not detectable in any condition, but on the contrary, PKA activation was significantly higher in PMO-SkpE23a treated. In addition, similar ERK phosphorylation levels were detected in PMO-SkpE23a and NGF treated cells with respect to PC12 cells treated with PMO-SkpE14 (depleted of neurofibromin) but the levels of PKA phosphorylation were extremely different, being much higher in PMO-SkpE23a and NGF treated cells (**Figure 37**). Thus this results point to a more direct regulation of cAMP/PKA pathway by the neurofibromin GAP activity, rather than an indirect regulation through the RAS/MAPK pathway.

The effect of the cAMP/PKA pathway activation on the morphological changes exhibited by differentiating PC12 cells is still not fully understood. It has been demonstrated that several cAMP analogues promote differentiation of PC12 cells (Vossler MR et al., 1997). In neurons neurofibromin regulates CNS neurite length

and growth cone areas in a cAMP/PKA/Rho/ROCK dependent manner *in vitro* and *in vivo* (Brown JA et al., 2012). Results obtained in this work show that the neurofibromin GAP activity regulates both the RAS/MAPK and the cAMP/PKA pathways in an opposite manner during neuronal differentiation. Further experiments will be required to dissect the contribution of each pathway to the morphological changes of differentiating PC12 cells.

Regulation of alternative splicing of E23a: a simple way to exert a coordinated time-dependent and opposite regulation of Ras/MAPK and cAMP/PKA signaling for a proper neuronal differentiation?

All together these results suggest the role of *NF1*-E23a alternative splicing as a fine-tuning regulatory mechanism to control two signaling pathways in a coordinated and time-dependent manner. The Ras/MAPK and cAMP/PKA pathways are regulated in an opposite manner (**Figure 63**). While an increase in neurofibromin GAP activity down-regulates RAS/MAPK signaling, and greatly enhance PKA phosphorilation, a decrease in GAP activity produces the opposite effect. Since the regulation of both pathways seem to be centered in the GAP activity, and both isoforms Type II and Type I have a ten-fold different GAP activity (Yunoue et al., 2003), the fine regulation of a simple and small alternative exon can exert an exquisite way to coordinate over time, two important pathways both required for a proper neuronal differentiation process.

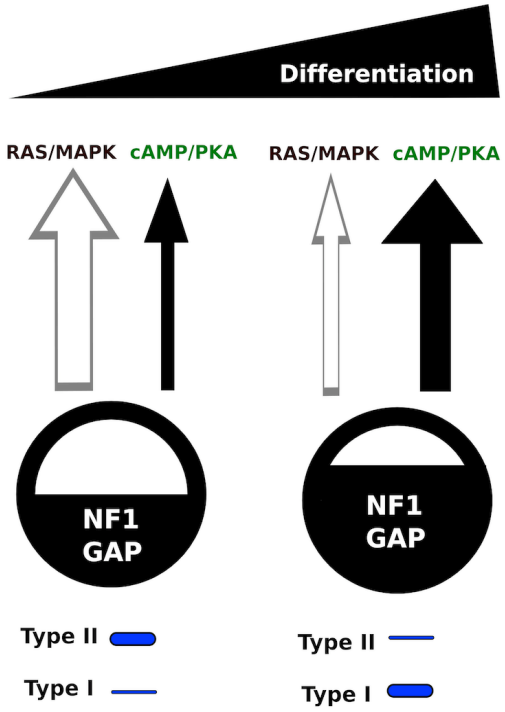

Figure 63: Schematic representation of how *NF1* alternative splicing allows the fine-tuning of the RAS/MAPK and cAMP/PKA pathways through its GAP activity in a coordinate and opposite way along process of neuronal differentiation**.**

Alternative splicing of E23a in neuronal and Schwann cell differentiation

Adequate set up and functional characterization of different neuronal model systems was necessary to perform experiments regarding the use of PMOs to modulate *NF1* alternatively-spliced exons. In this thesis we set up the use of two different cell lines, PC12 and H19-7, and a group of functional assays for assessing proliferation, differentiation, signaling and apoptosis. PC12 cells have been used as an *in vitro* model system to study neuron-like (sympathetic neurons) phenotypes. However, these cells have some limitations as a neuronal model such as the lack of formation of real central nervous system structures (axons,

dendrites and synapses) and the lack of information on their genetic and genomic alterations that can make these tumor-derived cells different from WT neurons. Thus in order to validate the results obtained in PC12 cells regarding the different effects of the PMOs used we set up another neuronal differentiation model based on the hippocampal cell line H19-7.

The use of H19-7 cell line, as a cellular model for neuronal differentiation has been quite limited. We have observed for the first time a switch from NF1 type II to type I isoforms upon bFGF differentiation and that the modulation of E23a alternative splicing using PMOs was interfering with the proper neuronal differentiation. These results reinforce the findings obtained using PC12 cells, making them not restricted to this cellular model, but a general finding in the context of neuronal differentiation, and specific to it, since the results obtained concerning the alternative splicing of E23 during Schwann cell differentiation were completely different. In the case of Schwann cell differentiation, we observed a slightly increase in type II isoform expression in accordance with previous observations (Gutmann DH et al., 1993). While differentiation of PC12 cells increased the levels of ERK1/2 phosphorylation, during SCs differentiation they were decreased. These results suggested that the regulation of E23a alternative splicing plays a different functional role in distinct differentiation processes depending on the cell type.

CONCLUSIONS

1. Different *Phosphorodiamidate Morpholino Oligomers* (PMOs) have been designed and tested that effectively modulate the expression of type I (-E23a) and type II (+E23a) isoforms of the *NF1* gene without altering its physiological expression. This tool could be used to study in detail the role of the alternative splicing of exon 23a in any *in vitro* model system relevant to NF1. In addition, it can serve as a model to study similar alternative splicings in other genes.

2. Forcing the alternative splicing of exon 23a is not sufficient for inducing PC12 neuronal differentiation in the absence of nerve growth factor (NGF); it does not alter the proliferation capacity of PC12 cells, neither the cell cycle arrest induced by NGF.

3. Any alteration of the proportion of isoforms type II and I resulting from the endogenous alternative splicing of E23a, either in a quantitative or time-dependent manner, interferes with the correct neuronal differentiation process of PC12 cells. In particular, it alters the correct formation of neurites, as well as the regulation of the RAS/MAPK and cAMP/PKA signalling pathways.

4. The alteration of the E23a alternative splicing also impedes the proper neuronal differentiation process in hippocampus neuronal cells (H19-7). In other models of differentiation, such as myelinating Schwann cells of the peripheral nervous system, it has been confirmed that the regulation of E23a alternative splicing plays a different functional role.

5. The NGF treatment of PC12 cells mainly expressing type I isoform (with higher GAP activity), results in the aberrant formation of neurites and in an altered RAS/MAPK and cAMP/PKA signalling pathways, similar to the aberrant

differentiation processes caused by neurofibromin knockdown. This phenomena, indicates the possible existence of a negative feed-back on the regulation of neurofibromin GAP function.

6. Depletion of neurofibromin in PC12 and H19-7 cells induces a generalized process of apoptosis that in the case of PC12 cells is partially reduced after NGF-triggered differentiation.

7. The modulation of E23a alternative splicing under physiological conditions has allowed, for the first time, to show that the GAP activity of neurofibromin (directly or indirectly) regulates the activation of PKA in the process of neuronal differentiation.

8. All together, the results of this thesis indicate that the regulation of the alternative splicing of exon 23a of the *NF1* gene allows the fine-tuning of the RAS/MAPK and cAMP/PKA pathways through its GAP activity in a coordinate and opposite way along the time-dependent process of neuronal differentiation.

BIBLIOGRAPHY

A

Anastasaki C, Gutmann DH. (2014). Neuronal NF1/RAS regulation of cyclic AMP requires atypical PKC activation. Hum Mol Genet. 2014 Dec 20;23(25):6712-21

Andersen LB, Ballester R, Marchuk DA, Chang E, Gutmann DH, Saulino AM, Camonis J, Wigler M, Collins FS. (1993). A conserved alternative splice in the von Recklinghausen neurofibromatosis (NF1) gene produces two neurofibromin isoforms, both of which have GTPase-activating protein activity. Mol Cell Biol 13:487–495.

Ars E, Serra E, de la Luna S, Estivill X, Lázaro C. (2000a). Cold shock induces the insertion of a cryptic exon in the neurofibromatosis type 1 (NF1) mRNA. Nucleic Acids Res 28(6):1307-1312.

Ars E, Serra E, García J, Kruyer H, Gaona A, Lázaro C, Estivill X. (2000b). Mutations affecting mRNA splicing are the most common molecular defects in patients with neurofibromatosis type 1. Hum Mol Genet 9(2):237-47.

Ars E, Kruyer H, Morell M, Pros E, Serra E, Ravella A, Estivill X, Lázaro C. (2003). Recurrent mutations in the NF1 gene are common among neurofibromatosis type 1 patients. J Med Genet 40(6):e82.

Ast G. (2004). How did alternative splicing evolve?. Nat Rev Genet 5(10):773-782.

B

Baralle M, Baralle D. (2012). Splicing Mechanisms and mutations in the NF1 gene. pp.135-50 In: Upadhyaya M, Cooper DN, editors. Neurofibromatosis Type I, Molecular and Cellular Biology. Springer-Verlag Berlina Heidelberg, Germany.

Barron VA, Zhu H, Hinman MN, Ladd AN, Lou H. (2010). The neurofibromatosis type I pre-mRNA is a novel target of CELF protein-mediated splicing regulation. Nucleic Acids Res 38:253–264

Barron VA, Lou H. (2012). Alternative splicing of the neurofibromatosis type I pre-mRNA. Biosci Rep 32(2):131-8

Bernards A, Snijders AJ, Hannigan GE, Murthy AE, Gusella JF. (1993). Mouse neurofibromatosis type 1 cDNA sequence reveals high degree of conservation of both coding and non-coding mRNA segments. Hum Mol Genet 2(6):645-650.

Buchberg AM, Cleveland LS, Jenkins NA, Copeland NG. (1990). Sequence homology shared by neurofibromatosis type-1 gene and IRA-1 and IRA-2 negative regulators of the RAS cyclic AMP pathway. Nature 347(6290):291-294

Bollag G, McCormick F, Clark R. (1993). Characterization of full-length neurofibromin: tubulin inhibits Ras GAP activity. Embo J 12(5):1923-1927.

Boyanapalli M, Lahoud OB, Messiaen L, Kim B, Anderle de Sylor MS, Duckett SJ, Somara S, Mikol DD. (2006). Neurofibromin binds to caveolin-1 and regulates ras, FAK, and Akt. Biochem Biophys Res Commun 340(4):1200-1208.

Brightman FA, Fell DA. (2000). Differential feedback regulation of the MAPK cascade underlies the quantitative differences in EGF and NGF signalling in PC12 cells. FEBS Lett 482(3):169-174.

Brown JA, Gianino S, Gutmann DH. (2010). Defective cAMP generation underlies the sensitivity of CNS neurons to neurofibromatosis-1 heterozygosity J Neurosci 30(16): 5579-5589.

Brown JA, Diggs-Andrews KA, Gianino SM, Gutmann DH. (2012). Neurofibromatosis-1 heterozygosity impairs CNS neuronal morphology in a cAMP/PKA/ROCK-dependent manner. Mol Cell Neurosci 49(1):13-22.

Bruno I, Jin W, Cote G. (2004) Correction of aberrant FGFR1 alternative RNA splicing through targeting of intronic regulatory elements. Hum Mol Genet 13:2409–2420

C

Caro-Gonzalez HY, Nejsum LN, Siemers KA, Shaler TA, Nelson WJ, Barth AI (2012). Mitogen-activated protein kinase (MAPK/ERK) regulates adenomatous polyposis coli during growth-factor-induced cell extension. J Cell Sci 125(5):1247-1258

Castellano E, Downward J. (2011). RAS Interaction with PI3K: More Than Just Another Effector Pathway. Genes Cancer 2(3):261-274

Castellanos E, Rosas I, Solanes A, Bielsa I, Lazaro C, Carrato C, Hostalot C, Prades P, Roca-Ribas F, Blanco I, Serra E. (2012). In vitro antisense therapeutics for a deep intronic mutation causing Neurofibromatosis type 2. EJHG 21(7):769-773.

Cawthon RM, Andersen LB, Buchberg AM, Xu GF, O'Connell P, Viskochil D, Weiss RB, Wallace MR, Marchuk DA, Culver M, et al. *(1991)*. cDNA sequence and genomic structure of EV12B, a gene lying within an intron of the neurofibromatosis type 1 gene. Genomics 9(3):446-460.

Chen M, Manley JL. (2009). Mechanisms of alternative splicing regulation: insights from molecular and genomics approaches. Rev Mol Cell Biol 10(11): 741–754

Clementi M, Boni S, Mammi I, Favarato M, Tenconi R. (1996). Clinical application of genetic polymorphism in neurofibromatosis type 1. Ann Genet 39:92–96.

Colman SD, Williams CA, Wallace MR. (1995). Benign neurofibromas in type 1 neurofibromatosis (NF1) show somatic deletions of the NF1 gene. Nat Genet 11:90–92

Corey DR, Abrams JM. (2001). Morpholino antisense oligonucleotides: tools for investigating vertebrate development. Genome Biol 2(5): 1015.1-1015.3

Costa RM, Yang T, Huynh DP, Pulst SM, Viskochil DH, Silva AJ, Brannan CI. (2001). Learning deficits, but normal development and tumor predisposition, in mice lacking exon 23a of Nf1. Nat Genet 27(4): 399-405

Costa RM, Federov NB, Kogan JH, Murphy GG, Stern J, Ohno M, Kucherlapati R, Jacks T, Silva AJ (2002). Mechanism for the learning deficits in a mouse model of neurofibromatosis type 1. Nature 415(6871):526-530.

Cui Y, Costa RM, Murphy GG, Elgersma Y, Zhu Y, Gutmann DH, Parada LF, Mody I, Silva AJ. (2008). Neurofibromin regulation of ERK signaling modulates GABA release and learning. Cell 135(3): 549-560.

D

Das KP, Freudenrich T, Mundy W. (2004). Assessment of PC12 cell differentiation and neurite growth: a comparison of morphological and neurochemical measures. Neurotoxicol Teratol 26(3): 397-406.

D'Angelo I, Welti S, Bonneau F, Scheffzek K. (2006). A novel bipartite phospholipid-binding module in the neurofibromatosis type 1 protein. EMBO Rep 7(2):174-9.

Danglot G, Regnier V, Fauvet D, Vassal G, Kujas M, Bernheim A. (1995). Neurofibromatosis 1 (NF1) mRNAs expressed in the central nervous system are differentially spliced in the 5′ part of the gene. Hum Mol Genet 4:915–920.

Daston MM, Scrable H, Nordlund M, Sturbaum AK, Nissen LM, Ratner N. (1992). The protein product of the neurofibromatosis type 1 gene is expressed at highest abundance in neurons, Schwann cells, and oligodendrocytes. Neuron 8(3):415-28.

DeBella K, Szudek J, Friedman JM. (2000). Use of the national institutes of health criteria for diagnosis of neurofibromatosis 1 in children. Pediatrics 105(3 Pt 1):608-14.

DeBella K, Poskitt K, Szudek J, Friedman JM. (2000b). se of "unidentified bright objects" on MRI for diagnosis of neurofibromatosis 1 in children. Neurology 54(8):1646-51

DeClue JE, Cohen BD, Lowy DR. (1991). Identification and characterization of the neurofibromatosis type 1 protein product. Proc Natl Acad Sci USA 88(22):9914-8.

DeFranco C, Damon DH, Endoh M, Wagner JA. (1993). Nerve growth factor induces transcription of NGFIA through complex regulatory elements that are also sensitive to serum and phorbol 12-myristate 13-acetate. Mol Endocrinol. 1993 Mar;7(3):365-79.

Denayer E, de Ravel T, Legius E. (2008). Clinical and molecular aspects of RAS related disorders. J Med Genet 45(11): 695-703.

De Raedt TM, Maertens O, Callens T, Neyaert JM, Lambert J, Messiaen L. (2008). Somatic NF1 mutations in tumors and other tissues. pp.143-153 In: Kaufmann D, editor. Neurofibromatoses, Vol 16. Monogr Human Genet. S Karger AG.

De Schepper S, Boucneau JM, Westbroek W, Mommaas M, Onderwater J, Messiaen L, Naeyaert JM, Lambert JL. (2006). Neurofibromatosis type 1 protein and amyloid precursor protein interact in normal human melanocytes and colocalize with melanosomes. J Invest Dermatol 126(3):653-9.

De Schepper S, Maertens O, Callens T, Naeyaert J-M, Lambert J, Messiaen L. (2008). Somatic mutation analysis in NF1 café au lait spots reveals two NF1 hits in the melanocytes. J Invest Dermatol 128(4):1050-3.

Desmet FO, Hamroun D, Lalande M, Collod-Béroud G, Claustres M, Béroud C. (2009). Human Splicing Finder: an online bioinformatics tool to predict splicing signals. Nucleic Acids Res 37(9):e6

Dhillon AS, von Kriegsheim A, Grindlay J, Kolch W. (2007) Phosphatase and feedback regulation of Raf-1 signaling. Cell Cycle 6: 3-7.

Diggs-Andrews KA, Gutmann DH. (2013). Modeling cognitive dysfunction in neurofibromatosis-1. Trends Neurosci 36(4):237-47

Doherty P, Ashton SV, Skaper SD, Leon A, Walsh FS. (1992). Ganglioside modulation of neural cell adhesion molecule and N-cadherin-dependent neurite outgrowth. J Cell Biol 117(5):1093-9.

Dougherty MK, Muller J, Ritt DA, Zhou M, Zhou XZ, Copeland TD, Conrads TP, Veenstra TD, Lu KP, Morrison DK. (2005) Regulation of Raf-1 by direct feedback phosphorylation. Mol Cell 17: 215-224

Dominski Z, Kole R. (1993). Restoration of correct splicing in thalassemic pre-mRNA by antisense oligonucleotides. Proc Natl Acad Sci U S A 90(18):8673-7

E

Evans DG, Baser ME, McGaughran J, Sharif S, Howard E, Moran A. (2002). Malignant peripheral nerve sheath tumours in neurofibromatosis 1. J Med Genet 39(5):311-4

Evans DG: Neurofibromatosis type 2 (NF2) (2009). a clinical and molecular review. Orphanet J Rare Dis 19: 4:16.

Eves EM, Tucker M, Roback J, Downen M, Rosner M, Wainer BH. (1992). Immortal rat hippocampal cell lines exhibit neuronal and glial lineages and neurotrophin gene expression. Proc. Natl. Acad. Sci. USA 89: 4373-4377

Eves EM, Skoczylas C, Yoshida K, Alnemri ES, Rosner MR. (2001). FGF induces a switch in death receptor pathways in neuronal cells. J Neurosci 21(14):4996-5006.

F

Fernández-Rodríguez J, Castellsagué J, Benito L, Benavente Y, Capellá G, Blanco I, Serra E, Lázaro C. (2011). A mild neurofibromatosis type 1 phenotype produced by the combination of the benign nature of a leaky NF1-splice mutation and the presence of a complex mosaicism. Hum Mutat 32(7):705-709.

Ferner RE, Huson SM, Thomas N, Moss C, Willshaw H, Evans DG, Upadhyaya M, Towers R, Gleeson M, Steiger C, Kirby A. (2007). Guidelines for the diagnosis and management of individuals with neurofibromatosis 1. J Med Genet 44(2): 81-88.

Fleming VA, Geng C, Ladd AN, Lou H. (2012). Alternative splicing of the neurofibromatosis type 1 pre-mRNA is regulated by the muscleblind-like proteins and the CUG-BP and ELAV-like factors. BMC Mol Biol 13:35.

Friedman JM, Birch PH. (1997). Type 1 neurofibromatosis: a descriptive analysis of the disorder in 1,728 patients. Am J Med Genet 70(2):138-143.

G

Geist RT, Gutmann DH. (1996). Expression of a developmentally-regulated neuron-specific isoform of the neurofibromatosis 1 (NFl) gene. Neuroscience 211: 85-88.

Greene LA, Tischler AS. (1976). Establishment of a noradrenergic clonal line of rat adrenal pheochromocytoma cells which respond to nerve growth factor. Cell Biology 73(7):2424-2428.

Greene LA. (1978). Nerve growth factor prevents the death and stimulates the neuronal differentiation of clonal PC12 pheochromocytoma cells in serum-free medium. J Cell Biol 78:747–755.

Gunning PW, Landreth GE, Layer P, Ignatius M, Shooter EM. (1981). Nerve growth factor-induced differentiation of PC12 cells: evaluation of changes in RNA and DNA metabolism. J Neurosci 1(4): 368-379.

Guo HF, Tong J, Hannan F, Luo L, Zhong Y. (2000). A neurofibromatosis-1-regulated pathway is required for learning in Drosophila. Nature 403(6772): 895-898.

Guan W, Cheng F, Huang Q, Kleiboeker S, Qiu J. (2011). Inclusion of the central exon of parvovirus B19 precursor mRNA is determined by multiple splicing enhancers in both the exon and the downstream intron. J Virol 85(5): 2463-2468

Gutmann DH, Wood DL, Collins FS. (1991). Identification of the neurofibromatosis type 1 gene product. Proc Natl Acad Sci USA 88(21): 9658-9662.

Gutmann DH, Tennekoon GI, Cole JL, Collins FS, Rutkowski JL. (1993). Modulation of the neurofibromatosis type 1 gene product, neurofibromin, during Schwann cell differentiation. J Neurosci Res 36(2):216-223.

Gutmann DH, Geist RT, Wright DE, Snider WD. (1995). Expression of the neurofibromatosis 1 (NF1) isoforms in developing and adult rat tissues. Cell Growth Differ 6:315–323

H

Hannan F, Ho I, Tong JJ, Zhu Y, Nurnberg P, Zhong Y. (2006). Effect of neurofibromatosis type I mutations on a novel pathway for adenylyl cyclase activation requiring neurofibromin and Ras. Hum Mol Genet 15(7):1087-1098.

Houston P, Campbell CJ, Svaren J, Milbrandt J, Braddock M. (2001). The transcriptional corepressor NAB2 blocks Egr-1-mediated growth factor activation and angiogenesis. Biochem Biophys Res Commun 283(2):480-486.

Huson SM, Compston DA, Clark P, Harper PS. (1989). A genetic study of von Recklinghausen neurofibromatosis in south east Wales. I. Prevalence, fitness, mutation rate, and effect of parental transmission on severity. J Med Genet 26(11):704-711.

Hinman M, Sharma A, Luo G, Lou H. (2014). Neurofibromatosis Type 1 Alternative Splicing Is a Key Regulator of Ras Signaling in Neurons. Mol Cell Biol 34(12): 2188-2197.

Hirayama M, Kobayashi D, Mizuguchi S, Morikawa T, Nagayama M, Midorikawa U, Wilson MM, Nambu AN, Yoshizawa AC, Kawano S, Araki N. (2013). Integrated proteomics identified novel activation of dynein IC2-GR-COX-1 signaling in neurofibromatosis type I (NF1) disease model cells. Mol Cell Proteomics 12(5):1377-1394.

Huang DW, Sherman BT, Lempicki RA. (2009a). Systematic and integrative analysis of large gene lists using DAVID Bioinformatics Resources. Nature Protoc 4(1):44-57.

Huang DW, Sherman BT, Lempicki RA. (2009b). Bioinformatics enrichment tools: paths toward the comprehensive functional analysis of large gene lists. Nucleic Acids Res 37(1):1-13.

I

Ito E, Sweterlitsch LA, Tran PB, Rauscher FJ 3rd, Narayanan R. (1990). Inhibition of PC-12 cell differentiation by the immediate early gene fra-1. Oncogene 5(12):1755-1760.

Izawa I, Tamaki N, Saya H. (1996). Phosphorylation of neurofibromatosis type 1 gene product (neurofibromin) by cAMP-dependent protein kinase. FEBS Lett 382(1-2):53-59.

K

Kaplan DR. (1998). Studying signal transduction in neuronal cells: the Trk/NGF system. Prog Brain Res 117:35-46

Kaufmann D, Leistner W, Kruse P, Kenner O, Hoffmeyer S, Hein C, Vogel W, Messiaen L, Bartelt B. (2002a). Aberrant splicing in several human tumors in the tumor suppressor genes neurofibromatosis type 1, neurofibromatosis type 2, and tuberous sclerosis 2. Cancer Res 62(5):1503-1509.

Kaufmann D, Muller R, Kenner O, Leistner W, Hein C, Vogel W, Bartelt B. (2002b). The N-terminal splice product NF1-10a-2 of the NF1 gene codes for a transmembrane segment. Biochem Biophys Res Commun 294:496–503.

Kaufmann D, Kenner O, Nurnberg P, Vogel W, Bartelt B. (2004). In NF1, CFTR, PER3, CARS and SYT7, alternatively included exons show higher conservation of surrounding intron sequences than constitutive exons. Eur J Hum Genet 12(2): 139-149.

Kayl AE, Moore BD 3rd, Slopis JM, Jackson EF, Leeds NE. (2000). Quantitative morphology of the corpus callosum in children with neurofibromatosis and attention-deficit hyperactivity disorder. J Child Neurol. 15(2):90-96

Kent WJ, Sugnet CW, Furey TS, Roskin KM, Pringle TH, Zahler AM, Haussler D. (2002). The human genome browser at UCSC. Genome Res 12(6):996-1006.

Klesse LJ, Meyers KA, Marshall CJ, Parada LF.(1999). Nerve growth factor induces survival and differentiation through two distinct signaling cascades in PC12 cells. Oncogene 18(12): 2055-2068.

Kluwe L, MacCollin M, Tatagiba M, Thomas S, Hazim W, Haase W, Mautner VF. (1998). Phenotypic variability associated with 14 splice site mutations in the NF2 gene. Am J Med Genet 77: 228-233

Kluwe L, Friedrich R, Mautner VF. (1999). Loss of NF1 allele in Schwann cells but not in fibroblasts derived from an NF1- associated neurofibroma. Genes Chromosomes Cancer 24: 283–285.

Knudson AG. (1971). Mutation and cancer: statistical study of retinoblastoma. Proc Natl Acad Sci USA 68: 820-823

Kuo WL, Abe M, Rhee J, Eves EM, McCarthy SA, Yan M, Templeton DJ, McMahon M, Rosner MR. (1996). Raf, but not MEK or ERK, is sufficient for differentiation of hippocampal neuronal cells. Mol Cell Biol 16:1458–1470.

L

Ladd AN. (2013). CUG-BP, Elav-like family (CELF)-mediated alternative splicing regulation in the brain during health and disease. Mol Cell Neurosci 56:456-464

Lazaro C, Fernández-Rodríguez J, Serra E. (2012). Deep Intronic *NF1* Mutations and Possible Therapeutic Interventions. pp.173-186 In: Upadhyaya M, Cooper DN, editors. Neurofibromatosis Type I, Molecular and Cellular Biology. Springer-Verlag Berlina Heidelberg, Germany.

Lebedeva I, Stein CA. (2001). Antisense oligonucleotides: Promise and reality. Annu Rev Pharmacol Toxicol. 41:403-419.

Legius E, Marchuk DA, Collins FS, Glover TW. (1993). Somatic deletion of the neurofibromatosis t00000ype 1 gene in a neurofibrosarcoma supports a tumour suppressor gene hypothesis. Nat Genet 3(2):122-126

Levine TM, Materek A, Abel J, O'Donnell M, Cutting LE. (2006). Cognitive profile of neurofibromatosis type 1. Semin Pediatr Neurol 13(1):8-20

Li C, Cheng Y, Gutmann DA, Mangoura D. (2001). Differential localization of the neurofibromatosis 1 (NF1) gene product, neurofibromin, with the F-actin or microtubule cytoskeleton during differentiation of telencephalic neurons. Brain Res Dev Brain Res 130(2): 231-248.

Li Y, O'Connell P, Breidenbach HH, Cawthon R, Stevens J, Xu G, Neil S, Robertson M, White R, Viskochil D. (1995). Genomic organization of the neurofibromatosis 1 gene (NF1). Genomics 25(1):9-18

Li W, Cui Y, Kushner SA, Brown RA, Jentsch JD, Frankland PW, Cannon TD, Silva AJ. (2005). The HMG-CoA reductase inhibitor lovastatin reverses the learning and attention deficits in a mouse model of neurofibromatosis type 1. Curr Biol 15(21):1961-1967.

Lin Y, Hsueh Y. (2008). Neurofibromin interacts with CRMP-2 and CRMP-4 in rat brain. Biochem Biophys Res Commun 369(2): 747-752.

Listernick R, Ferner R, Liu G, Gutmann DH. (2007). Optic pathway gliomas in neurofibromatosis-1: Controversies and recommendations. Ann Neurol 61(3): 189-198.

M

MacCollin M, Woodfin W, Kronn D, Short MP. (1996). Schwannomatosis: a clinical and pathologic study. Neurology 46 (4): 1072–1079.

Maertens O, Brems H, Vandesompele J, De Raedt T, Heyns I, Rosenbaum T, De Schepper S, De Paepe A, Mortier G, Janssens S, Speleman F, Legius E, Messiaen L. (2006). Comprehensive NF1 screening on cultured Schwann cells from neurofibromas. Hum Mutat 27(10):1030-40

Maertens O, De Schepper S, Vandesompele J, Brems H, Heyns I, Janssens S, Speleman F, Legius E, Messiaen L. (2007). Molecular dissection of isolated disease features in mosaic NF1 patients. Am J Hum Genet 81(2): 243-251

Mantani A, Wakasugi S, Yokota Y, Abe K, Ushio Y, Yamamura K. (1994). A novel isoform of the neurofibromatosis type-1 mRNA and a switch of isoforms during murine cell differentiation and proliferation. Gene 148: 245–251

Marchuk DA, Saulino AM, Tavakkol R, Swaroop M, Wallace MR, Andersen LB, Mitchell AL, Gutmann DH, Boguski M, Collins FS. (1991). cDNA cloning of the type 1 neurofibromatosis gene: complete sequence of the NF1 gene product. Genomics 11(4): 931-940.

Marshall CJ. (1995). Specificity of Receptor Tyrosine Kinase Signaling: Transient versus Sustained Extracellular Signal-Regulated Kinase Activation. Cell 80: 179-185.

Martin GA, Viskochil D, Bollag G, McCabe PC, Crosier WJ, Haubruck H, Conroy L, Clark R, O'Connell P, Cawthon RM. (1990). The GAP-related domain of the neurofibromatosis type 1 gene product interacts with ras p21. Cell 63:843–849

Martin I, Andres C, Védrine S, Tabagh R, Michelle C, Jourdan M, Heuze-Vourc'h N, Corcia P, Duittoz A, Vourc'h P. (2009). Effect of the oligodendrocyte myelin glycoprotein (OMgp) on the expansion and neuronal differentiation of rat neural stem cells. Brain Research 1284: 22-30.

Matlin AJ, Clark F, Smith CW. (2005). Understanding alternative splicing: towards a cellular code. Nat Rev Mol Cell Biol 6(5):386-398.

Matsushita T, Amagai Y, Terai K, Kojima T, Obinata M, Hashimoto S. (2006). A novel neuronal cell line derived from the ventrolateral region of the suprachiasmatic nucleus. Neuroscience 140(3):849-856

McClorey G, Fall AM, Moulton HM, Iversen PL, Rasko JE, Ryan M, Fletcher S, Wilton SD. (2006). Induced dystrophin exon skipping in human muscle explants. Neuromuscul Disord 16:583–590

Meijering E. (2010). Neuron Tracing in Perspective. Cytometry A 7(77):167-176. 693-704

Meijering E, Jacob M, Sarria JC, Steiner P, Hirling H, Unser M. (2004). Design and validation of a tool for neurite tracing and analysis in fluorescence microscopy images.Cytometry A 58(2):167-176.

Messiaen LM, Callens T, Mortier G, Beysen D, Vandenbroucke I, Van Roy N, Speleman F, Paepe AD. (2000). Exhaustive mutation analysis of the NF1 gene allows identification of 95% of mutations and reveals a high frequency of unusual splicing defects. Hum Mutat 15:541–555.

Messiaen L, Wimmer K. (2008). NF1 mutational spectrum. pp. 63-77. In: Kaufmann D editor. Neurofibromatoses. Monogr Hum Genet (16), Basel.

Metheny LJ, Skuse GR. (1996). NF1 mRNA Isoform Expression in PC12 Cells: Modulation by Extrinsic Factors. Experimental cell research 228: 44–49.

Mingorance-Le Meur A, Mohebiany A, O'connor T, Hendricks M. (2009). Varicones and Growth Cones: Two Neurite Terminals in PC12 Cells. PLoS ONE 4(2): e4334.

Morcos PA. (2001). Achieving efficient delivery of morpholino oligos in cultured cells. Genesis 30(3): 94-102.

Morcos PA. (2007). Achieving targeted and quantifiable alteration of mRNA splicing with Morpholino oligos. Biochem Biophys Res Commun 358(2): 521-527

Mori D, Yamada M, Mimori-Kiyosue Y, Shirai Y, Suzuki A, Ohno S, Saya H, Wynshaw-Boris A, Hirotsune S. (2009). An essential role of the aPKC-Aurora A-NDEL1 pathway in neurite elongation by modulation of microtubule dynamics. Nat Cell Biol 11(9):1057-1068.

N

Nakagawa T, Zhu H, Morishima N, Li E, Xu J, Yankner BA, Yuan J. (2000). Caspase-12 mediates endoplasmic-reticulum-specific apoptosis and cytotoxicity by amyloid-beta. Nature 403(6765):98-103

NIH (1988). NIH consensus development conference statement (1988) Neurofibromatosis. Arch Neurol 45:575-78

North KN, Riccardi V, Samango-Sprouse C, Ferner R, Moore B, Legius E, Ratner N, Denckla MB. (1997). Cognitive function and academic performance in neurofibromatosis. 1: consensus statement from the NF1 Cognitive Disorders Task Force. Neurology 48(4):1121-1127.

O

Oh D, Cho J, Park S, Kim YS, Yoon YJ, Yoon SH, Chung KC, Lee K, Han J. (2008). A novel role of hippocalcin in bFGF-induced neurite outgrowth of H19-7 cells. J Neurosci Res 86(7): 1557-1565.

Ohuchi T, Maruoka S, Sakudo A, Arai T. (2002). Assay-based quantitative analysis of PC12 cell differentiation. J Neurosci Methods 118(1): 1-8.

Ozonoff S. (1999). Cognitive impairment in neurofibromatosis type 1. Am J Med Genet 89(1):45-52.

P

Park VM, Kenwright KA, Sturtevant DB, Pivnick EK. (1998) Alternative splicing of exons 29 and 30 in the neurofibromatosis type 1 gene. Hum Genet 103(4):382-385.

Phillips SE, Vincent P, Rizzieri KE, Schaaf G, Bankaitis VA, Gaucher EA. (2006). The diverse biological functions of phosphatidylinositol transfer proteins in eukaryotes. Crit Rev Biochem Mol Biol 41(1):21-49.

Popplewell L, Malerba A, Dickson G. (2012). Optimizing antisense oligonucleotides using phosphorodiamidate morpholino oligomers. pp143-167. In: Exon skipping: Methods and Protocols. Vol (867**).** Aartsma-Rus A. ed. Springer Science+Business Media.

Pride N, Payne JM, Webster R, Shores EA, Rae C, North KN. (2010). Corpus callosum morphology and its relationship to cognitive function in neurofibromatosis type 1. J Child Neurol 25(7):834-841

Pros E, Fernández-Rodríguez J, Canet B, Benito L, Sánchez A, Benavides A, Ramos FJ, López-Ariztegui MA, Capellá G, Blanco I, Serra E, Lázaro C. (2009). Antisense therapeutics for neurofibromatosis type 1 caused by deep intronic mutations. Hum Mutat 30(3):454-462.

Q

Qu Z, Wolfraim LA, Svaren J, Ehrengruber MU, Davidson N, Milbrandt J. (1998). The transcriptional corepressor NAB2 inhibits NGF-induced differentiation of PC12 cells. J Cell Biol 142(4):1075-1082

R

Régnier V, Meddeb M, Lecointre G, Richard F, Duverger A, Nguyen VC, Dutrillaux B, Bernheim A, Danglot G. (1997). Emergence and scattering of multiple neurofibromatosis (NF1)-related sequences during hominoid evolution suggest a process of pericentromeric interchromosomal transposition. Hum Mol Genet 6(1):9-16.

Reilly KM. (2009). Neurofibromatosis and lessons for the war on cancer. EMBO Mol Med 1(4):198-200.

S

Sadek CM, Pelto-Huikko M, Tujague M, Steffensen KR, Wennerholm M, Gustafsson JA. (2003). TACC3 expression is tightly regulated during early differentiation. Gene Expr Patterns 3(2):203-11.

Sawada S, Florell S, Purandare SM, Ota M, Stephens K, Viskochil D. (1996). Identification of NF1 mutations in both alleles of a dermal neurofibroma. Nat Genet 14:110–112.

Sazani P, Kang SH, Maier MA, Wei C, Dillman J, Summerton J, Manoharan M, Kole R. (2001) Nuclear antisense effects of neutral, anionic and cationic oligonucleotide analogs. Nucl. Acids Res 29: 3965–3974.

Bibliography

Scheffzek K, Lautwein A, Scherer A, Franken S, Wittinghofer A. (1998). Crystallization and preliminary X-ray crystallographic study of the Ras-GTPase-activating domain of human p120GAP. Proteins 27(2):315-318.

Scheffzek K, Welti S. (2012). Neurofibromin: Protein Domains and Functional characteristics. pp. 305-319 In: Upadhyaya M, Cooper DN, editors. Neurofibromatosis Type I, Molecular and Cellular Biology. Springer-Verlag Berlina Heidelberg, Germany.

Schnerwitzki D, Perner B, Hoppe B, Pietsch S, Mehringer R, Hänel F, Englert C. (2014). Alternative splicing of Wilms tumor suppressor 1 (Wt1) exon 4 results in protein isoforms with different functions. Dev Biol 393(1):24-32.

Selvanathan SK, Shenton A, Ferner R, Wallace AJ, Huson SM, Ramsden RT, Evans DG. (2010). Further genotype-phenotype correlations in neurofibromatosis 2. Clin Genet 77: 163-170

Serra E, Puig S, Otero D, Gaona A, Kruyer H, Ars E, Estivill X, Lazaro C. (1997). Confirmation of a double-hit model for the NF1 gene in benign neurofibromas. Am J Hum Genet 61:512–519.

Serra E, Rosenbaum T, Winner U, Aledo R, Ars E, Estivill X, Lenard HG, Lázaro C. (2000). Schwann cells harbor the somatic NF1 mutation in neurofibroma: evidence of two different Schwann cell subpopulations. Human Molecular Genetics 9: 3055-3064.

Shieh JJ, Liu KT, Huang SW, Chen YJ, Hsieh TY. (2009). Modification of alternative splicing of Mcl-1 pre-mRNA using antisense morpholino oligonucleotides induces apoptosis in basal cell carcinoma cells. J Invest Dematol 129:2497–2506

Silva AJ, Frankland PW, Marowitz Z, Friedman E, Laszlo GS, Cioffi D, Jacks T, Bourtchuladze R.(1997). A mouse model for the learning and memory deficits associated with neurofibromatosis type I. Nat. Genet 15:281–284

Sorek R, Ast G. (2003). Intronic sequences flanking alternatively spliced exons are conserved between human and mouse. Genome Res 13(7):1631-1637.

Stevenson DA, Zhou H, Ashrafi S, Messiaen LM, Carey JC, D'Astous JL, Santora SD, Viskochil DH. (2006). Double inactivation of NF1 in tibial pseudarthrosis. Am J Hum Genet 79(1):143-148

Stocker A. (2004). Molecular mechanisms of vitamin E transport. Ann N Y Acad Sci 1031:44-59.

Sugnet C, Srinivasan K, Clark T, O'brien G, Cline M, Wang H, Williams A, Kulp D, Blume J, Haussler D, Ares M. (2005). Unusual Intron Conservation Near Tissue-regulated Exons Found by Splicing Microarrays. PLoS Comp Biol. e4.

Summerton J, Weller D. (1997). Morpholino antisense oligomers: design, preparation, and properties. Antisense Nucleic Acid Drug Dev 7(3): 187-195.

Summerton J. (2005). Endo-Porter: a novel reagent for safe, effective delivery of substances into cells. Ann N Y Acad Sci 1058: 62-75.

Summerton J. (2007). Morpholino, siRNA, and S-DNA compared: impact of structure and mechanism of action on off-target effects and sequence specificity. Curr Top Med Chem 7(7): 651-660.

Sun Y, Kim NH, Ji L, Kim SH, Lee J, Rhee HJ. (2013). Lysophosphatidic acid activates β-catenin/T cell factor signaling, which contributes to the suppression of apoptosis in H19-7 cells. Mol Med Rep 8(6):1729-1733

Suzuki Y, Suzuki H, Kayama T, Yoshimoto T, Shibahara S. (1991). Brain tumors predominantly express the neurofibromatosis type 1 gene transcripts containing the 63 base insert in the region coding for GTPase activating protein-related domain. Biochem Biophys Res Commun. 181(3):955-961.

T

Takahashi K, Suzuki H, Kayama T, Suzuki Y, Yoshimoto T, Sasano H, Shibahara S. (1994). Multiple transcripts of the neurofibromatosis type 1 gene in human brain and in brain tumours. Clin Sci (Lond) 87(5):481-485.

Tokuo H, Yunoue S, Feng L, Kimoto M, Tsuji H, Ono T, Saya H, Araki N. (2001). Phosphorylation of neurofibromin by cAMP-dependent protein kinase is regulated via a cellular association of N(G), N(G)-dimethylarginine dimethylaminohydrolase. FEBS Lett 494(1-2):48-53.

Thomson SA, Wallace MR. (2002). RT-PCR splicing analysis of the NF1 open reading frame. Hum Genet 110(5):495-502.

U

Uchida T, Matozaki T, Suzuki T, Matsuda K, Wada K, Nakano O, Konda Y, Nishisaki H, Nagao M, Sakamoto C, et al. (1992). Expression of two types of neurofibromatosis type 1 gene transcripts in gastric cancers and comparison of GAP activities. Biochem Biophys Res Commun 187: 332–339

Upadhyaya M, Kluwe L, Spurlock G, Monem B, Majounie E, Mantripragada K, Ruggieri M, Chuzhanova N, Evans DG, Ferner R, Thomas N, Guha A, Mautner V. (2008). Germline and somatic NF1 gene mutation spectrum in NF1-associated malignant peripheral nerve sheath tumors (MPNSTs). Hum Mutat 29(1):74-82.

V

Vaisid T, Barnoy S, Kosower NS. (2008). Calpastatin overexpression attenuates amyloid-beta-peptide toxicity in differentiated PC12 cells. Neuroscience 156(4):921-931.

Vaudry D, Stork PJS, Lazarovici P, Eiden LE. (2002). Signaling Pathways for PC12 Cell Differentiation: Making the Right Connections. Science 296(5573): 1648-1649.

Vandenbroucke I, Callens T, De Paepe A, Messiaen L. (2002a). Complex splicing pattern generates great diversity in human NF1 transcripts. BMC Genomics 3(1): 13

Vandenbroucke I, Vandesompele J, De Paepe A, Messiaen L. (2002b). Quantification of NF1 transcripts reveals novel highly expressed splice variants. FEBS Lett 522(1-3):71-76.

Viskochil DM, Cawthon R, O'Connell P, Xu GF, Stevens J, Culver M, Carey J, White R. (1991). The gene encoding the oligodendrocyte-myelin glycoprotein is embedded within the neurofibromatosis type 1 gene. Mol Cell Biol 11(2):906-912.

Viskochil DM. 1998. Gene structure and expression. pp. 39-56 In: Upadhyaya M, Cooper DN, editors. Neurofibromatosis Type I: from genotype to phenotype. Oxford: Bios Scientific Publishers Ltd.

Vossler MR, Yao H, York RD, Pan MG, Rim CS, Stork PJ. (1997) cAMP activates MAP kinase and Elk-1 through a B-Raf- and Rap1-dependent pathway. Cell 89:73-82.

von Kriegsheim A, Baiocchi D, Birtwistle M, Sumpton D, Bienvenut W, Morrice N, Yamada K, Lamond A, Kalna G, Orton R, Gilbert D, Kolch W. (2009). Cell fate decisions are specified by the dynamic ERK interactome. Nat Cell Biol 11(12):1458-1464.

W

Wang S, Watanabe T, Noritake J, Fukata M, Yoshimura T, Itoh N, Harada T, Nakagawa M, Matsuura Y, Arimura N, et al. (2007). IQGAP3, a novel effector of Rac1 and Cdc42, regulates neurite outgrowth. J. Cell Sci 120: 567–577.

Wang Q, Yin H, Camelliti P, Betts C, Moulton H, Lee H, Saleh A, Gait MJ, Wood MJ. (2010). In vitro evaluation of novel antisense oligonucleotides is predictive of in vivo exon skipping activity for Duchenne muscular dystrophy. J. Gene Med 12(4): 354-364.

Wimmer K, Roca X, Beiglböck H, Callens T, Etzler J, Rao A, Krainer A, Fonatsch C, Messiaen L. (2007). Extensive in silico analysis of NF1 splicing defects uncovers determinants for splicing outcome upon 5′ splice-site disruption. Hum. Mutat 28(6): 599-612.

Wimmer K, Yao S, Claes K, Kehrer-Sawatzki H, Tinschert S, De Raedt T, Legius E,Callens T, Beiglbock H, Maertens O, Messiaen L. (2006). Spectrum of single- and multiexon NF1 copy number changes in a cohort of 1,100 unselected NF1 patients. Genes Chromosomes Cancer 45(3):265-276.

X

Xu GF, O'Connell P, Viskochil D, Cawthon R, Robertson M, Culver M, Dunn D, Stevens J, Gesteland R, White R, et al. (1990a). The neurofibromatosis type 1 gene encodes a protein related to GAP. Cell 62(3):599-608.

Xu GF, Lin B, Tanaka K, Dunn D, Wood D, Gesteland R, White R, Weiss R, Tamanoi F. (1990b). The catalytic domain of the neurofibromatosis type 1 gene product stimulates ras GTPase and complements ira mutants of S. cerevisiae. Cell 63(4):835-841.

Y

Yao H, York RD, Misra-Press A, Carr DW, Stork PJS. (1998) The Cyclic Adenosine Monophosphate-dependent Protein Kinase (PKA) Is Required for the Sustained Activation of Mitogen-activated Kinases and Gene Expression by Nerve Growth Factor. J. Biol. Chem 273: 8240-8247.

York RD, Yao H, Dillon T, Ellig CL, Eckert SP, McCleskey EW, Stork PJS. (1998). Rap1 mediates sustained MAP kinase activation induced by nerve growth factor. Nature 392: 622-626.

Yunoue S, Tokuo H, Fukunaga K, Feng L, Ozawa T, Nishi T, Kikuchi A, Hattori S, Kuratsu J, Saya H, Araki N. (2003). Neurofibromatosis type I tumor suppressor neurofibromin regulates neuronal differentiation via its GTPase-activating protein function toward Ras. J Biol Chem 278(29): 26958-26969.

Z

Zhou H, Janghra N, Mitrpant C, Dickinson RL, Anthony K, Price L, Eperon IC, Wilton SD, Morgan J, Muntoni F. (2013). A novel morpholino oligomer targeting ISS-N1 improves rescue of severe spinal muscular atrophy transgenic mice. Hum Gene Ther 24(3):331-42

Zhu H, Hinman MN, Hasman RA, Mehta P, Lou H. (2008). Regulation of neuron-specific alternative splicing of neurofibromatosis type 1 pre-mRNA. Mol Cell Biol 28:1240–1251